Master Thesis in Geographical Information Science nr 136

Comparing radar satellites.

Use of Sentinel-1 leads to an increase in oil spill alerts in Norwegian waters.

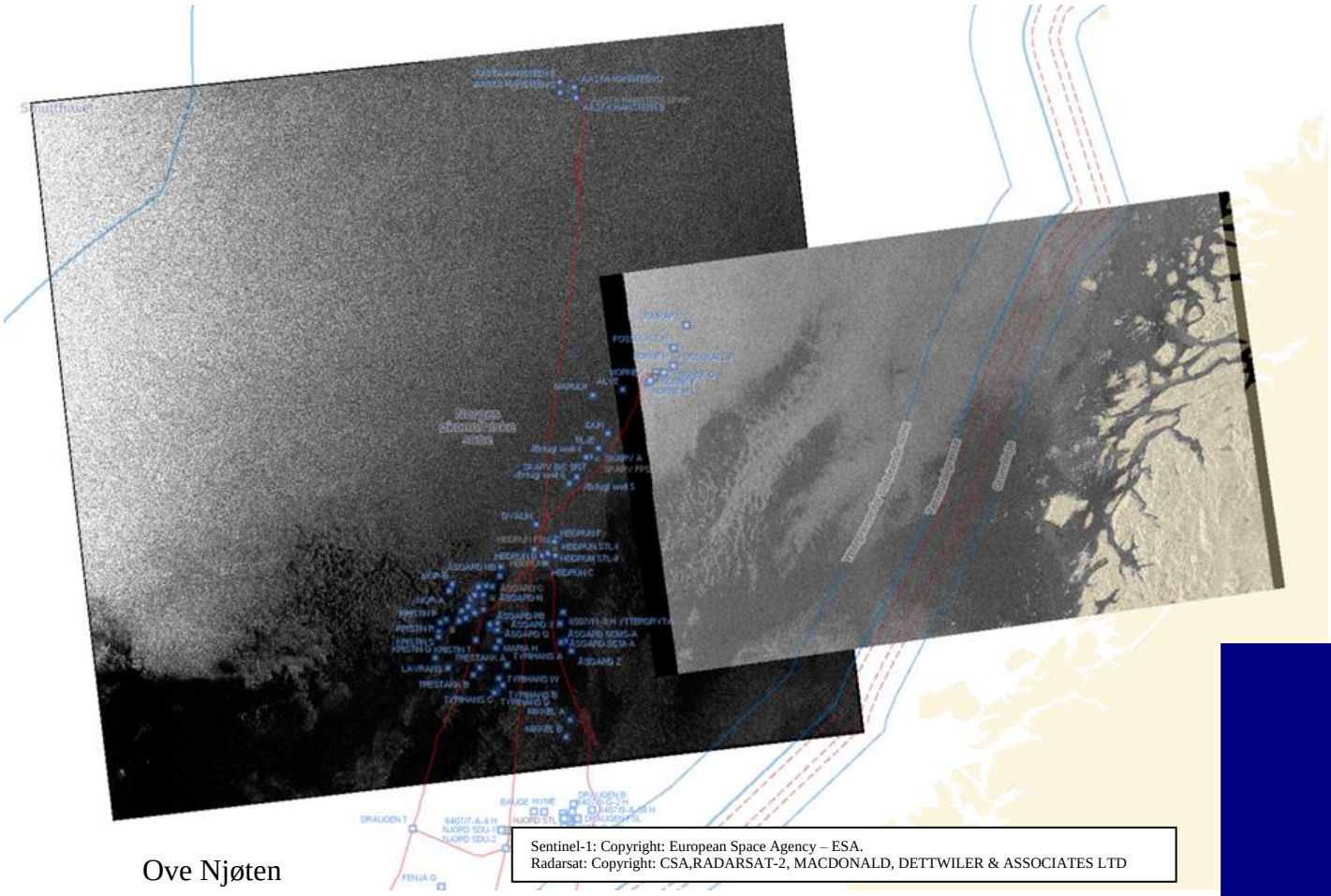

Ove Njøten

2021
Department of
Physical Geography and Ecosystem Science
Centre for Geographical Information Systems
Lund University
Sölvegatan 12
S-223 62 Lund
Sweden

Ove Njøten (2021). Title of thesis
Master degree thesis, 30/ credits in Master in Geographical Information Science
Department of Physical Geography and Ecosystem Science, Lund University

Acknowledgments

I would like to thank my supervisor, Jonathan Seaquist, for all his advice, discussions, and guidance throughout my thesis work. I also want to thank Rune Bergstøm and Even Widerøe Kristoffersen at the Norwegian Coastal Administration for all their support and for making it possible to use in-house data for my thesis. Also, thanks to Jon-Arve Røyset at the Norwegian Coastal Administration for help and discussions on Havbase. Also, thanks to Tony Bauna and Line Stenbakk at KSAT for their support on data collection. Thanks to Sonia Santos at EMSA for her support on data use from EMSA.

Finally, I need to thank my family, partner Silje, and children Tommy, Elvira, Adrian, and Alva. Without their patience and support, this would not be possible.

Abstract

Since the introduction of Sentinel-1A and 1B in 2015-2016, oil spill alerts have increased by 250% in Norwegian waters. This increase does not track the slight decreasing trend in oil spills at sea detected by Norwegian remote sensing aircraft, nor is it consistent with the decreasing trends for both the number of oil spills and the yearly oil spill volume registered by international monitoring programs. This study, therefore, aims to explain the increase in the number of oil spill alerts, discover how much additional mineral oil is discharged into Norwegian waters, and analyze the service provider's likelihood settings for oil spill alerts being mineral oil. Approximately *9400 satellite images from 2011-2018, with almost 3900 oil spill alerts*, are analyzed. To estimate the additional mineral oil discharged into the sea, 25% of the oil spill alerts are analyzed by connecting oil spill alert with the source, using historical ship tracks for Automatic Identification System (AIS) and data from the oil and gas industry. An assumption on the most likely discharged substance estimates the mineral oil impact by having detailed information on the source connected to the oil spill alerts. The result shows only a marginal increase in mineral oil (2.65%) when comparing 2013-2015 to 2016-2018, although the average number of oil spill alerts had increased by 154%. The increase in oil spill alerts is analyzed by comparing Sentinel-1A/B to Radarsat-2 using nonparametric tests on oil slick size. The results show statistically significant differences in performance between Sentinel-1A/B and Radarsat-2 on small-size oil spills. Hotspot analysis shows significant spatial clustering in oil spill alerts that overlap with offshore industry areas, fishing activities areas, and major shipping lanes. By contrast, clusters comprised of small size oil spills mainly overlap with offshore industry areas. Finally, service provider likelihood settings for flagging an alert as mineral oil is analyzed using *in situ* data. The results show that confidence settings are inaccurate and therefore unsuitable for operational applications without additional information. This thesis shows a need for further research regarding mineral oil and oil spill lookalikes. The thesis also concludes that service providers should further develop the use of ancillary source data to improve decision-making for end-users.

Content

Keywords
Radar satellites, Oil spill, Alert service, End-user, Service provider, High-resolution images. Impact, Small size oil spills.

List of abbreviations and Acronyms

AIS	Automatic Identification System (Ship Tracing).
CSN	CleanSeaNet, EMSA's satellite Service name.
EEZ	Exclusive Economic Zone.
EMSA	European Maritime Safety Agency (Service provider).
ESA	European Space Agency.
IMO	International Maritime Organization.
KSAT	Kongsberg Satellite Servises (Service provider).
LRIT	Long Range Tracking and Identification (Ship Tracing).
MARPOL	The International Convention for the Prevention of Pollution from Ships.
MET	Meteorological data.
NCA	Norwegian Coastal Administration, Kystverket (Norwegian name).
RIG	Source class for this study, connected to the oil and gas industry/offshore industry.
SHIP	Source class for this study connected to shipping.
VMS	Vessel monitoring System (Fishing vessel Tracing).
UNK	Source class for this study, for observations that are not connected to SHIP or RIG.
WEB GUI	Service provider's web-based graphical interface offered to the end-user organizations on the alert services, to include an operational geographical interface and search possibilities to archive.

Tables

Figures

1 Introduction

In Norway, mineral oil spill monitoring is used for early warning to the national authority to enforce appropriate remedial actions (NCA, 2021). These remedial actions are enforced to support two main objectives. The first objective is to assess the environmental impact and, if necessary, take action to reduce possible damage. This applies to both small and large oil spills (oil spill accidents). The second objective is to support legal prosecution by the national authority, based on both national and international law on oil pollution in the marine environment. Furthermore, monitoring is also a source of information on the state of our sea areas. The use of monitoring and efficiency in legal prosecution act as deterrents, hopefully contributing to fewer oil spills and fewer adverse effects to the environment.

Specially equipped monitoring aircraft and radar satellites do this monitoring of oil spills at sea in Norway. This monitoring has been conducted in Norwegian waters since the early 1980s by pollution authorities(AirHistory.net, 2018, NCA, 2021) and since 2003 by The Norwegian Coastal Administration (NCA) as the governmental authority on acute pollution. The introduction of radar satellites to the oil spill monitoring was mainly based on cost efficiency and more efficient use of monitoring aircraft. Polar-orbiting satellites have good coverage/revisit times over Norwegian waters as they are situated far north. Satellite images also cover a large area in one "snapshot," making the monitoring cost per km^2 less than monitoring aircraft. Radar satellites have been an integrated part of oil spill monitoring in Norwegian waters since 1996(FFI, 2003). The benefit of using radar is mainly monitoring oil spills during darkness, cloudy and foggy conditions.

Today, Norway uses two radar satellite monitoring services from two different service providers. These are near real-time oil spill alert services, providing NCA end-users with "possible oil spill" alerts. The service is near real-time, as the time elapsed from image acquisition to the end-user receiving the result of an analysis is typically 20 - 40 minutes depending on the size (area covered) and complexity of the radar image(EMSA, 2013b, KSAT, 2021). Detection of oil at the sea surface by radar has also known limitations. For example, wind influences the result with limitations for discriminating between natural phenomena and different oil types(Espedal, 1999). By this limitation, the oil spill alerts states "possible oil spill." The service providers account for this by applying measures/rules when analyzing the radar images and stating a likelihood for a "possible oil spill alert"/observation being mineral oil or not(EMSA, 2010, KSAT, 2021). The limitation in detecting mineral oil with radar also applies to the radar on NCA remote sensing aircraft. However, assessing mineral oil spills, other oils, or natural phenomena can be categorized more reliably using additional sensors and visual assessment by trained system operators in remote sensing aircraft. NCA data from the monitoring aircraft is the most reliable source for assessing and classifying substances at sea(NCA, 2021).

Despite the service provider applying likelihood measures, the oil spill services give false mineral oil alerts for satellite monitoring. The end-user/decision maker's level has to account for this uncertainty. The end user's follow-up of a possible oil spill alert includes making time-critical decisions on what type of action/verification is needed. An *in situ* verification of the oil spill alert can be needed to account for the uncertainty. As the observations are often far out at sea, verification/assessment using ships, platform personnel (if the alert is in an oil and gas platform area), or NCA

remote sensing aircraft comes with a substantial financial cost. When enforcing appropriate remedial actions, this cost has to be considered, together with environmental and legal factors. Today, this is done by NCA, considering each "spill alert" concerning observation size, potential environmental impact, and if the "spill alert" can be connected to a possible source. The connection to a possible source is essential for two reasons. The first reason is that a connection between spill alert and a possible source will "red flag" the observation as more likely to be mineral oil, hence having a negative environmental impact. The second reason is the legal aspect, where one needs to identify a potential culprit for an investigation to be prosecuted by national and international legislation on discharges at sea.

The pollution authorities acquired one to two radar satellite images per week in the early operational years of the oil spill alert service. However, there was a large increase in the use of radar satellite imagery in 2004 when the Norwegian Space Centre signed a contract with Canada's Radarsat on behalf of all governmental users, reducing the price per area/image for the end-user (Norwegian_Space_Agency, 2021). In addition, the European Maritime Safety Agency (EMSA) introduced an alert service in 2007 to all member states in Europe, free of charge for the end-user (EMSA, 2010, EMSA, 2013b). Together, these services have given three to four radar satellite images per day for the last ten years, covering 200 000 km2 to 400 000 km2 of Norwegian waters daily(NCA, 2016a). In the last two decades, satellite oil spill alert services have developed from serving only a few countries to more or less all European coastal states. The use of radar satellites has become a natural part of oil spill monitoring. The quality of the service delivered to the end-user is of the highest importance to use such a service efficiently.

1.1 Rationale

An overall decreasing trend in the number of mineral oil spills detected by the Norwegian surveillance aircraft is found when examining the last two decades(Bonn_Agreement, 2018a). This trend is also supported by other nations' surveillance aircraft findings in the North Sea basin, where the overall trend shows a decreasing number of oil spills found per flight hour of monitoring (Bonn_Agreement, 2018a).

On the contrary, examining the results of radar satellite monitoring, there has been a steep increase in the number of possible oil spill alerts from 2015 to 2018(NCA, 2016a, NCA, 2017b, NCA, 2018b). The increase is approximately 250% in the number of oil spill alerts reported in Norwegian waters in this period. This shift and rather steep increase are highly surprising and unexpected for the NCA. This trend is also registered internationally. The European Commission (EC) states this increase in oil spill alerts as a trend shift (EC, 2018).

During this period (2015-2016), two new radar satellites, the European Sentinel-1A and Sentinel-1B were introduced to the services, parallel with other radar satellites. These new satellites offer higher resolution and therefore are most likely able to detect more minor oil spills, indicating the new satellites may play a part in the large increase in the number of possible oil spill alerts. Still, this increase is not consistent with other verified surveillance data (by aircraft). There are many unanswered questions regarding the origin (activity and source) and the impact of additional oil spills.

Research rationale
Norway is now (2018) facing an average of nearly three possible spills per day from the oil spill services. This is challenging operationally, where NCA needs to prioritize what to follow up and how. For example, verifying one observation by surveillance aircraft can exceed €10 000, which is a high cost if the detected oil spill turns out to be false. Different national management plans also use oil spill surveillance data as part of the input for discussing the state of our seas, pollution trends, and preparedness at a governmental/ national level. This new surprising shift in trends needs to be verified and explained when data are used in these types of assessments and policy-making. Service providers will also benefit from further knowledge of the product they deliver, thereby enabling further service improvement for end users' needs.

There is a need to verify if the increase of oil spill alerts is due to Sentinel-1A and Sentinel-1B(NCA, 2017b).

There is also a need to know the increase in oil spill alerts in terms of substance. In-depth knowledge on why there is an increase and what the added "spills" mean, in terms of source origin, spatial distribution, substance, and impact are of high importance.

Finally, as the service providers use a likelihood setting on each oil spill alert being mineral oil, the fit of this likelihood setting should be further explored. It is essential for the end-user that this likelihood setting adds confidence to the alert used for decision-making.

As the 250% increase only account for the number of oil spill alerts and the satellite monitoring is not uniform in time and space (cover), there is a need to account for this when comparing oil spill alert trends over time. Results from this will be used as a reference for confirming the problem, its magnitude and for discussing other results.

The knowledge and results from such a study are beneficial for the Norwegian end-user NCA and other European end-users, using the same service with the same satellites and service providers.

In sum, the NCA faces a knowledge gap on ***what, where,*** and ***why*** there is a major increase in possible oil spill alerts(NCA, 2017b).

1.2 Overall Aim, Objectives, and hypothesis

The overall aim of this thesis is to determine whether the increase in oil spill alerts can be attributed to Sentinel-1A and 1B, investigate trends, and assess whether there has been any change in mineral oil discharges in Norwegian waters associated with this increase. The specific objectives are:

1. To determine if the increase in oil spill alerts in Norwegian waters is due to the use of Sentinel-1 from 2015-2018.
2. To quantify oil spill type, size, and variability.
3. To validate/verify the service provider's likelihood settings with historical observations.

My hypothesis is:

H_0: The increase in alerts is not due to increased “mineral oil” at sea.

H_1: The increase in alerts is due to increased “mineral oil” at sea.

2 Background

This chapter will shortly present how the oil spill service works, the type of technology used, and the influences and limitations to consider within the study and study area. As the operational services aim to provide mineral oil spill alerts to the end-user, there is a short presentation on the sources of mineral oil within the Norwegian area. The sources must be capable of creating a visible and large enough oil cover on the sea surface to be detected by radar satellites. As radar satellites also have limitations for detecting and establishing mineral oil spills, the rest of this chapter will focus on climate factors as well as those factors that generate signatures that can look like mineral oil spills

2.1 Oil spill satellite service

Norway has used operational oil spill services since 1996 (FFI, 2003). Briefly, the end-user organization decides which area they want to monitor and how often. The service provider undertakes the acquisition of satellite images from the satellite owner, processes/downloads the radar images, and performs the oil spill analysis. The time from the image capture to the oil spill alert report received by the end-user is typically 20-40 minutes and is considered a ”near real-time” oil spill alert service(EMSA, 2013b, KSAT, 2021).

The product delivered from the service provider to the end-user is an alert call (if ordered) and a pdf report of the alert, including metadata on the reported spill and the surroundings. The report also shows the radar observation (oil spill) at a suitable scale. A representation of the observation/alert is also available as a polygon or a multipolygon (multiple “oil slicks” assumed from the same origin/source). Several polygons can represent the alert if the service provider analyses a fragmented/discontinuous “oil slick” probably originating from the same spill/source. The alert polygon/polygons also include important attribute data, with id, timestamp, confidence classification, size of the observation, and others (Figure 1).

Norway has used the national service provided by KSAT(KSAT, 2019) since 1996 and EMSA CSN(CleanSeaNet) Service (CleanSeaNet, 2019) since 2007. KSAT is also one of several service providers used in the EMSA CSN service. *The radar image analysis operator decides if the oil spill alert is a confidence A (more likely a mineral oil spill) or confidence B (less likely to be a mineral oil spill). Both, EMSA CSN service and the KSAT service set an observation to a confidence B alert when the probability of the observation of being mineral oil (oil spill) is less than 50%. If the oil spill alert is set to confidence A the probability of the observation being mineral oil (oil spill) is more than 50%.*
Both services also apply a possible source connected to an oil spill alert based upon a set of ancillary source data. In addition, the NCA (Norwegian Coastal Administration), as the end-user, also analyzes the observation in a GIS regarding a possible source connection. As NCA has more ancillary data on possible sources than the service provider, all no source connected oil spill alerts are analyzed on possible source connections. The findings from this analysis are the basis of what kind of follow-up is applied to the alert (Figure 1). Since 2018, NCA has implemented rules regarding the possible oil spill alerts. The service provider will sort the alert into “Green alert” or a “Red alert.” This alert setting is based upon an algorithm, taking distance to a source, observation size, confidence A/B, and if an observation is inside or outside a specially defined area that NCA has established as of high interest. Such

areas originate either from an activity perspective or an environmental vulnerability assessment. A green alert has a random follow-up, whereas a red alert will have a follow-up from NCA. The content of this alert algorithm is considered classified information from NCA and is not accessible for more details.

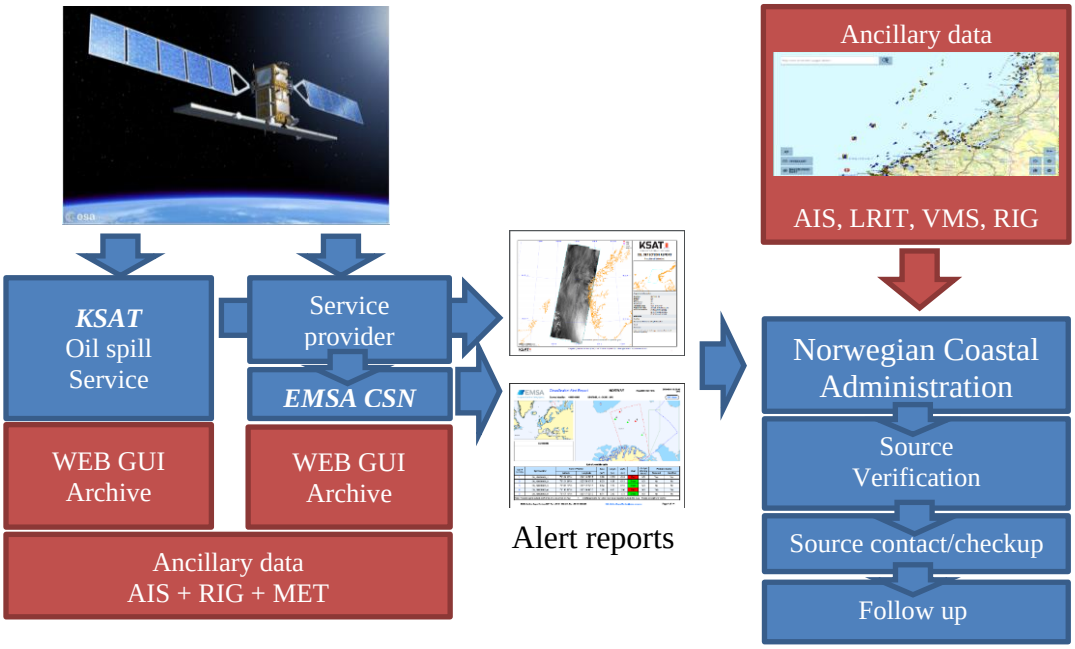

Figure 1: Flowchart of the two Radar Satellite services used in Norway. Starting at the top left, the two services, KSAT, and EMSA CSN (CleanSeaNet), use imagery from radar satellites. The illustration shows Sentinel1 (ESA, 2019c). KSAT order and download raw data directly, and for EMSA CSN, an additional service provider is used for this. The service provider analyzing the radar image both deliver a possible oil spill alert with a likelihood setting of the alert being mineral oil., A report of all observations in the satellite image, the observations(possible oil spill) can be downloaded as polygons with a set of attribute data from the alert report. NCA uses ancillary data to connect oil spill alert to likely source (NCA, 2018a). If no possible oil spills are detected in a radar image, a clean sea report is sent by mail, showing the area of the image and some basic metadata.

2.2 The use of radar satellites in oil spill alert services

Radar satellites can detect and distinguish areas of possible oil spills, characterized by smooth surface areas compared to their surroundings. The surface roughness will influence the backscatter being sensed by the radar(Fingas, 2016). The oil will flatten small surface waves formed by the wind on the surface (Bern et al., 1993, Fingas and Brown, 1997). A darker signature from an area with oil (less/no backscatter) in comparison to lighter signature surroundings (stronger backscatter) can be a candidate for a possible oil spill (Figure 2). The observation signature, shape, wind conditions, surrounding areas are all data used when analyzing the likelihood of a darker signature being a possible mineral oil spill. As the radar measures the backscatter from the sea surface, other natural phenomena that influence the sea surface characteristics create “oil spill lookalike” signatures (Espedal, 1999, Gade et al., 1998). Radar satellites used in an oil spill service and false “mineral oil” alerts are some of the significant challenges for the end-user (Alpers et al., 2017). Another limitation of the radar satellites used in the operational services is in estimating oil thickness (Fingas, 2018). The modes used in the operational services do not offer any oil thickness estimation today.

When looking at the established services offered in Europe, the radar satellite analysis and classification are done manually by a radar operator or semi-automatically (with

the help of algorithms finding spill candidates). Different service providers have used different approaches classifying the possible “oil spills” and their likelihood of being mineral oil (Ferraro et al., 2010). The use of other ancillary data for a possible “oil spill” alert might help the end-user to establish the right level and means for a follow-up (Ferraro et al., 2010).

2.3 Satellites used in the study

The satellites and their characteristics used in the Norwegian services from 2011 are listed in Table 1. Envisat (ESA, 2019b) and Radarsat-1(CSA, 2019a) were used on a large scale in oil spill services until 2012, but when both failed in 2012, there was a gap in multi-satellite coverage for the next couple of years. Radarsat-2 (CSA, 2019b), only supported by some images from Cosmo SkyMed (ESA, 2019a), was the primary satellite over the services in this period. The two TerraSAR satellites have been used since 2016 (ESA, 2019d, ESA, 2019e), but in smaller quantities. Sentinel-1A was introduced into the service on a large scale in late 2015 and Sentinel-1B in 2016.

Little has been found in the literature comparing studies for the three satellites (Sentinel-1 A and 1B and Radarsat-2) used for oil spill monitoring. Some studies compare these satellites’ performance on ship detection, where Sentinel1 satellites show better performance due to higher resolution (Pelich et al., 2015). There is also a study on ice sheet velocity mapping where the satellites are compared, but in another mode and resolution than operationally used for oil spill detection. Therefore, it is difficult to draw parallels to oil spill services (Mouginot et al., 2017).

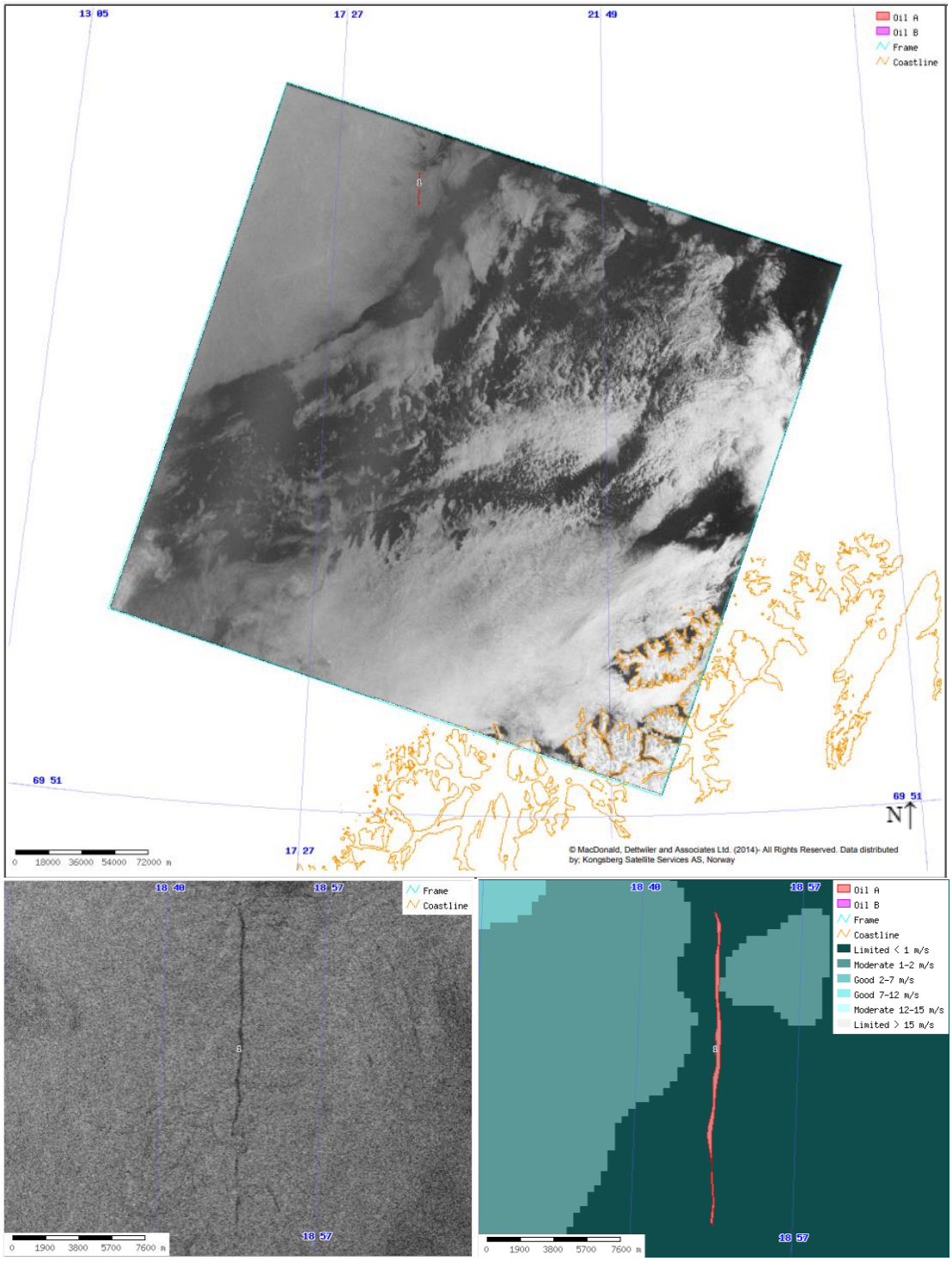

Figure 2: Example of an oil spill alert report. The image shows a linear oil spill, where the vessel was connected to the observation and admitted an accidental spillage of 40 liters of hydraulic oil into the sea. The picture shoved is from a KSAT report delivered to NCA (KSAT, 2014). © MacDonald, Dettwiler and Associates Ltd. (2014)- All Rights Reserved. Data distributed by; Kongsberg Satellite Services AS, Norway

Table 1: The different radar satellites used in the Norwegian services since 2011. The three most used satellites are Sentinel-1A and 1B and Radarsat-2, where they have delivered 97 % of the total observations from 2011 until 2018.

Satellite	Instrument	Typical Mode used (Oil spill)	Resolution (m)	Cover(Km)	Percent of total number of observations	Status
Envisat	C band Radar (SAR)	Wide swath	150x150	400	0.9	Ended mission 2012
Sentinel-1A	C band Radar (SAR)	Interferometric Wide Swath	5x20	250	34.2	In operation
Sentinel-1B	C band Radar (SAR)	Interferometric Wide Swath	5x20	250	22.6	In operation
Radarsat-1	C band Radar (SAR)	ScanSAR Narrow/Wide	50x50/100x100	300/500	0.5	Ended mission 2012
Radarsat-2	C band Radar (SAR)	ScanSAR Narrow/Wide	50x50/100x100	300/500	40.2	In operation
COSMO-SkyMed1	X band Radar (SAR)	HugeRegion	100x100	200	0.03	In operation
COSMO-SkyMed2	X band Radar (SAR)	HugeRegion	100x100	200	0.06	In operation
COSMO-SkyMed4	X band Radar (SAR)	HugeRegion	100x100	200	0.08	In operation
TerraSAR TSX-1	X band Radar (SAR)	ScanSAR mode	16x16	287	0.5	In operation
TerraSAR TDX-1	X band Radar (SAR)	ScanSAR mode	16x16	287	0.6	In operation

2.4 Satellite monitoring area and influences acting on the oil spill alert analysis

The area covered and frequency of the oil spill service in Norwegian waters is based on the accessibility of images within a department budget used on monitoring. Both area (Figure 3) and monitoring frequency have changed over the years (Figure 4). Additionally, flights by remote sensing aircraft collect data over the area as part of the planning of satellite monitoring cover. These flights fill in the gaps in satellite monitoring cover (Figure 4).

As discussed in section 2.2, several influences need to be considered when analyzing and using radar satellites to monitor oil spills. The monitoring is aimed at shipping along the coast and other hotspots of shipping activities, offshore oil and gas industry, and particular environmentally sensitive areas. This prioritization results in non-uniform monitoring of the area in Figure 3.

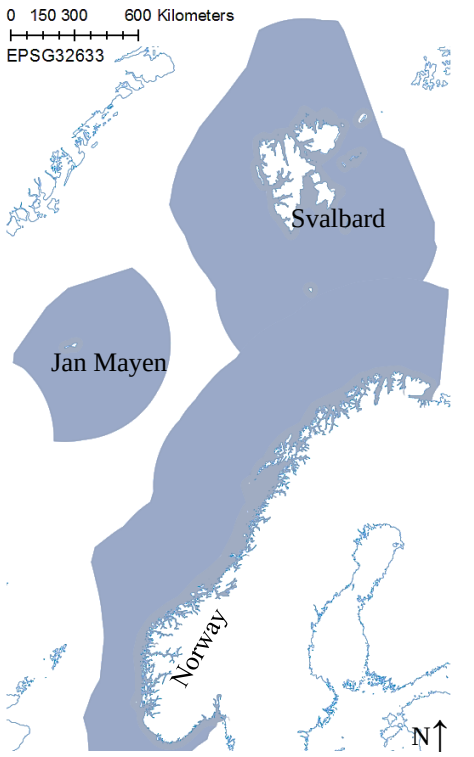

Figure 3: Map of Norwegian EEZ, and the Fishery protection zones. Area of interest with EEZ, and the Fishery protection zones around Svalbard and Jan Mayen. The area is approximately 2 million km^2, and includes both temperate and arctic climate.

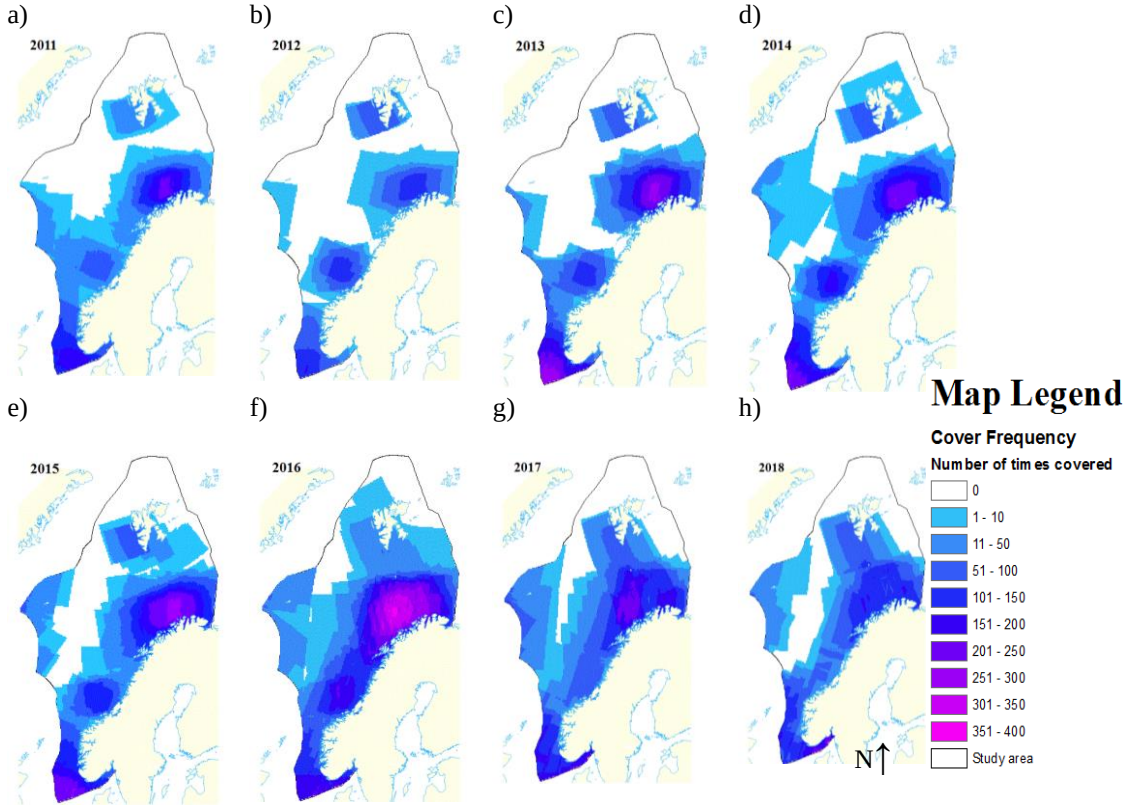

Figure 4: Satellite monitoring frequency per year. Maps for the years, (a) 2011, (b) 2012, (c) 2013, (d) 2014, (e) 2015, (f) 2016, (g) 2017, (h) 2018. The satellite images' footprints in this thesis have been analyzed for a 10x10 km raster frequency map. The footprint of 9442 satellite images is included for all the years.

2.4.1 Sources of mineral oil discharges in Norwegian waters

Shipping and the offshore industry are the two primary sources of mineral oil discharged to visible oil slicks on the sea surface in Norwegian waters. Other sources might be land-based oil spills, oil leakage from shipwrecks, and natural mineral oil seepage.

2.4.1.1 *Ship as source*

Visible mineral oil slicks on the sea surface from ships are considered illegal. Under certain strict conditions, a 15 ppm maximum mineral oil discharge is allowed from certain ship types (IMO, 2019). Trials have shown that a 15 ppm and below discharge of oil will not be visible on the sea surface (Carpenter, 2018). Figure 5 shows the magnitude of shipping activity within the Norwegian EEZ and the Fishery protection zone around Svalbard and Jan Mayen. The figure also shows the different ship categories and the overall increasing trend in operation hours for all ship categories from 2014- 2018.

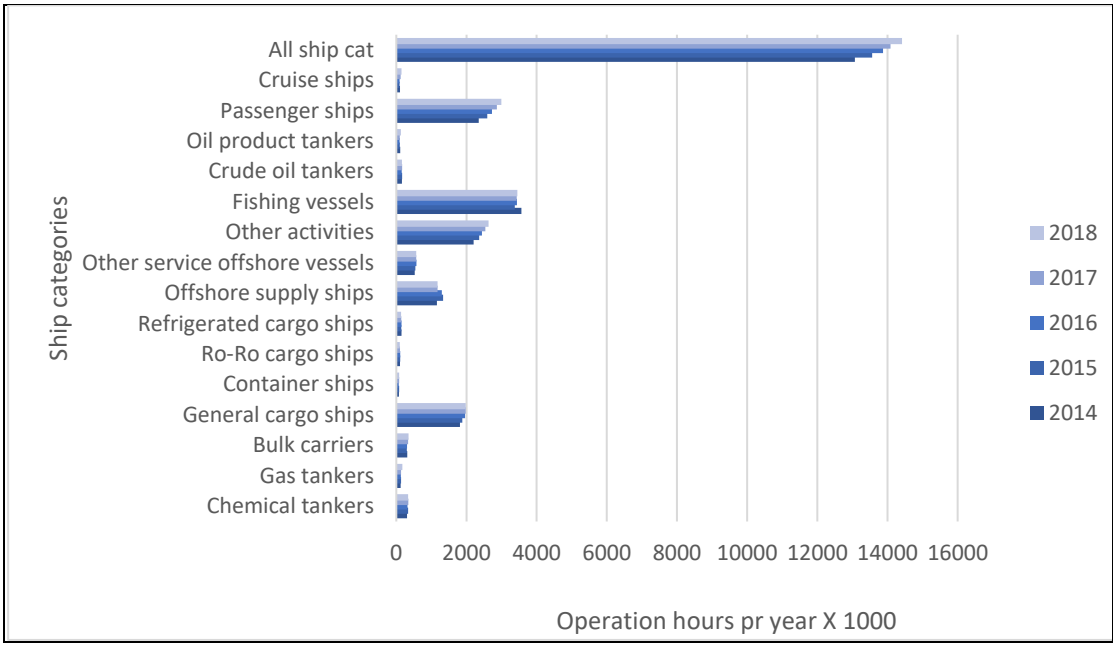

Figure 5: Ship traffic within the study area. The activity is shown in thousands of hours of operation. The all ship category is shown on top, with a 10.3% increase from 2014 until 2018. Fishing has the most operation hours with approximately 3500 000 work hours/year, data extracted from NCA Havbase: www.havbase.no (2019 ship categories).

2.4.1.2 *Oil and Gas industry offshore as source*

Mineral oil from the oil and gas industry in Norwegian waters can be discharged up to a monthly average of 30 mg of oil per liter of water (OSPAR, 2020). This mineral oil discharge will often give a visible oil slick on the sea surface, especially with calm winds(Morandin and O'Hara, 2016). Many of the oil-producing platforms in Norwegian waters discharge produced water into the sea.

2.4.1.3 *Shipwrecks as source*

Shipwrecks are a possible source of mineral oil pollution. A register of shipwrecks containing ships built after 1914 is available in a national shipwreck database at NCA (Idaas, 1995). Twelve wrecks, shortlisted as high risk for oil discharge, were listed in 2019. NCA conducts regular follow-up on these wrecks, using remote sensing and visual inspection by surveillance aircraft(NCA, 2016b).

2.4.1.4 *Natural seepage as a source*

Seepage of hydrocarbons from oil and gas reservoirs (natural leakage from the seabed) is present within Norwegian waters (Hovland, 1990, Hovland, 1992, Roy et al., 2016). However, there have been no areas registered by NCA monitoring, with seepage quantities large enough to produce mineral oil slicks, persistent over time, and detectable either visually or by radar.

2.4.2 Oil spills "lookalikes."

The discrimination between "oil spill lookalikes" and mineral oil is maybe the single most challenging aspect for both service providers and end-users. Much of the research done over the last 30 years on using radar satellites as a tool for reporting oil spills deals with this topic (Alpers et al., 2017, Bern et al., 1993, Brekke et al., 2014, Espedal, 1999, Fingas and Brown, 2018, Gade et al., 1998). *Biological activity in the*

water, like algal blooms and upwelling, influences a radar satellite image by detecting these phenomena as darker features than the surroundings, resulting in a possible "oil spill alert." It is also essential to keep in mind that there is a distinct seasonality to the distribution of phytoplankton and zooplankton throughout the year (Richardson, 1989).

2.4.3 Other oil types, non-mineral oils

Vegetable or animal oils are discharged by ships into the sea, both legally and illegally. The International Maritime Organization (IMO) and the international marine pollution regulations for ships (MARPOL) regulate the discharge of Noxious Liquid Substances. MARPOL Annex II covers the discharge of Noxious Liquid Substances, and MARPOL Annex V covers garbage pollution. These regulations include legal disposal/discharges from some category ships (IMO, 2020), resulting in a possible oil spill alert on a radar image under certain weather conditions. These oil types behave in many cases like mineral oil on the sea surface, and it is challenging to separate these slicks from mineral oil slicks by the radars used (Alpers et al., 2017, Bonn_Agreement, 2011, Skrunes et al., 2012).

2.4.4 Weathering of oil

The weathering of oil can, in some cases, be seen in a satellite image. The weathering of oil on the sea surface depends on the chemical composition of the oil and environmental influences like temperature and winds, and waves (Fingas, 2016). These factors influence how long a mineral oil spill will be visible on the sea surface before evaporating or dissolving into the water column. Weathering of oil is something one has to consider as an end-user. For example, when a satellite image gives an oil spill alert, the oil spill might be ongoing or be 5 -15 hours old. Oil type, oil amount, and climate factors influencing the oil are essential factors when linking a possible oil spill and a possible source. The likely "lifespan" of visible oil on the sea surface, the movement of the oil carried by current and wind, and a possible source moving have to be accounted for when connecting a link between a source and an oil spill alert.

2.4.5 Ship-based discharge of waste products

There are three main types of oily waste produced on a ship: *oily bilge water, oil residue, also called sludge, and cargo residue from carrying oil products*. Even though there is a considerable variation from ship to ship, the content of the bilge oil is considered to be "lighter and thinner" than sludge oil. The oily bilge water is a mixture of different oils from maintaining in machinery spaces and leakages from machinery. It also contains some detergents and solvents used in these spaces. Regarding washing cargo tanks residues and discharges of oily water, the physical properties, and chemicals of the oil depend on the cargo oil that is being washed (EMSA, 2013a). The physical and chemical properties of the oil decide how resistant the oil is to the weathering process when discharged into the sea (Fingas, 2016).

2.4.6 Sea surface current

The movement of oil is vital to consider when connecting a link between an oil spill observation and a potential source using satellite images, as they both might have moved since the time and place of the discharge. Oil on the sea surface will follow the sea surface current influenced by the wind. One rule of thumb is the 3% wind

influence rule (Fingas, 2016). This means, for example, that a10 m/s wind speed will create a force of 0.3 m/s with its direction calculated against the sea current speed and direction. Then if the current also has a velocity of 0.3 m/s, the oil trajectory (direction and speed) will result in a movement at a maximum velocity of 0.6 m/s (if both the current and wind has the same direction) or 0 m/s (if the current and wind directions are opposite another). The current within different parts of the study area varies a lot in velocity with the time of year, measured from 0.05 m/s to 0.6 m/s within the Norwegian continental shelf (Haugan et al., 1991). Sea surface currents on the west side of Spitsbergen have a maximum velocity of 0.024-0.035 m/s (Gyory et al., 2013).

2.4.7 Climate as an influencing factor

Some climate factors, like wind, do influence how oil on the sea surface is detected by radar satellites. Low temperature, the formation of sea ice, and sea ice, in general, can complicate the radar image. These influences might contribute to false alerts, as "oil spill lookalikes" (Brekke et al., 2014).

2.4.7.1 *Wind/Sea state*

Wind influences the radar satellites' capability to detect mineral oil on the sea surface. Both a low wind limitation and a high wind limitation influence the sea state and the backscatter detected by the radar (Alpers et al., 2017, Bern et al., 1993, Fingas and Brown, 2011). Wind criteria are also part of the confidence setting of class A or confidence B, where either low wind or high wind will lower the confidence settings (Ferraro et al., 2010). The mean wind velocity within the study area varies from high winds in the winter and low in the summer (Figure 6).

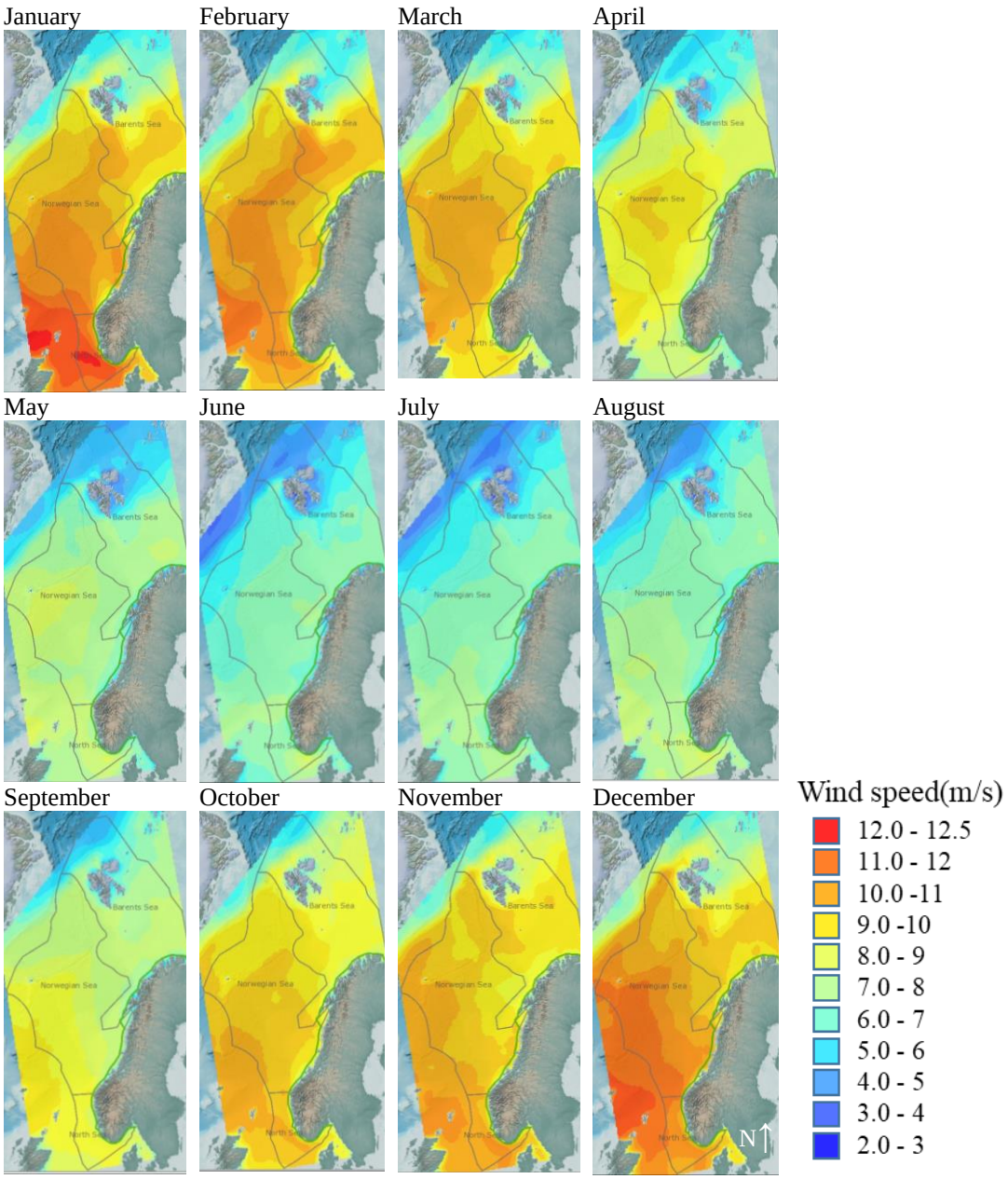

Figure 6: Wind Model data/hind cast (NORA 10) for mean wind speed 10 years. (1.1.2007 – 31.12.2016). (. The three areas showed in the maps, is marine action plan areas in Norway. The figure has been extracted from the oil spill response viability tool used in the Norwegian Coastal Administration, where month by month, average met data on wind, waves, ice condition, horizontal visibility, is used to model the efficiency of different oil spill combat strategies (Dahlslett et al., 2018). Source DNV: Oil Spill Response Viability Analysis Model, (DNV-GL, 2018).

2.4.7.2 *Sea Ice*

The interpretation of radar satellite images for oil on the water surface is very demanding, and the discrimination of the signature between oil and new/young ice is difficult (Brekke et al., 2014). The Norwegian Coastal Administration experienced this in the outer Oslo fjord in February 2011, in connection with the grounding of a ship and its associated mineral oil spillage. Satellite images were used as part of the ongoing monitoring of the oil spill tracking. However, it did not prove easy due to the complexity of the sea state, where oil and different forms of sea ice influenced the

signatures in the radar images (DLR, 2011) (Figure 7). Both solid sea ice and drift ice is present within the study area, varying by season. The sea ice is present on the north, east, and south-side of Svalbard (Vaughan et al., 2013).

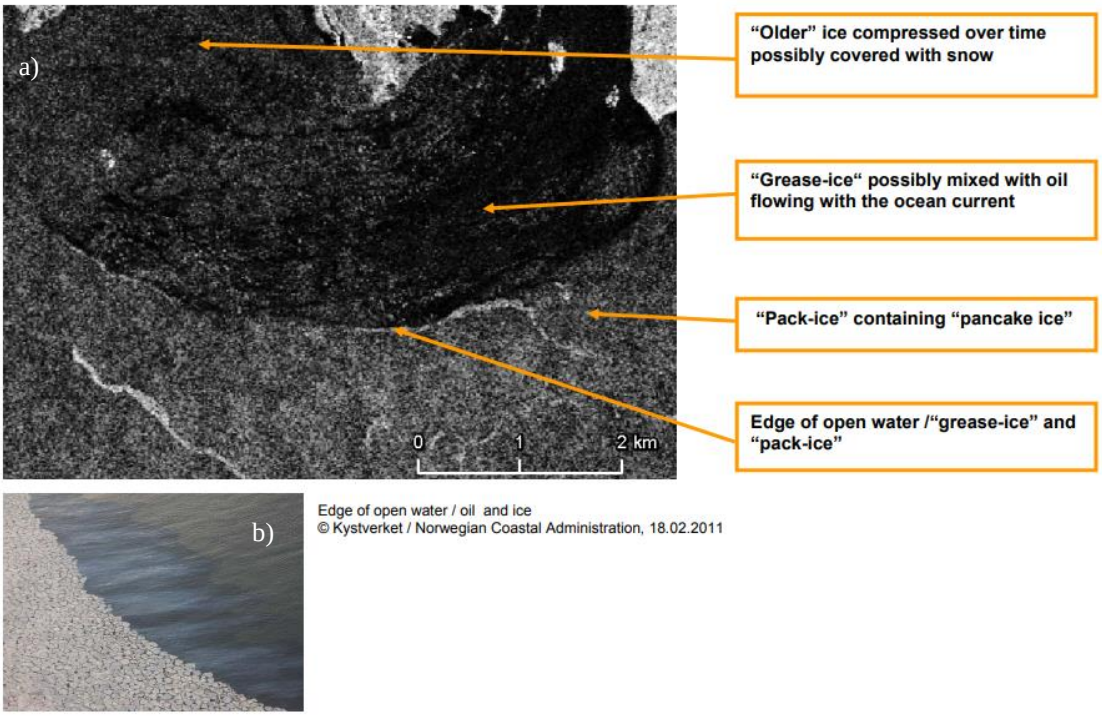

Figure 7: Example of ice conditions in the area of a mineral oil spill in 2011. (a) Radarsat-2 image. Ancillary remote sensing and in situ data have been used to overlay the ice conditions to the radar image. (b) Photograph from NCA remote sensing aircraft showing the edge from open water to oil, and the ice, ice/oil (DLR, 2011): ***©DLR****.*

3 Study Area, Data and Methods

To be able to address the overall aim of this study, three specific objectives have been established (see Section 1.2). These three specific objectives are all grounded in each potential oil spill alert. The dataset holds 3694 oil spill alert observations. *These data are not the satellite images themselves but geographical objects and attribute data derived from the radar images by an oil spill alert service provider.* These geographical objects are the primary input to the analyses, and the dataset content is essential for answering the specific objectives. There is also a need for high-quality ancillary data to meet these objectives.

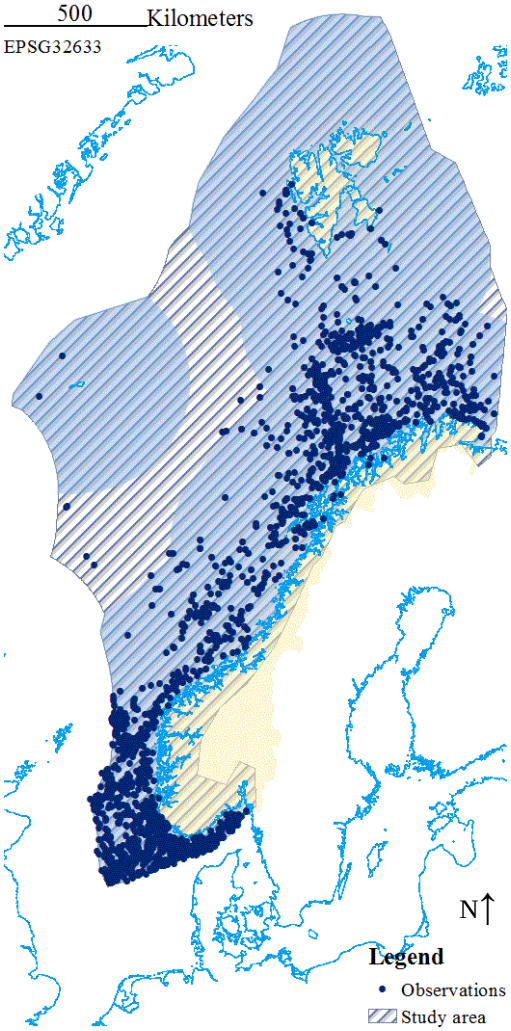

Figure 8: Map of the study area and all observations used in the study. The light ocean areas are international waters included in the study. The study area is generalized for the coast areas and cover some land areas as part of this generalization as there it is a lot of fjords and small islands included in territorial waters.

Study Area

The study area includes international waters between mainland Norway and Jan Mayen, including all three marine management areas of Norway (NEA, 2019) (Figure 8). Territorial waters (12 nautical miles) are also included in the study area. The study area falls within the monitoring area discussed in section 2.4, and it consists of an approximately 2.4 million km^2 sea area. The area is characterized by a temperate (mainland coastal), cool and polar climate (Peel et al., 2007). The marine ecosystem is rich in both marine flora and fauna, including cold-water corals, large populations of fish, seabirds, and marine mammals (Ministry_of_Climate_and_Environment, 2020, Norwegian_Government, 2015)

3.1 Data collection and format

There is a need to analyze available data to establish a suitable time series to meet objectives and produce a common ground for discussion. A time series of oil spill alerts from 2011-2018 is used for this study. Within this time series, Radarsat-2 has been used all of the years, and Sentinel-1 is used in parallel from 2015 to 2018. Also, the oil spill alert data have a good set of attributes to cover the three objectives. Spill size can be obtained for all oil spill alerts(point dataset and polygon dataset). Likelihood settings from a service provider are available, and the time tag of all oil

spill alerts. This oil spill alert dataset is considered the primary dataset used to answer all three objectives and produce common ground for discussion.

Four different format datasets are used to obtain a complete oil spill alert dataset due to changes in databases and deliveries from the service providers during 2011-2018 (Table 1), dataset 1.0-1.1, and 2.0-2.1. These four datasets hold different vector formats (multi-polygons, polygons, points), different attributes, spatial coverage, units in attribute data. All data collected were checked and prepared for analysis. *The data were checked by importing all data into a GIS, by examining the data visually in its original format, datum, and extent, controlling basic statistics.*

The following four sections (3.1.1-3.1.4) present the data needed for analyzing a common ground for discussion and the three objectives. The last section (3.1.5) presents how the data is prepared and standardized.

Table 2: Data used in the analysis. Each dataset has been numbered, named, and is referenced by this in the text, the method flow chart, and the data tables

Dataset	Format	File/data Size Approx.	Objects Approx.	Resolution / Scale	Temporal resolution	Extent	Data owner
1.0 KSAT Alert Polygons 2011-2015	GML Database – Multi polygon – EPSG 4326	25MB	690	Polygons based on 5mx20m to 150m X 150m resolution	seconds	0-100km^2 per obs	**NCA** /KSAT
1.1 KSAT Alert Polygons 2015-2018	Single Shape files – Multi-polygon - EPSG 4326	15MB	1380	Polygons based on 5m X 20m to 150m X 150m resolution.	Seconds	0-100km^2 per obs	**NCA**/ KSAT
2.0 EMSA Alert Polygons 2011-2018	KMZ - Polygons EPSG 4326	<1MB	2450	Polygons based on 5mx20m to 150m X 150m resolution.	Seconds	0-100km^2 per obs	**NCA**/ EMSA
2.1 EMSA Alert Points Late 2018	CSV, x.y. EPSG 4326	<1MB	630	Polygons based on 5mx20m to 150m X 150m resolution.	Seconds		**NCA** /EMSA
1.2 KSAT Satellites scenes footprints	Excel, xy1, xy2, xy3, xy4. EPSG 4326	<1MB	4300	Estimated by 150 m for lowest resolution	Seconds	200 000-400 000 km^2	**NCA**/KSAT
2.2 EMSA Satellites scenes footprints	KML, EPSG 4326	<1MB	5200	Estimated by 150 m for lowest resolution	Seconds	200 000-400 000 km^2	**NCA**/EMSA
3.0 Study Area	Shape files	<1MB	1	1:50000	Not relevant	Norwegian waters	Norwegian Environment Agency
4.0 Ship movements 2015-2016, Havbase, AIS data	CSV files	50GB	500 x10^6 ship observations	GPS accuracy, typical 4 m +/-	Mainly 6 minutes	Norwegian waters	NCA
5.0 Offshore Installations	Shape file		200	1:000000		Not relevant	Norwegian Petroleum Directorate
6.0 Oilrig oil discharge data on four representative	Reports	Not relevant		Not relevant	Not relevant	Norwegian waters	Norske Shell, Statoil, Wintershall
7.0 Ship movement statistical data	Havbase database	Not relevant		GPS accuracy, typical 4 m	Mainly 6 minutes	Norwegian waters	NCA
8.0 Viability study	Reports/web tool	Not relevant		10x10km rasters	Months	Norwegian waters	NCA
9.0 NCA Archive Validation data	Database report	Not relevant		Not relevant	Not relevant	Norwegian waters	NCA

3.1.1 Intensity analysis of oil spill alerts

There is a need to account for the monitoring coverage when discussing the number of oil spill alerts, as the satellite images differ in the area covered. To do this, satellite image footprints, representing the actual satellite image coverage (polygons), image by image, of all satellite images used by the satellite services 2011-2018, are needed (Table 1). By having all the footprints, one can analyze the magnitude of the increase by intensity/ratio. One will also need a complete set of oil spill alert data, and dataset 1.0-1.1 and 2.0-2.1 contain this.
Available data are collected from 2 different datasets (Table 2), dataset 1.3 and 2.3. The footprint data were partly collected and partly produced (made geographical feature polygons from the excel file), and the footprint data were checked in a GIS.

3.1.2 Objective 1: To determine if the increase in alerts due to the use of sentinel1

To meet objective 1, alert data where both the Sentinel-1 satellites and Radarsat-2 satellite is available in parallel is used.
The oil spill alert data, dataset 1.0-1.1 and 2.0-2.1, the year 2015-2018 contains oil spill alerts from these instruments, and oil spill observation size (km^2) is either included in the attribute data (point features) or can be derived from the dataset (polygon features).

3.1.3 Objective 2: To quantify oil spill type, size, and variability

A time series of oil spill alert data includes data before the increase (2011-2015) in alerts are needed to meet objective 2 on variability. This, to be able to analyze the status before this increase. Dataset 1.0-1.1 and 2.0-2.1 hold these data.

To establish the oil spill type, a connection between a most likely source and the oil spill alert can also determine the most likely oil spill type. As discussed in Background section 2.4, offshore oil and gas platforms and shipping are the two main oil spill sources for mineral oil discharges. Some non-mineral oils as animal oils and vegetable oils can also connect to certain types of ships and activities. To be able to connect source and oil spill alerts, a geographical dataset with a high-resolution time tag (shipping dataset) is used on:

- Oil and gas installations.
- Ship movements within the study area, where each single ship position is recorded approximately every 6 minutes.

In addition, NCA Archived validated data on satellite oil spill alerts and confirmed oil type is used when quantifying the size of oil type from the oil and gas industry.

As discussed in Background section 2.4, data on some known influences are used to analyze possible relationships on seasonal variations on the number of oil spill alerts. For this, a dataset of:

- Oil and gas industry, mineral oil discharges, with a monthly resolution.
- Ship operation statistics,
- Wind/Sea state and ice influence, with a monthly resolution.
- The number of satellite images used, with a monthly resolution.

A short presentation on the content and format of these datasets is presented below in sub paragraph 3.1.3.1-3.1.3.6.

All data used are referenced in the flowchart in Figure 9 and Table 2.

3.1.3.1 *Havbase – Historical ship movement data for source analysis (dataset 4.0)*

Regarding ship movement, NCA manages a ship movement database named Havbase, which is used as input for different assessments. The database contains data from 2011 onward with a 6 minute (on average) temporal resolution for each ship (NCA, 2017a). The records of each ship contain the data as shown in Table 3. Statistical data on ship movements, working hours, sailed distance, and others can be produced from this database by a web interface, www.havbase.no.

Table 3: Havbase data records (Example, sorted by vessel name). The following database recording attributes are included in the CSV data.. MMSI Vessel name, Imo number is ship-specific identification data, where Date-time-UTC, lat, long is the time and position of the vessel recording (point). Lloyds-type, Nor-vessel-category, and Size group-gross-ton are general ship class categorizations according to both Lloyds and Norwegian ship categorization systems. Dist_nextpoint and sec_next-point can be used to calculate speed and is used in calculating emission footprint.

MMSI	Date-time-utc	Lat	Lon	Lloyds type	Nor-vessel-category	Size-group-gross-ton	Vessel-name	Imo-number	dist_nextpoint	sec_next-point
229767000	01.04.2015 00:04	68.95915	12.6555516666667	850	3	7	ARCTIC AURORA	9645970	1301.7633865584	371
229767000	01.04.2015 00:10	68.96674	12.6802083333333	850	3	7	ARCTIC AURORA	9645970	1354.1920913828	380
229767000	01.04.2015 00:16	68.975205	12.704455	850	3	7	ARCTIC AURORA	9645970	1385.3132012021	380

3.1.3.2 *Oil and gas surface facilities for source analysis (dataset 5.0).*

The Norwegian Petroleum Directorate does facilitate data on fixed facilities, floating production facilities, and primary facilities onshore offered as a shape file. This file is filtered for this study to only contain surface facilities in operation.

3.1.3.3 *Oil rig discharge data on four representative oilrigs (dataset 6.0)*

Oil and gas industry *in situ* data are available on the amount of oil discharged into the sea. These data are only available for the public in yearly reports for each platform and have been extracted manually. Based on the results of the source analysis, section 3.5.1, the four platforms that contribute to most oil spill alerts is chosen as a sample (Wintershall, 2017, A/S_Norske_Shell, 2017, Statoil, 2017a, Statoil, 2017b, Wintershall, 2016, A/S_Norske_Shell, 2016, Statoil, 2016a, Statoil, 2016b). The mean discharge of mineral oil per month is used as input for a regression test against the monthly number of alerts.

3.1.3.4 *Ship movement statistical data*

NCA has available AIS data on ship movements and operating hours on the different ship types. Data has been extracted from the NCA ship movement database, Havbase. The four ship categories chosen as a sample are the categories that contribute to most observations in the dataset (
Table 16). The mean operating hours per month are used.

3.1.3.5 *Viability study, the influence of wind, waves, and ice (dataset 8.0)*

The viability study and tool discussed in 2.4.7 has a parameter on the viability of applying chemical dispersant from a ship on an oil slick. This is a method of removing oil from the sea surface into the water column. The tool shows the method's efficiency (in percent) in a monthly temporal resolution and spatially on the study area's 10 x10 km grid. The efficiency measured in this tool is driven by the influence of climate factors, being wind, sea state, and ice conditions, and the result is a map showing where the method efficiency is considered "good," "challenging," and "impossible."

As the climate limitations set for applying chemical dispersant from a ship on oil spills are approximately the same as for a radar image of an oil slick, the data can be used to discuss seasonal variations.

3.1.3.6 *NCA Archive Validation data (dataset 9.0)*

NCA internal duty officer log system is used for recording all acute pollution incidents, including follow-up on oil spill alerts from the satellite services. These follow-ups do include *in situ* verification of the satellite oil spill alerts. The *in situ* data is useable for supporting assumptions and for discussing results.

3.1.4 Objective 3: To validate/verify the service provider's likelihood settings with historical observations.

Likelihood settings from the service provider are needed on all oil spill alerts to meet objective 3.

The NCA archive validation data, dataset 9.0, is used for objective 3, in addition to the oil spill alert observation dataset 1.0-1.1 and 2.0-2.1.

3.1.5 Preparing alert data and attributes

The overall uniformity decided for all datasets is shown in Table 4 and applied both for analyzing data and results.

Table 4: Datasets uniform file formats, spatial elements, attributes, and datum.

Vector data:				
Dataset	File format	datum	Geographical feature	Attributes
Alert data 1.0-1.1 and 2.0-2.1	Shape file	EPSG 3426 (WGS84) and EPSG 32633 (WGS84/UTM Zone33).	Alert as Mulitipolygon and weighed points.	See Table 5
Satellite image footprints 1.2 and 2.2	Shape file	EPSG 32633 (WGS84/UTM Zone33).	Polygon	
Study Area 3.0	Shape file	EPSG 3426 (WGS84) and EPSG 32633 (WGS84/UTM Zone33).	Polygon	
4.0 Ship movements	Shape file	EPSG 3426 (WGS84)	Points	See Table 3
5.0 Offshore Installations	Shape file	EPSG 3426 (WGS84)	Points	
Raster data				
Results Alerts 4.1	Geo TIFF.	EPSG 32633 (WGS84/UTM Zone33)	Aligned 10x10km resolution.	Number of alerts
Results Footprints 4.1	Geo TIFF.	EPSG 32633 (WGS84/UTM Zone33)	Aligned 10x10km resolution.	Number of revisits (monitoring frequency)

As described, the oil spill alert data consists of 4 different datasets, where different methods have to be applied to meet the uniformity defined for the datasets (Table 4). Each oil spill alert (polygon feature and point feature) would also need a unified set of attributes, and the attributes and format decided are shown in Table 5. Some attributes are available from the satellite provider dataset, and some, for example, the attribute source, are filled in as results after analysis. The attribute SAT_PASS is not used in this study but can be used for further studies by NCA.

Table 5: Standardization of observation datasets attributes. The standardization applies to polygons and points dataset of all observations.

Attribute Data	Standard text	Format
Name	”Unique” name	String
Satellite	S1A, S1B, S1X, RS1, RS2, TDX1, TSX1,ASA, CSKS1, CSKS2, CSKS4	String
Class	A, B	String
Source:	RIG, SHIP, UNK	String
S_C_NOR	1-13	Integer
S_C_Loyds	Lloyds Ship classes	Integer
Poll_Type	FISH_OIL, MIN_OIL, VEG/AN_OIL	String
Year	yyyy	integer
Month	01-12	integer
SAT_PASS	Time or M,E (Morning, Evening)	String
Area_Km^2		float

3.2 Methods

This section covers the methods used to answer the objectives. The method chapter is divided into sections, each linked to answering each of the objectives. An overall method flowchart and specific method flowcharts are produced according to the flow chart legend in Figure 9. The different color-codes show dataset status and objectives the methods and results support (Figure 9). Each specific method includes a more detailed flowchart and is explained in more detail under the subparagraphs, including the primary tool used.

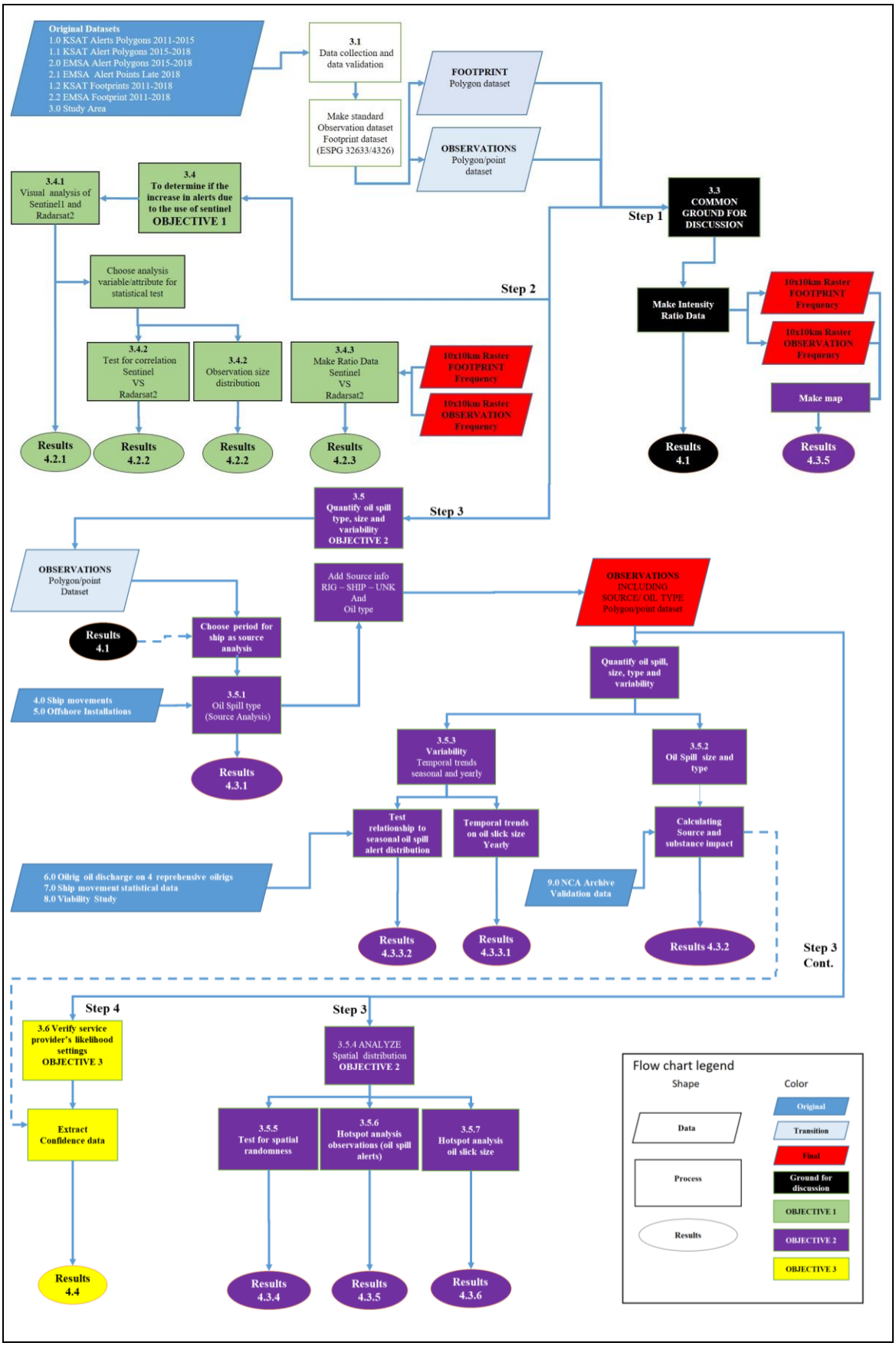

Figure 9: Flow chart of the methods. The flowchart shows how the data is collected, and a step by step method chart. It is referenced to the method chapters on the processes/analysis, and the results are referenced to the result chapter.

3.3 Intensity analysis of oil spill alerts

To support the objectives and have a common ground for discussion, there is a need to normalize the data in reference to the problem, so far just discussed as an increase in the number of oil spill alerts per year. Variations in the number of satellite images and their yearly area coverage need to be accounted for to give a more precise understanding of the increase in oil spill alerts. For this, an intensity analysis of the number of alerts per area per year is calculated, step 1in Figure 9. The intensity is calculated based on the footprints of all the satellite images used in the alert service for 2011-2018 within the fixed geographical study area (see Figure 8). *An intensity ratio states the number of possible oil spills per area observed over a given time.* The result is a ratio calculation, using the sum of all observations of cell frequency value and the sum of all footprint cells frequency number multiplied with cell size(Figure 10).

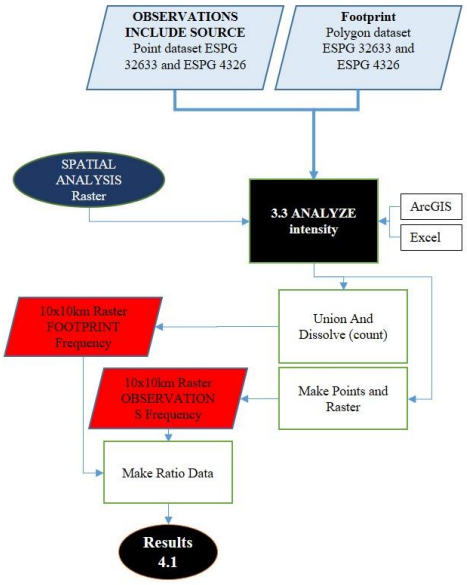

Figure 10: Method for intensity analysis of the problem. The method results in a ratio, where number of observations is compared with the number of times the area is observed yearly.

3.4 Objective 1: To determine if the increase in alerts is due to the use of Sentinel1

As discussed in section 1.1, the higher resolution sensor, Sentinel-1, might be one of the reasons for the increasing number of oil spill alert recorded. A chosen way forward is by comparing Sentinel-1 and Radarsat-2 data, where observation size, Area_Km^2 in Table 5, is available for all oil spill alerts.
Visually comparing the same oil spill in a Sentinel-1 and a Radarsat-2 image is an excellent first step and a basis for choosing if the spill area attribute can fit further testing. Oil spill area size attribute *could* then, as the next step, be used in a correlation test to check significant differences in performance between Sentinel-1 and Radarsat-2.

3.4.1 Visual analysis of Sentinel-1 and Radarsat-2 radar images

As a first step, a visual investigation of the two satellites by high-resolution radar image of the same mineral oil at the same time could add insight into the difference in performance as comparing size, shape, and noise/backscatter. The clear visual difference can help evaluate if the oil spill size variable is a sound basis for further analysis. The best opportunity to get the overlapping satellite images from Sentinel-1 and Radarsat-2 is to search on verified oil spills as far north as possible, as these are polar-orbiting satellites. The starting point was to use already available Radarsat-2 observations connected to an oil rig far north and search for Sentinel1 data from Copernicus Open Access Hub over the same area and time as the Radarsat-2 observation. When getting overlapping images, both are checked at full/high

resolution together with NCA follow-up data from the oil rig to get a verified example, where it is confirmed mineral oil at the sea surface (see Figure 11).

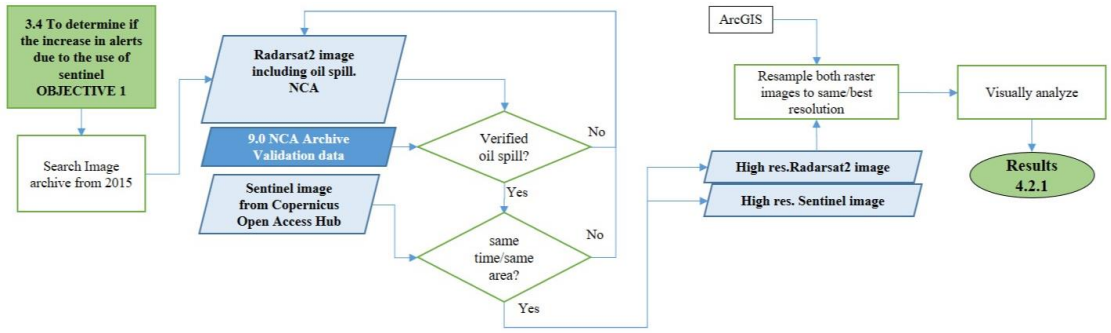

Figure 11: Visual analysis of the difference in performances between Radarsat2 and Sentinel1.

Visual analysis can confirm if oil spill size is a suitable attribute for analyzing the difference in the performance of the instruments.

3.4.2 The detection performance of the instruments

The approach is shown in the flow chart (Figure 12). The first step is to plot observation size distribution between Sentinel-1, and Radarsat-2, as shown on the right side of the flow cart. This is a frequency plot for 17 different oil spill size categories.

The non-normality test is the next step in choosing a suitable correlation test comparing the attribute chosen for analysis. The test chosen is a Shapiro-Wilk, based up on its overall performance. A comparison of four different normal tests, Shapiro-Wilk (SW) test, Kolmogorov-Smirnov (KS) test, Lilliefors (LF) test, and Anderson-Darling (AD), concludes the Shapiro-Wilk test is concluded the most powerful normality test (Razali and Wah, 2011). A non-normality test ($p>.05$), where the data can be visually inspected in the resulting histogram and normal q and q plot has been applied (Razali and Wah, 2011, Shapiro and Wilk, 1965). The next step is to choose a test of the instruments to see if they behave differently regarding oil spill alert observation size. As the same oil spill seems to give different results in detection between Sentinel-1 and Radarsat-2 regarding detected spill size (km^2), a non-parametric rank test on spill size is chosen. Some attribute data in the alert observation dataset do not separate between Sentinel-1A and 1B,

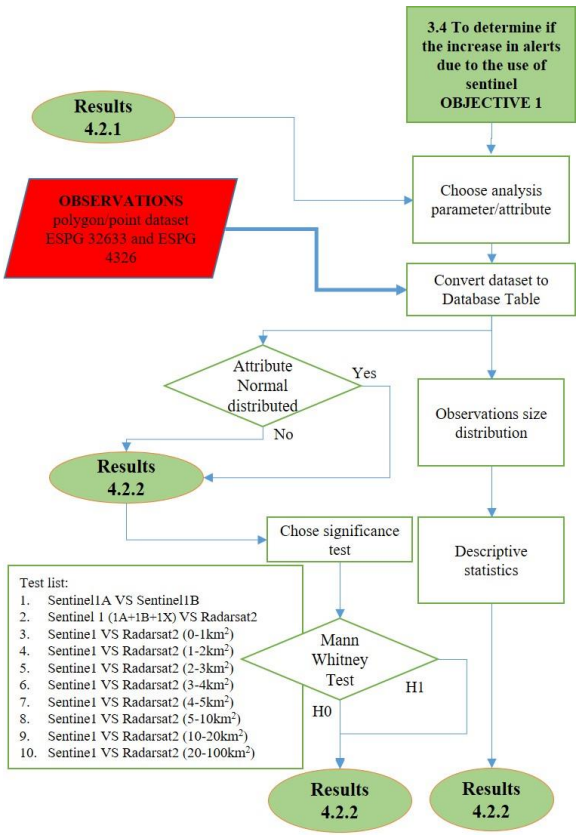

Figure 12: Method for analyzing Objective 1. To determine if the increase in alerts due to the use of Sentinel.

which is denoted as Sentinel-1X. For testing rank between Sentinel-1 and Radarsat-2, all Sentinel-1 data is merged (1A+1B +1X).

A Mann–Whitney U test is chosen as the oil spill size is not normally distributed. It is suitable as it tests two datasets simultaneously and applies for datasets different in size, i.e., number of observations (n) (Mann and Whitney, 1947, Nachar, 2008).
This is a rank test where oil spill observation size (km^2) is tested, first to see if there is a difference between Sentinel-1A and 1B, next to do the test of Sentinel-1(A+B+X) VS Radarsat-2. These two tests are shown in the test overview box in Figure 12. To further analyze observation size distribution and how Sentinel-1 differs from Radarsat-2, different spill size categories are tested using the Mann–Whitney U test. Testing one category at a time can isolate where they significantly differed from one another, test 3-10 (Figure 12).

A 95% significance Mann–Whitney U test is performed (10 tests):
Hypothesis tested:

H_0: There is no difference in satellite performance based on spill size capability
H_1: There is a difference in satellite performance based on spill size capability

3.4.3 How the oil spill per area ratio for the two instruments compare 2015-2018.

The difference between Sentinel-1 and Radarsat-2 on the number of spills per area can be derived from the two final datasets of the intensity analysis (section 3.3 and Figure 10).

3.5 Objective 2: To quantify oil spill type, size, and variability

To be able to quantify the oil spill type, there is a need to connect the oil type to the possible oil spill alerts in the dataset. To connect an oil type to an observation, one needs to connect a source to the oil spill alert.
Two years of alert data of the observations 2011-2018 dataset, 1.0-1.1 and 2.0-2.1 (Figure 9, Table 2), chosen to connect oil spill alerts and ship as a source due to the complexity and time-consuming nature of the analysis. The ship-based spills and ship-based oil types have to be estimated for all other years in the dataset.

Connecting oil rigs, being static objects, is relatively straightforward and has been done for all years in the study.

The thesis hypothesis can be tested by calculating oil type and oil spill size by having source/oil type connected to all oil spill alerts in the dataset.

The hypothesis to be tested:

H_0: The increase in alerts is not due to increased “mineral oil” at sea.
H_1: The increase in alerts is due to increased “mineral oil” at sea.

At last, in this section, both temporal and spatial analysis on oil spill type, size, and variability for oil spill alerts is conducted.

3.5.1 Oil spill origin (Source Analysis)

A mineral oil slick on the sea surface has an origin. As highlighted in section 2.4, the most likely source of any mineral oil slick on the water within the study area is from the oil and gas industry or shipping.

There is a need to connect a source to a two-year subsample of the oil spill alerts observations to meet the specific objectives 2 and 3. One part of objective 2 is to analyze if the big increase in oil spill alerts also can relate to a similar increase in mineral oil at sea. There is a need to establish this to test the hypothesis. As volume estimation of mineral oil is not possible using radar satellite images, discussed in section 2.2, the measure to answer the hypothesis will be based on the oiled area (km^2), observation size, and where the oil is most likely mineral oil.

Two years of the dataset are chosen based on the results from the intensity analysis, section 3.3, where the "big shift in intensity" (alerts/km^2 x 10^6) was registered from 2015 until 2016 (see Table 6). This includes all three of the satellites, where all observations are available as polygons. The period also has good spatial and temporal resolution regarding the source data.

The three different source categories chosen are (and in this order):

1. Category "RIG," where the most likely source is an offshore surface facility linked to the possible oil spill alert.
2. Category "SHIP," where the most likely source linked to the possible oil spill alert is a ship, also recording ship type category
3. Category "UNK," unknown is the source categorization where there is no link between an oil spill alert and a likely source.

In general, the method used is a buffer analysis, where a source and observation intersects within a set buffer distance. A more detailed flow chart shows the workflow, criteria for the analysis, and the expected result (see Figure 13). The results of this source analysis are mainly a basis for further analysis in answering objective 2 and 3. However, findings on how the different sources contribute to the oil spill alerts are presented in the results chapter.

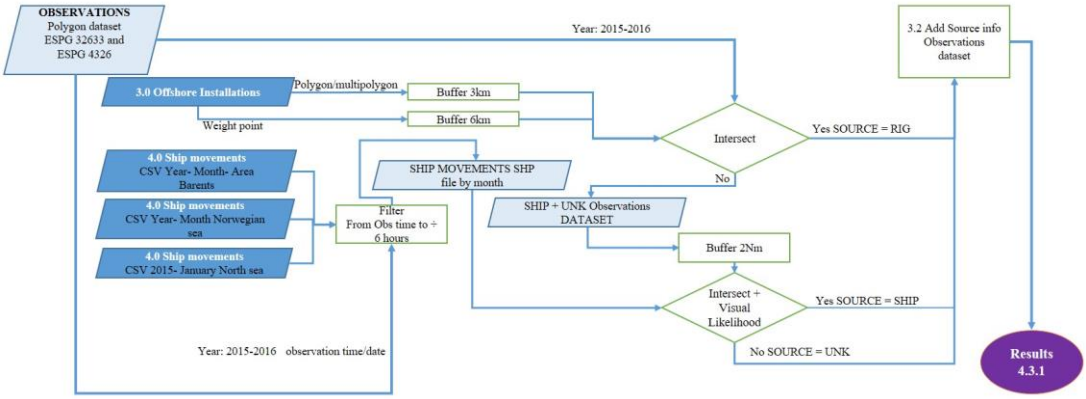

Figure 13: Method of source analysis. The flow chart shows steps determining if a most likely source is connected to the observations, resulting in adding source data in the standard format defined in Table 5.

The first step is to flag RIG as a source. *A 3000 m buffer around the oil installation connects the oil spill alerts when the oil slicks are represented as a polygons*
The 3000 m buffer is chosen as NCA uses this in yearly reports from 2017, and the buffer is based on *in situ* observations compared with satellite images/polygons (NCA, 2017b). An example from the analysis is shown in Figure 14.

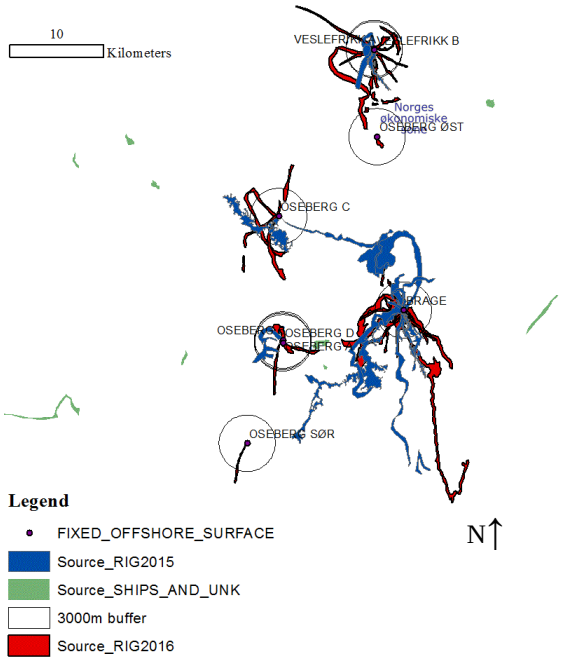

Figure 14: Example of observations in offshore industry area. Shows the observations in blue, 2015 and, red, 2016 that intersect with a 3000 m buffer for some platforms in the North Sea. Green observations is passed on to the ship + unknowns dataset for further analysis.

A part of the oil spill alert observations only is available as point features (Table 2, dataset 2.1.) These points represent the center position of observation. *A 6000 m buffer around the oil installation connects the oil spill alerts when the oil slicks are represented as a point.*
This buffer should connect a point to an offshore installation like the 3000 m buffer used on polygons. To calculate the point buffer, one of the datasets (Table 2Dataset 1.0) includes the length and width of each observation. The average length of the observations in this dataset is 6870 m, counting 1848 observations from 2012-2018. The average center position is 3435 m of the observations and would not connect to the offshore installation using the 3000 m buffer. A polygon would connect to a 3000 m buffer if it only touches on the edge of the buffer, so if a 6870 m long feature (straight) also should connect at the edge of the same 3000 m buffer, the center position would be 3435 m outside this buffer. As this is a rough estimate, the point buffer was set to 6000 m. The performance of this buffer was tested on the 2015 and 2016 datasets, available as both a point and polygon dataset. By using the point dataset and 6000 m buffer, 413 observations were connected to RIG as a source. By using the polygon dataset and 3000 m buffer, 419 observations were connected to RIG.

The next step of the source analysis is to determine if the observations that do *not* intersect with oil and gas installations intersect with ships or are classified as unknowns. For the SHIP + UNK category, here, the observation polygon/point is given a buffer of a predefined measure due to the many points representing ship movements, typically between 2 and 5 million points per month after filtering. This is analyzed by applying an intersection operation to ship movement points. *If they intersect, a likely SHIP source candidate is recorded.*

In most cases, connecting a ship is more challenging as there in most cases is no direct connection between the ship and the observation. Looking at an example of a ship discharging oil from 14:00 to14:20 UTC on a given day, sailing at 10 knots on a steady course, one has to consider that time has passed from the oil discharge from the ship to the time of the satellite image, that might be at 17:00 UTC the same day. In the

radar image taken at 17:00 UTC, the ship, often visible as a white dot in the radar image, and the observation, a dark three nautical miles long “oil” feature, are approximately 30 nautical miles apart. By overlaying the radar image with 17:00 UTC AIS ship data, the AIS ship feature will align over the white dot in the radar image. Using the historical AIS position data, the ship track of the alleged polluter will pass near the darker oil spill feature in the radar image. It will not be a perfect alignment between the ship track and the oil spill represented in the image, which is caused by the movement of the oil slick over the intervening time period. For the analysis, the following variables need to be accounted for, and due to the complexity highly generalized:

- Oil drift being maximum of 2 nautical miles
- Weathering of the oil, where the there is still oil on the sea surface after 6 hours

A maximum conservative drift of 2 nautical miles between the observation and a ship track and maximum backtrack of ship movements of 6 hours have been chosen for the ship as source analysis.

The 2 nautical miles drift within 6 hours represents a velocity of 0.17 m/s along a straight line. This is approximately half of the maximum speed of the sea surface current west of Svalbard, and 28% of the current maximum speed at the Norwegian continental shelf, referring to section 2.4.6. There is also wind to consider in the calculation. For example, ten m/s wind will influence the oil slick movement by 3% of its force, being 0.3m/s drift that needs to be calculated against the current, for example, 0.2m/s, with 100% of its force (Figure 15). A resulting drift trajectory of both current and wind, calculating speed and direction, is given in Figure 15. Wind and current might also change velocity and direction during the lifespan and drift of the oil slick, and with this in mind, the 2 nautical mile constant seems feasible and conservative.

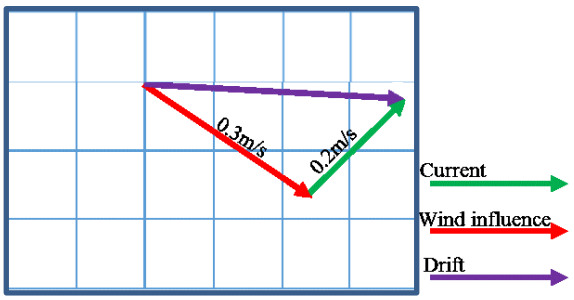

Figure 15: Example of oil drift trajectory. The velocity of the drift is influenced by the current speed (100%) and by wind speed (3%), and the calculation of the drift is the diagonal of a parallelogram.

When a 6 hour backtracked ship route and an oil spill polygon with an applied 2 nautical mile buffer intersect, representing the ability for up to 2 nautical miles of oil drift in all directions, there is a high likelihood that these are related.

The 6-hour backtrack chosen is related to the lifespan of the oil on the sea surface when discharged by a ship, as discussed in section 2.4.5. This minimum lifespan is estimated using diesel to represent a “light” type of mineral oil at the sea surface. Marine diesel represents a “light” non-persistent oil type carried as fuel by a majority of vessels.

The SINTEF oil weathering model can be used to predict oil slick lifetime at sea (Daling and StrØm, 1999). Next, there is a need to investigate the threshold of the environmental factors that influence the lifespan of the oil at the sea surface as the

diesel oil's minimum lifespan results from the weathering of the oil. The diesel oil is weathering most rapidly at high temperatures and high winds. Running the model at 10 m/s, being at the threshold of the radar satellites detection capability, and 15 degrees Celsius as a high sea temperature results in a lifespan of the marine diesel on the sea surface to 9 hours when looking at the mass balance in Figure 16. At 6 hours, there is approximately still 10% of the discharged marine diesel on the sea surface.

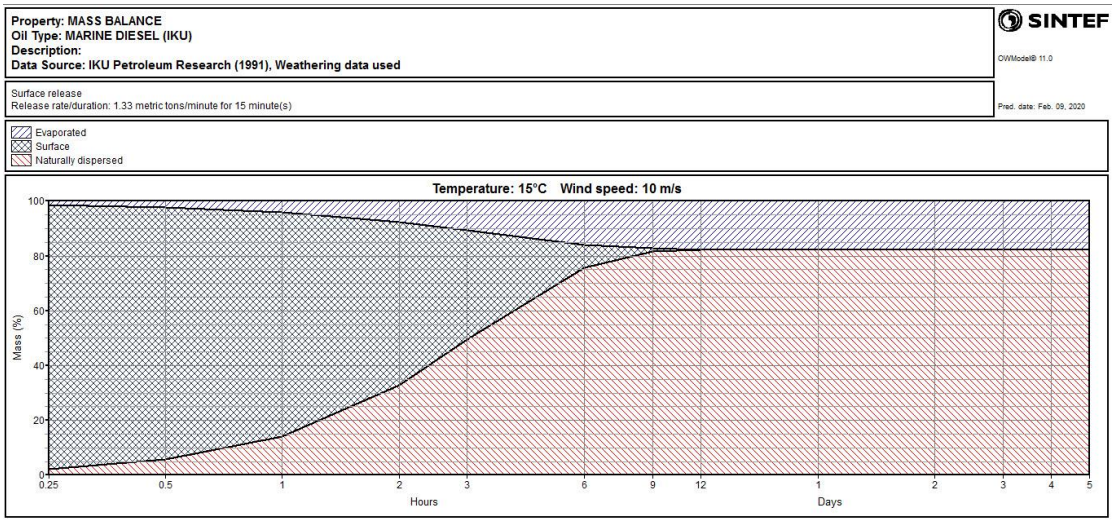

Figure 16 SINTEF Oil Weathering Model mass balance results. The graph shows the mass balance of a marine diesel at 10m/s wind and a sea temperature at 15C°. The diagram shows the balance between surface oil, evaporation, and dispersed oil.

Before flagging the ship as a source of oil, there is a need to assess the ship's heading and the observation's physical characteristics. This is done to exclude ship tracks that intersect but are going in a totally different direction than the oil spill, as the ship is unlikely to be the source. The ship's timestamp and observation also need to be considered, as shown in Figure 17d. Figure 17 shows five examples from the analysis. 4 of them intersect by less than 2 nautical miles, and the visual assessment is deciding the ship is a likely source or not.

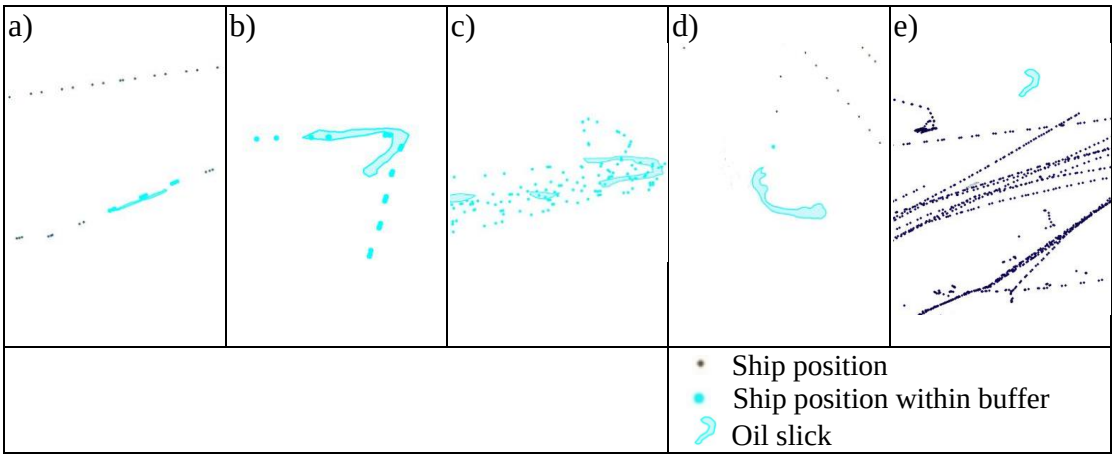

Figure 17: Examples of intersection between observations and ship movements. (a) Shows a good match between ship movement and observation, in this case, a chemical tanker. (b) Shows a good match in observation shape and ship movement, in this case, a fishing vessel. (c)Area with more than one operating fishing vessel in the same area within the same 6 hour period, connecting this observation to fishery activity. (d) In this case, the last point, ship movement, is at the same time as the observation, so this vessel cannot be connected to the observation, even though they intersect according to distance. The vessel is approaching (Sailing towards the oil spill alert observation) the observation (e) Observation that does not intersect to vessel movements in the area.

3.5.2 Oil spill size and type (substance impact)

One of the main indications of a possible oil spill alert from a radar satellite service is observation size. As oil volume is not available, observation size is considered the best available measurement for impact and calculation of the increase of mineral oil. In addition, a categorization of the most likely substance is connected to the spill alert.

Observations connected to RIG as a source are considered mineral oil (MIN OIL). The final result will be adjusted by a mineral oil/no mineral oil ratio derived by *in situ* data from NCA verification data on oil and gas installations (dataset 9.0, Figure 18). The ratio oil/no oil is used in two places in the analysis. It is used where already source RIG is part of the polygon observation dataset. The following use of oil/no oil ratio is where there is no source data in the input observation point dataset.
Here the first step is to connect RIG as a source category. The RIG category observations are then adjusted by the oil/no oil ratio from the *in situ* 9.0 NCA Archive validation dataset. *The RIG category now consists of two oil types, Mineral oil (MIN OIL) and unknown substance (UNK).*

In Figure 18, following the flow chart where the dataset has source data, observations connected to unknown sources are considered unknown substances (UNK). On the same part of the flow chart, observations connected to ships are divided into two types of substance, where *ship category 2 (chemical tankers) and category13 (fishing vessels) as the source are considered fish/animal/vegetable oils (OTH OIL). All other ship categories are not allowed any discharge,* and these *are considered mineral oil (MIN OIL).*
The argument for this categorization of oil and ship type is based up on the legal/illegal aspect of discharging, as discussed in section 2.4.

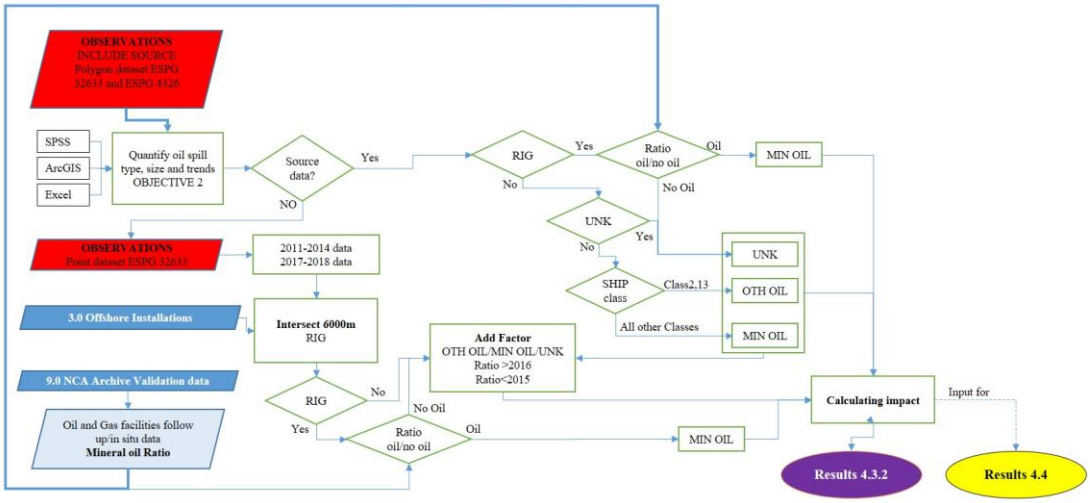

Figure 18: Flow chart of overall calculation of oil spill size and substance.

Following the flow chart, where there is no source connected in the input observation dataset, a separate analysis and estimation are needed to calculate source type and substance type for these observations. As the subsample of data analyzed for all sources only applies for two years (2015-2016), data before 2015 and after 2016 need to be analyzed estimated regarding sources connected to the alerts. Regarding Oil and Gas as source (RIG), a spatial buffer (6000 m) analysis, where the 4.0 Oil and gas facilities dataset is given a 6000 m buffer (decided and calculated in section 3.5.1) to the point alert observation dataset (2011-2014 and 2017-2018).

There is a need to estimate the ship origin alerts and unknown origin alerts for the years outside the timespan of the source analysis to investigate all the oil spill alerts in the study and how they connect to a source (section 3.5.1).

Estimating 2011-2014 and 2017-2018 data on SHIP and UNK as a source is done in two steps. The first step is to calculate two sets of ratio data for a ship as the source. The first ratio for the 2011-2014 data, based on the 2015 source results, and the second ratio is for the 2017-2018 data, based on the 2016 source results. The 2015 data and 2016 data on the number of observations connected to SHIP is calculated by:

$$Ratio_{SHIP} = \frac{SHIP_{COUNT} + UNK_{COUNT}}{SHIP_{COUNT}} \qquad 3.1$$

Where $Ratio_{SHIP}$ is the ratio of Ship-based origin alerts for 2015 and 2016, $SHIP_{COUNT}$ is the number of alerts connected to ship as the source from the 2015-2016 analysis, and UNK_{COUNT} is the number of alerts connected to an unknown source2015-2016 analysis.

The next step is to apply a MIN OIL/OTH OIL ratio to SHIP source data using 2015 and 2016 data on ship categories 2 and 13 (Chemical tankers and Fishing vessels), as OTH Oil and the rest of the ship categories as MIN Oil. An Oil type ratio based on the 2015 oil type results is applied to the 2011-2014 data, and a 2016 ratio is applied to the 2017-2018 data.

The remaining data are unknowns as the source, UNK, and the substance is also categorized unknown, UNK.

These two steps are applied to oil spill alert observation size (km^2), calculating the impact ("oiled area") of the different substances. Further, the same steps are applied to the number of alerts, calculating the trends and impact for the end-user organization to handle each alert.

3.5.3 Oil spill variability analysis (non-spatial methods)

Objective 2 sets to analyze temporal and seasonal variability within the dataset. Such analysis will add knowledge concerning the problem of increasing the number of oil spill alerts, how the introduction of the Sentinel-1 satellites might influence, and how other factors might influence the number of oil spill alerts. One of the questions addressed here is how oil spill alert observation sizes (km^2) are distributed over time. Another question is if there is temporal (seasonal, yearly) variation in the number of oil spill alerts, which can relate to other temporal factors, like monitoring effort, environmental influence (wind), and variation in "oil spill activities."

First, descriptive statistical analysis of the oil spill alert observation size (km^2) on a monthly temporal resolution is applied to address these two questions. Second, an analysis of the seasonal distribution of the number of oil spill alerts is undertaken together with a regression analysis where y is the dependent variable and x1, x2, …,xn are the independent variables

3.5.3.1 *Analyzing oil spill alert observation size (km^2) distribution.*

A monthly plot of the median oil spill alert observation size (km^2) is made. First, outliers (large oil spill observations that clearly are not an oil spill candidate) within this dataset are investigated. There have not been any major oil spills within the study area in the time period from 2011 that would cause large areas of oil at sea (ITOPF, 2018). Therefore, observation sizes over 100 km^2 are considered to be outliers concerning mineral oil. Monthly median observation size is analyzed throughout the observation dataset to investigate the variation year by year for each month of the year.

3.5.3.2 *Analyzing Seasonal variations on the number of oil spill alerts*

A Spearman rank correlation analysis is applied as a suitable method for analyzing the correlation between oil spill alerts and an "influence." Four tests will be applied to test the correlation of oil spill alerts against four different independent "influences" (Figure 19). *As one of the influences, wind/sea state, discussed in section 2.4.7.1, based on the mean wind speed NORA 10 model, shown in Figure 6, mean value data over a January until December scale should be used for all variables*. Seasonal distribution, where the variable is calculated as a mean value by month, is considered nonparametric data, and a Spearman rank method is considered a good test(Prion and Haerling, 2014).

To analyze the strength of association, the variable 'oil spill alerts' and several possible influence variables (number of satellite scenes, *In situ* Oil rig discharge of oil data, ship movement in operational hours, Wind/wave) are calculated at a monthly scale. The wind data from the viability study uses mean wind speed over ten years (2007-2017), and the result used is the percentage of the time of favorable conditions (%) for each month (see section 3.1.3.5 on the dataset). For offshore oil and gas and ships, a sample of the years 2015-2016 is chosen. The offshore oil and gas industry sample includes a monthly discharge amount of mineral oil to the sea (m^3) from the four oil rigs that connect to most of the oil spill alerts from the source analysis (section 3.5.1 oil spill type - source analysis). The ship sample includes a monthly operation time (h) from the four ship-categories that connect to most of the oil spill alerts from the source analysis (section 3.5.1 Oil spill type - source analysis). For the analysis, the year is divided into 12 months, and the mean value of all variables is used.

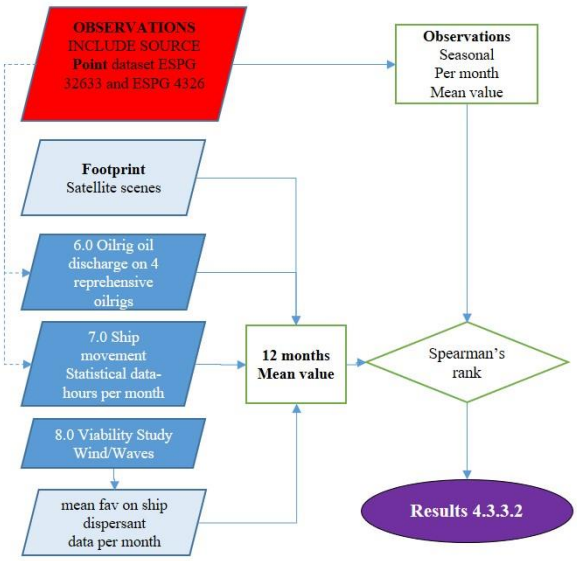

Figure 19: Method for analyzing seasonal trends in the observations data. Spearman's correlation test is used by comparing mean oil spill alerts frequency on each of the influences (mean values), over a 12 month "season".

The resulting Spearman's ρ is used for discussing the influencing variables analyzed.

3.5.4 Spatial distribution Analysis

The main methods used are Ripleys K function (Ripley, 1977) test for randomness, and hotspot analysis, Getis-Ord Gi*. (Getis and Ord, 1996), (see Figure 9 and Figure 20). These methods are chosen based on the dataset's characteristics and how well the method accounts for limitations within the data used. One limitation is that alerts only can occur at sea, limiting the study area to exclude land areas. This, together with the study area shape, the method chosen should account for the shape of the study area.

3.5.5 Test for spatial randomness

As a first step, a test of complete spatial randomness is applied to the alert dataset. This test aims to test the oil spill alert spatial distribution, whether it is considered random or not (e.g., clustered or dispersed).

The hypothesis to be tested:

H_0: The alerts are spatial random distributed.
H_1: The alerts are clustered/dispersed

There are many different methods that can be applied. One spatial statistical tool that fits the aim, takes the study area into the calculation, tests for multiple distances, and is well available in GIS tools is the Ripleys K function multi-distance test for spatial randomness.

The hypothesis to be tested by using Ripleys K function:

> H_0: the K function does not vary significantly from the line *y=x (Random distribution)*.
> H_1: there are scales at which the K function varies significantly from the line *y=x (Random distribution)*.

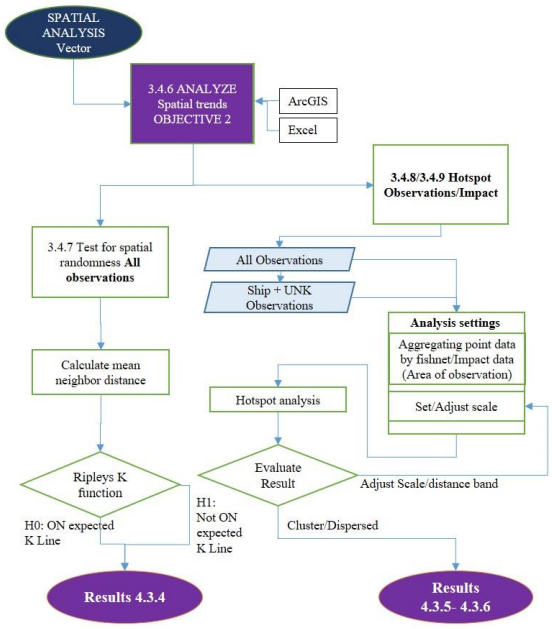

Figure 20: Method on spatial clustering and complete spatial randomness

This test includes a null hypothesis that the pattern is random. The random pattern is plotted as a line, with the expected L(d) being the K value for complete spatial randomness along the neighborhood distance scale chosen for the analysis. K values above the random line state significant clustering, and below the line states significant dispersal. The result will answer if the data are random, cluster, or dispersed, tested for multiple neighborhood distances. As it is known that many of the oil and gas installations have multiple surface installations within a relatively close range of another, the starting neighborhood used is a little less than the calculated mean distance to at least one neighbor within the point oil spill alert dataset. Ten different neighborhood distances are tested, where some test runs with different spacing between each neighborhood distance are done to ensure a representative result.

3.5.6 Test for spatial Hotspots/Significant clustering, based on spatial distribution by Getis-Ord Gi*.

In order to obtain further information on the alert dataset and to meet the aim of analyzing variability, it is essential to analyze where clustering, randomness, and dispersion appear within the study area. As the two primary sources of mineral oil discharges are the oil and gas industry (static source) and ships (dynamic source), a separate set of analyses on oil spill alerts might add important information on the spatial pattern results throughout the study area. The methods so far in answering objective 2 have mainly been non-spatial. A local spatial statistics method for identifying statistically significant hotspots and cold spots is chosen to investigate the spatial patterns. In general, local spatial statistics analyze smaller areas and compare the local area results with the global area result, giving a significance (p) value. The GIS tool can then visualize the results in a map showing an area of clustering or dispersion. There are many tools and methods available for this type of analysis, and one statistical method chosen that fits the aim is Getis-Ord Gi*. In this analysis, the study area is divided into smaller polygons, each holding a value (oil spill alert count). Locally, each polygon and its neighboring value is compared to the study area to see if the neighborhood differs significantly (higher or lower mean alerts counts) than the

mean alert count within the study area. A fixed polygon grid can be used in the study area, being the ocean, and where oil spills can occur anywhere within the study area. A fixed neighborhood distance where the dataset obtains maximum autocorrelation (maximum clustering) is chosen as a start. The dataset is also analyzed with smaller neighborhood distances to investigate clustering with high z scores. Small distances can be essential to identify a single source or an area of activity. The method is shown in Figure 20.

The analysis is carried on all alert data and on a dataset where all oil and gas-related alerts are subtracted. The reason for having the two analyses is because the oil and gas offshore industry constantly discharges mineral oil. As these are also fixed installations, clustering can be expected on such objects. By only analyzing the oil spill alerts connected to ship and the unknowns, a new spatial pattern of oil spill alerts can give a different result for discussing the contribution from shipping.

3.5.7 Test for spatial Hotspots/Significant clustering, based on observation size, by Getis-Ord Gi*.

This analysis aims to investigate how the "oil spill" size (oil slick area in km^2) of the alerts cluster within the study area. The main subject here is analyses for clusters of large "spills" and clusters of small "spills." This has also been analyzed non spatially, on a timeline section 3.5.3.1. The spatial distribution of oil spill size is essential in regards to both areas of large size observations (hot spots) and areas of small size observations (cold spot). Such results can be discussed in regards to the activity in the area. This, like oil spills, mineral and vegetable/animal oils, is closely connected to human activity as shipping and offshore oil and gas industry. Also, here, the analysis is done on all alert data, as well as a dataset where all oil and gas-related alerts are subtracted.

On observation size, all observations are analyzed using Getis-Ord Gi*. *However, outliers and observations over 100 km^2 are removed from the dataset (15 of 3694 alerts), as they are unlikely to be a mineral oil observation, and they will influence the result.* Values and evaluation for the different neighborhood distances follow the same method as for section 3.5.6. The value chosen for the neighborhood in the maps produced is adjusted from the default neighborhood value, as several oil spill alerts had more than 1000 neighbor alerts.

3.6 Objective 3: To validate/verify the service provider's likelihood settings with historical observations.

Historical remedial actions data from NCA are needed to address this objective. These historical validated data on satellite observations and how these compare with the dataset produced in the specific objective 2 are the basis of meeting objective 3.

To answer the third specific objective on the services confidence level settings and the performance of the services, a set of basic statistics (frequency distribution, standard deviation, and probability) derived from the dataset produced for the impact results are calculated and presented. Each observation has a confidence level of 'A' if it is more likely to be mineral oil or 'B' if it is less likely to be mineral oil. The EMSA CSN service and the KSAT service set confidence level to confidence B when the probability of an alert being mineral oil (Oil spill) is less than 50%, and to confidence

A if the probability of the alert being mineral oil (Oil spill) higher than 50%. Data for all years and satellites (Radarsat-2 VS Sentinel-1, (2015-2018) and source connected by analysis - 2015-2016) are developed and presented.

Using the two results on impact (3.5.2) (where trends on observation size and the number of observations, both calculating/estimating substance), the probability of a spill being mineral oil, other oils, and unknown can be calculated and discussed in regards to the two confidence levels 'A' and 'B.'

For observations where RIG is confirmed as the source, *in situ* verification data is used to estimate the probability of mineral oil observation.

For observations where RIG is not confirmed as the source, these alerts then belong to the source categories SHIP or UNK, and the probability for the observation than being mineral oil is calculated by:

$$P_{(M_{OIL},SHIP)} = \frac{n_{SHIP\_M\_OIL}}{n_{total} - n_{RIG}} \quad (3.2)$$

Where $P_{(MOIL,SHIP)}$ are the probability of an alert being mineral oil and connected ship as the source. $n_{SHIP\_M\_OIL}$ is the number of alerts oil spills calculated as mineral oil from ships. n_{total} is the total number of alerts. n_{RIG} is the number of oil spills mineral oil alerts connected to RIG as the source.

By estimating and calculating these two probabilities, one can measure how well confidence A and B categorization comply with the results.

This will also answer if the results are consistent with the probability setting of the service providers, and it can also answer if the implementation of Sentinel-1A and 1B as the new sensors gives the service a higher, equal, or lower probability delivering correct confidence setting then before.

4 Results

4.1 Intensity analysis of oil spill alerts.

The number of oil spill alert increase is shown in Figure 21a on the number of oil spill alerts, printed as the yellow plot, and shown in numbers in Table 6, Observations. The increase from 2015 until 2018 calculates to 249%.
The results of the raster analysis where the area (km^2) covered by all satellite images used in the monitoring is shown in Figure 21a, the orange plot, and in Table 6, the Satellite area covered. The satellite monitoring coverage varies for all years in the study and shows an overall increasing trend until 2016, where there is a shift towards less coverage the two following years.
The results by calculating oil spill alerts and variation in monitoring coverage for 2015 until 2018 show an increase of 297% in intensity/ratio. Figure 21b and Table 6 show the ratio calculated in observations per 1 million km^2 (10^6 Km^2).

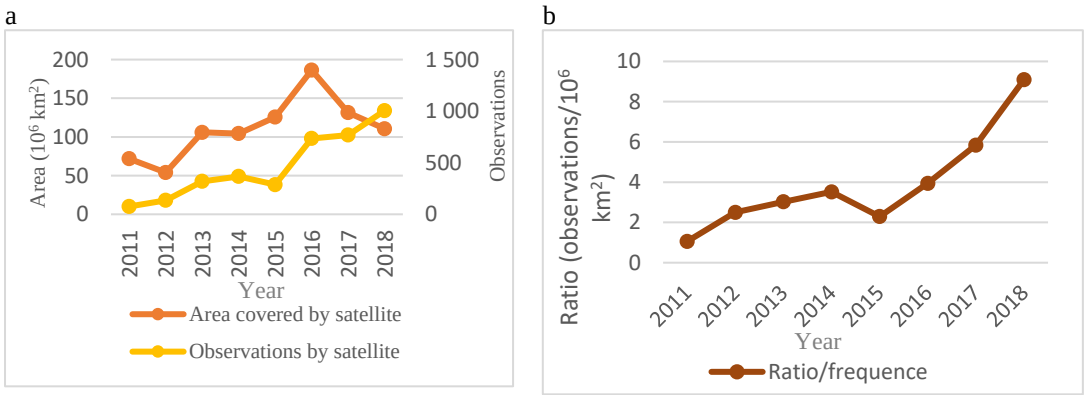

Figure 21: Result on oil spill trend by ratio 2011-2019. (a) Trend analysis results, with total satellite footprint of covered area per year and the number of observations per year. (b) Ratio, showing the number of spills per 1 million km^2.

Table 6: Observation and accumulated yearly coverage by ratio. Area per year is coverage added up using the footprint on each satellite image as part of the oil spill service. Observations are the number of possible spills reported by the service and the ratio/frequency quantifying spills/area.

	2011	2012	2013	2014	2015	2016	2017	2018	Mean
Satellite area covered (x10^6 Km^2)	71.825	54.031	105.907	104.341	125.697	186.394	131.496	110.541	111.279
Observations of oil spills (n)	76	135	320	367	288	735	768	1 005	461.750
Ratio/intensity (n/area x10^6 Km^2)	1.058	2.498	3.022	3.517	2.291	3.943	5.840	9.092	4.149

4.2 Objective 1: To determine if the increase in alerts is due to the use of Sentinel-1

The results in this section give an overview of the satellite used in the analysis, the visual comparing analysis of Sentinel-1 and Radarsat-2 on a verified oil spill, and a correlation test
Table 7 shows that Radarsat-2, Sentinel-1A, and Sentinel-1B satellites have delivered 7478 out of a total of 9442 satellite scenes in the study.

Table 7: Number of scenes from Radarsat-2 and Sentinel-1.

	2011	2012	2013	2014	2015	2016	2017	2018	Sum
Radarsat2	355	511	463	490	1106	813	406	329	4473
Sentinel 1					40	384	738	749	1911
Sentinel1A					141	476	127	80	824
Sentinel1B						63	131	76	270
Sum	355	512	463	490	1287	1736	1402	1234	7478

4.2.1 Visual analysis of Sentinel-1 and Radarsat-2 radar images

The *in situ* measurements consist of two essential confirmations. 1. The oil slick is visible on the sea surface and covers an area large enough to be picked up by satellite, and 2, it is mineral oil. As the satellite alert triggers the *in situ* measurement, there is a time delay between the satellite images and *in situ* measurement data. This data is presented in Table 8.

Table 8: Data sources for visual analysis between Radarsat-2 and Sentinel-1A.

Dara source	Date	Time UTC	Mineral oil?	Oil slick size
In situ Report from Norne platform operator	2016.10.11	19:00	Confirmed	Visible
In situ Report from NCA Remote sensing aircraft LN-TRG	2016.10.12	12:50	Confirmed	1.5 km x 0.3km slick with 50% oil cover
Radarsat-2 image – basis of Oil spill alert + national archive	2016.10.11	16:55:09		1.23km^2
Sentinel-1A (from ESA archive)	2016.10.11	16:47:30		Not measured

The possible oil spill alert was confirmed as mineral oil on water on the day of the satellite image by the platform operator and the next day by NCA Remote sensing aircraft (see Table 8 and Figure 22*). It is essential to state that this is a legal discharge from the Norne FPSO, reported within legal limits by the platform operator.* The oil slick reported by the remote sensing aircraft confirms the visual appearance of a typical mineral oil slick and covers an area of approximately 0.45 km^2, 20 hours after the satellite detections.
Figure 23a,b, shows the oil slick where both Radarsat-2 and Sentinel-1A have covered the same area at approximately the same time, clearly confirming different performance when looking at noise and resolution (see Figure 23 a and b). Both satellite images show homogenous “lighter” surroundings around the “darker” spill, making it a high likelihood confidence A, “Possible oil spill” observation. Further, investigating the Sentinel-1A image (Figure 23b), looking at the right-hand side in this image shows a” thin tail” going left, where there is a 160-degree turn of the oil slick. This same “oil slick tail” mixes into the noise on the Radarsat-2 image and is not visible (Figure 23a). The images show that smaller oil slicks can be visual on Sentinel-1A compared to Radarsat-2.

a b

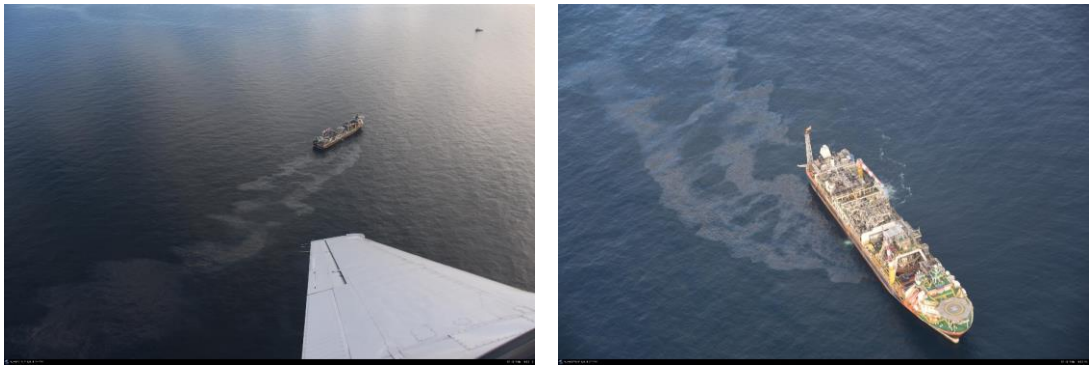

Figure 22: Mineral oil slick example from an oil rig. Norne FPSO2016.10.12 at 13:00UTC, oil on water, and calm sea conditions. Photo: Norwegian Coastal Administration (Kystverket, 2016).

Both satellite images are level 1 products VV polarization, Radarsat-2 with a spatial resolution of 50 m, and Sentinel-1A GRD High resolution of 20x22 m resolution. This is typically the operational mode used within the oil spill services. Both images show an oil slick signature connected to Norne FPSO (oil-producing installation, Figure 22). Norne FPSO is the only surface facility in the area and can legally discharge oil into the sea (up to 30 mg/l monthly average). The two white point features in the radar image are large objects, where one is the NORNE FPSO and the other a stand-by vessel. The oil slick size reported (alert report to NCA) on the Radasat-2 image is 1.23km^2.

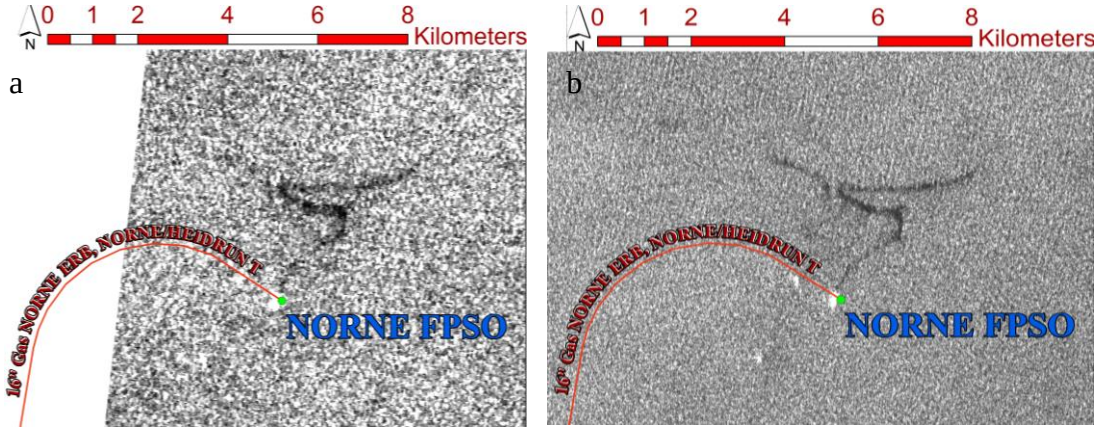

Figure 23: Example of Radarsat-2 and Sentinel-1A on the same oil slick. Both images are shown with an offshore industry overlay including, pipelines and fixed installations. (a) Radarsat-2 image on the left, taken 2016.10.11 at 16:55:09 UTC and, (b) Sentinel-1A taken 2016.10.11 at 16:47:30 UTC, 7 minutes and 39 seconds apart. Sentinel 1: Copyright: European Space Agency – ESA. Radarsat: Copyright: CSA, RADARSAT-2, MACDONALD, DETTWILER & ASSOCIATES LTD

4.2.2 Detection performance of the instruments

The first result when looking at how Sentinel-1 and Radarsat-2 perform towards oil slick size, a histogram of all oil spill alerts from these two instruments, Radarsat-2 and Sentinel-1 (Sentinel-1A + 1B + 1X) are shown in Figure 24. Here, all available oil spill alert data within this study (Table 9) are categorized regarding the detected oil slick size. Even though there is more Sentinel-1 with 2096 alerts than Radarsat-2 with 1473 alerts, the histogram shows more small oil slicks for Sentinel-1 than for Radarsat-2. There is a slight difference in the number of alerts shown in Figure 24, and Table 9 (Sentinel-1 2096 VS 2098 and Radarsat-2 1472 VS 1485) due to the scale of classes not showing oil spill alerts over 100 km^2. Observations above 100 km^2 are considered outliers.

Figure 24: Histogram on the distribution on observation size. The histogram shows the number of observations within 10 different classes from 0-1 km^2, 4 classes from 1-5 km^2, and 3 classes for large observations. 1473 observations are from Radarsat-2 and 2096 are from Sentinel-1 (Sentinel-1A + 1B + 1X)

Table 9: All oil spill alerts 2011-2018 sorted by detecting satellite. Sentinel-1X is either Sentinel-1A or Sentinel-1B and is used as one service provider only stated Sentinel-1 from late 2018 (It is the same radar instrument, on the two different satellites).

Satellite	2011	2012	2013	2014	2015	2016	2017	2018	Sum
Envisat	47	0							47
Sentinel-1A					39	483	478	262	1262
Sentinel-1B						20	214	450	684
Sentinel-1X								152	152
Radarsat-1	3	15	1						19
Radarsat-2	26	120	315	365	249	227	64	119	1485
COSMO-SkyMed1			1						1
COSMO-SkyMed2			2						2
COSMO-SkyMed4			1	2					3
TerraSAR TSX-1								8	8
TerraSAR TDX-1						5	4	22	31
								Total	3694

Table 10: Descriptive statistics on oil slick areas for oil spill alerts. Statistics for Radarsat-2, Sentinel-1A, Sentinel- 1B and Sentinel-1X.

Table 10: Descriptive statistics on oil slick areas for oil spill alerts. Statistics for Radarsat-2, Sentinel-1A, Sentinel- 1B and Sentinel-1X

Satellite	Radarsat-2		Sentinel-1A		Sentinel-1B		Sentinel-1X	
	Statistic	Std. Error	Statistic	Std. Error	Statistic	Std. Error	Statistic	Std. Error
N	1472		1262		683		152	
Mean unit (km^2)	4.710	0.234	2.362	0.172	2.202	0.164	0.931	0.14
Median(km^2)	1.850		0.912		0.911		0.377	
Mode (smallest) (km^2)	0.571		0.125		0.044		0.034	
Variance	80.822		37.164		18.433		2.967	
Std. Deviation(km^2)	8.990		6.096		4.293		1.722	
Minimum (km^2)	0.046		0.000		0.044		0.000	
Maximum (km^2)	88.69		90.537		59.835		14.200	
Skewness	4.684	0.064	8.928	0.069	6.609	0.094	5.119	0.197
Kurtosis	27.135	0.127	101.854	0.138	65.144	0.187	32.846	0.391
Z value Skewness	71.188		129.391		70.309		25.985	
Z value Kurtosis	213.661		738.072		348.364		84.005	

All four satellite datasets show a positive skew when looking at mean, median, and mode. All four satellites' oil slick area data show mean>median>mode (Table 10). Also presented in Table 10, Z values are calculated by Skewness/std.error and are well outside the range of +/- 1.96 for all four datasets. The kurtosis value is also positive for all four datasets and has a value outside a normal distribution assumption. The Z values may also be calculated here by kurtosis/std.error and are also well outside a +/- 1.96 range for all four datasets

The histogram plot of the oil slick size distribution is shown in Figure 25. In the same figure, a Q-Q plot for the oil slick size distribution is compared to a normal distribution fit line for each of the four oil slick size datasets. All four datasets on oil slick size distribution show a histogram with a positive skew. A normal distribution should ideally have a mean=median=mode distribution. The three values of mean, median, and mode are shown in Figure 25 on each of the four datasets, clearly diverting from a mean=median=mode distribution, where mean>median>mode indicates a positive skew. A Q-Q plot test for all four datasets is also shown in Figure 25, and all show a clear deviation to the normal fit line. Finally, the results of a Shapiro-Wilk test are shown in Table 11, and the significance level, Sig column in the table, concludes to reject the H_0, which in this test states that the dataset is normally distributed.

Table 11: Result of Shapiro-Wilk normality test on oil slick size distribution. Results for Radarsat-2, Sentinel-1A, Sentinel-1B and Sentinel-1X,

Satellite	Radarsat-2			Sentinel-1A			Sentinel-1B			Sentinel-1X		
Shapiro-Wilk test	Statistic	df	Sig	Statistic	df	Sig	Statistic	df	Sig	Statistic	df	Sig
SPSS results	0.476	1472	0.000	0.307	1262	0.000	0.442	683	0.000	0.479	152	0.000

The results of the tests, examination of statistics, and inspection of the histogram and normal q and q plot show that the data do not follow a normal distribution.

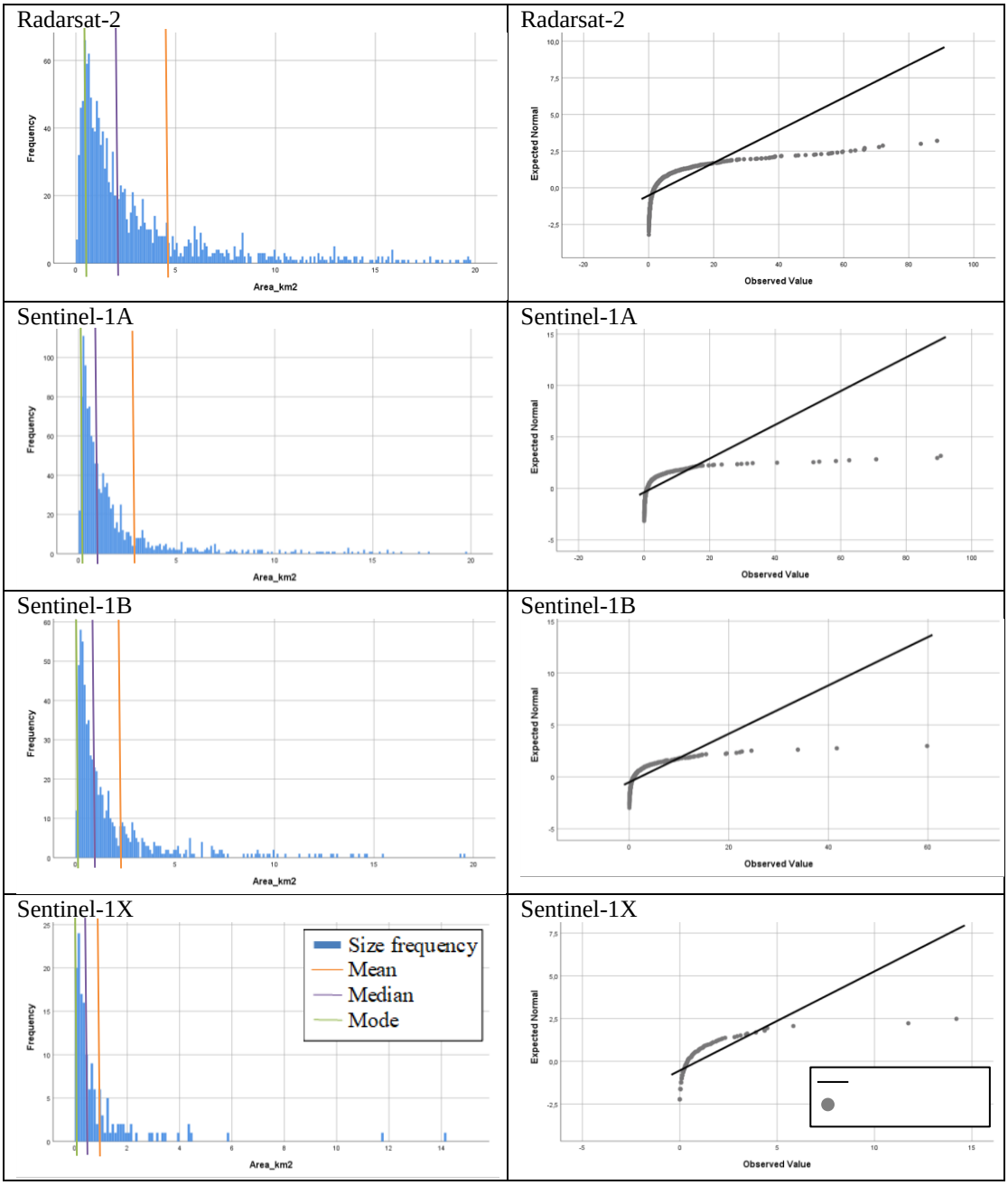

Figure 25: Histogram of the oil spill size distribution and Q-Q plot. Histograms (number of oil spill alerts/oil spill size) for the four datasets on the left-hand side and Q-Q plot (quartile/quartile). The plot shows the fit to the normal distribution fit line.

Results of the first test Mann-Whitney U-test is Sentinel-1A VS Sentinel-1B supports the 0 hypotheses with a sig (2-tailed) p-value of 0.695. The statistics are shown in Table 12 state a very similar value on mean rank on oil slick size, supporting an equal performance.

Table 12: Sentinel-1A VS Sentinel-1B results. Rank test on oil slick size.

Satellite	Number of observations N	Mean Rank	Sum of Ranks	Asymp. Sig (2-tailed)
Sentinel 1A	1264	969.84	1225872.00	0.695
Sentinel 1B	682	980.29	668559.00	
Total	1946			

In the second test, all Sentinel-1 data is merged (Sentinel-1A + Sentinel-1B + Sentinel-1X), and tested against Radarsat-2 data. The results of this test do not support the 0 Hypothesis with a sig (2-tailed) p-value of 0.000. The statistics (Table 12) state a higher value on mean rank on oil slick size than Sentinel-1, indicating a larger oil slick size for Radarsat-2.

Table 13: Mann-Whitney U-test results on Sentinel-1A/B VS Radarsat-2. Rank test on observation size.

Satellite	Number of observations N	Mean Rank	Sum of Ranks	Asymp. Sig (2-tailed)
Sentinel-1A/1B	2096	1536.53	3222113.50	0.000
Radarsat-2	1486	2152.51	3198622.50	
Total	3583			

A plot on spill sizes from both satellites, Sentinel-1 and Radasat-2, ranked from low to high, limited to 1 km^2 for Sentinel-1, counting 1143 observations from each satellite, is shown in Figure 26.

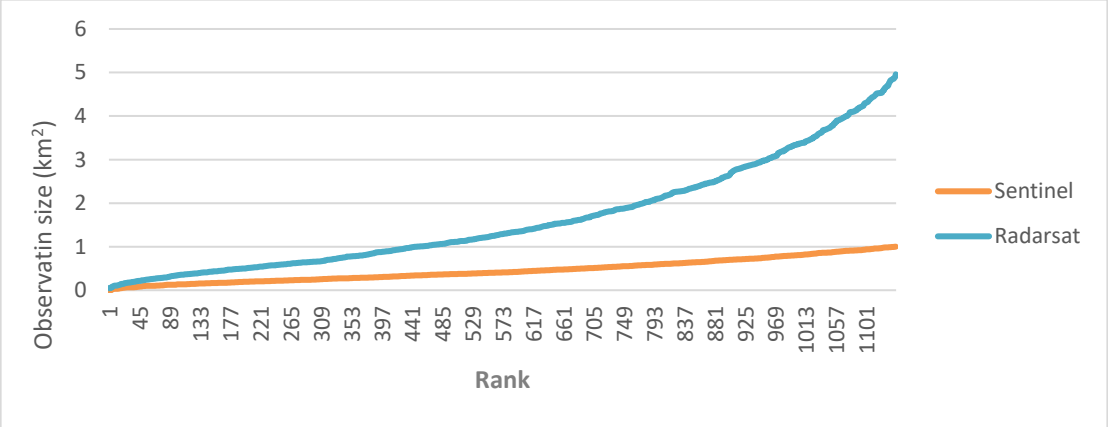

Figure 26: Plot of Sentinel-1 and Radarsat-2 by rank on observation size. A plot of observations, the first 1143 observations from each instrument, by observation size

To further analyze which parts of the size scale the difference in performance applies, the data has been divided into eight sets of size classes and analyzed one by one. The result shows only a significant result in the small oil slick size category, 0-1km2 (see Table 12)

Table 14: Result of Mann-Whitney U significance test. Test including eight oil slick size categories.

Oil slick size	0-1km^2	1-2km^2	2-3km^2	3-4km^2	4-5km2	5-10km^2	10-20km^2	20-100km^2
Sentinel-1A/1B VS Radarsat-2 Asymp. Sig (2-tailed) probability?	0.000	0.949	0.398	0.880	0.889	0.418	0.338	0.641

4.2.3 How the oil spill per area ratio for the two instruments compare 2015-2018.

The results plot shows (Figure 27) the difference in ratio, the number of observations per 1million km^2 for Sentinel-1A/B and Radarsat-2. The ratio for Sentinel-1A/B is increasing and separate from the relatively stable ratio of Radarsat-2.

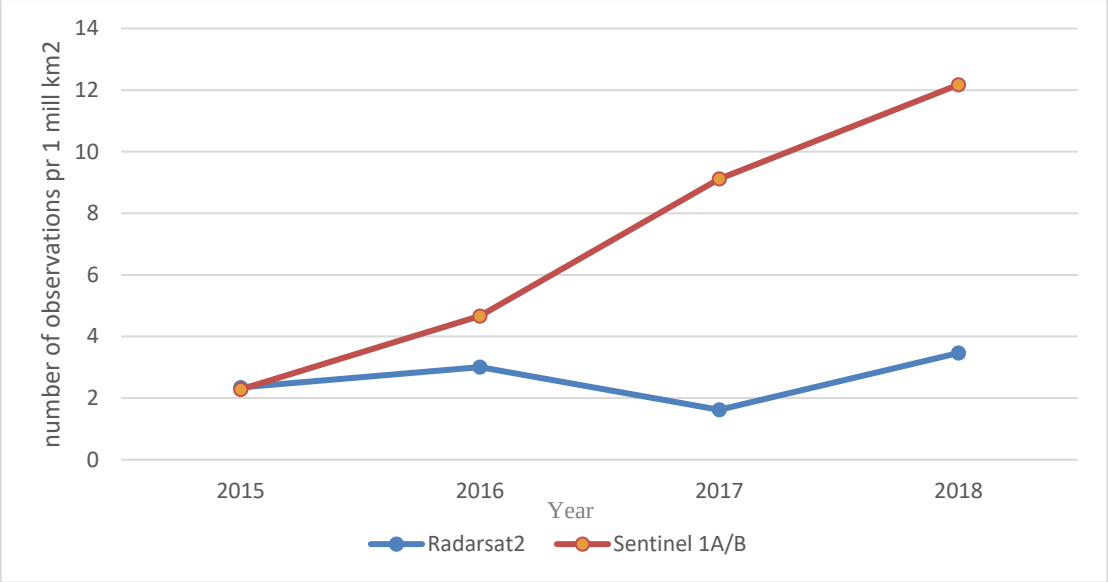

Figure 27: Radarsat-2 and Sentinel-1A/B ratio plot. The plot shows oil spill observations per million km^2 observed area.

4.3 Objective 2: To quantify oil spill type, size, and trends

4.3.1 Oil spill origin (source analysis)

The results in this section show how different sources connect to the oil spill alerts. Further, the substance of the oil spill alerts is analyzed based on the source data. The overall impact of the increase is calculated, also testing the hypothesis. Finally, the spatial distribution is analyzed.

The source analysis results show an increase, from 2015 to 2016, in oil spill alerts for all three source categories (Figure 28). The increase on rigs is 79%, on ships 271%, and unknowns 189%. The results show a percentage reduction on a rig as source category and an increase for a ship as source category.

When looking at all oil spill alerts from all source categories, there was an increase from 288 to 735 alerts (153%) from 2015- 2016. In the same period, the area covered is from 126 to 186 million km^2 (48%) (Table 6)

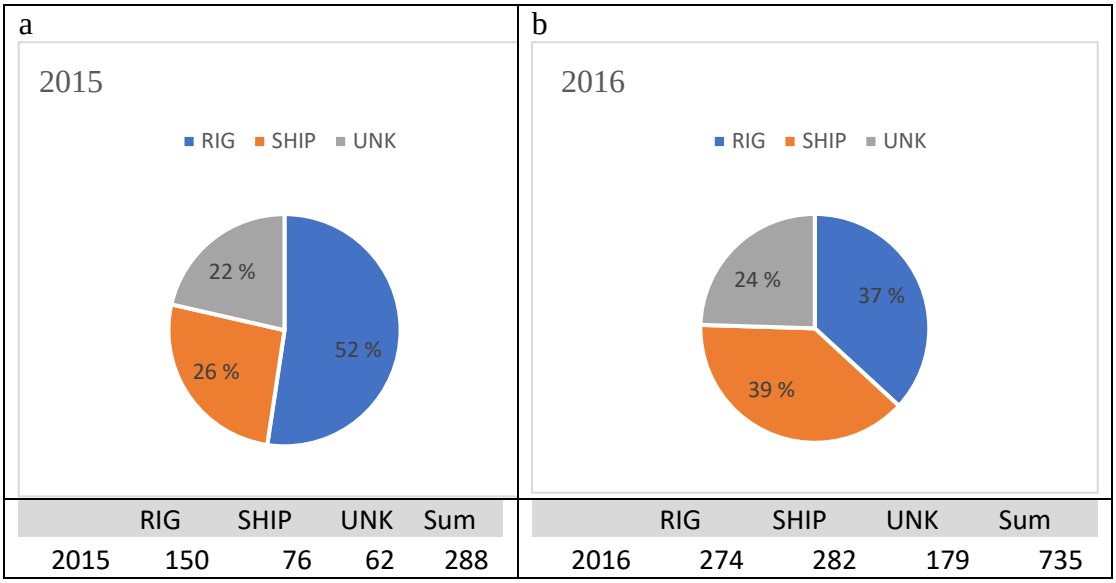

	RIG	SHIP	UNK	Sum
2015	150	76	62	288

	RIG	SHIP	UNK	Sum
2016	274	282	179	735

Figure 28: Source analysis results. Result of source analysis/observations for the dataset (a) 2015 and (b) 2016. The unknown category is relatively stable, with a slight increase from 22% to 24% of the yearly total. Looking at the percentage distribution, there is a shift going between RIG and SHIP as Source.

The result of how oil slick size developed from 2015 until 2016 are shown in Table 15. The results show a decreasing average oil slick size per alert for alerts connected to oil rigs and ships. For the unknown category, there is an increase in slick oil size.

Table 15: Oil slick size for the Source categories, 2015 and 2016.

Source	2015		2016	
	Oil slick size total Area (km^2)	Area per alert (km^2/alerts)	Oil slick size total Area (km^2)	Area per alert (km^2/alerts)
RIG category	344	2.29	551	2.05
SHIP category	393	5.17	1010	3.58
Unknowns category	295	4.75	1017	5.68

The last result from the source analysis shows how each of 14 different ship categories contributes to where a ship is found as a source.

Table 16 shows that fishing vessels contribute by far the most, both for the number of alerts (203) connected to fishing vessels and for oil slick surface area(649 km^2). The next in line are chemical tankers on the number of alerts (44) and oil slick surface area (257 km^2). Figure 29 shows the same data as percentage distribution for each of the 14 different ship categories.

Table 16: Ship category distribution. The table summarizes the ship categories by the Norwegian categorization system (2015-2016). It shows the number of observations connected to each ship category and the total size of the observations within each ship category for each year.

Ship Cat	Oil Tankers	Chem Tankers	Gas Tankers	Bulk Carrier	Gen Cargo	Container	RoRo Cargo	Refridge Cargo	Passenger	Offshore Supply	Oth serv/ Offshore	Oth activities	Fishing	Unk	Sum
2015 obs	1	17	1	3	5	0	0	1	8	12	1	3	21	3	76
2016 obs	1	27	2	5	23	3	0	2	7	5	2	9	182	14	282
SUM	2	44	3	8	28	3	0	3	15	17	3	12	203	17	358
2015 Size Km^2	1	135	0	81	28	0	0	0	14	65	0	3	60	6	393
2016 Size km^2	1	122	5	38	102	16	0	8	23	18	2	71	589	15	1010
SUM	2	257	5	119	130	16	0	8	37	83	2	74	649	10	1403

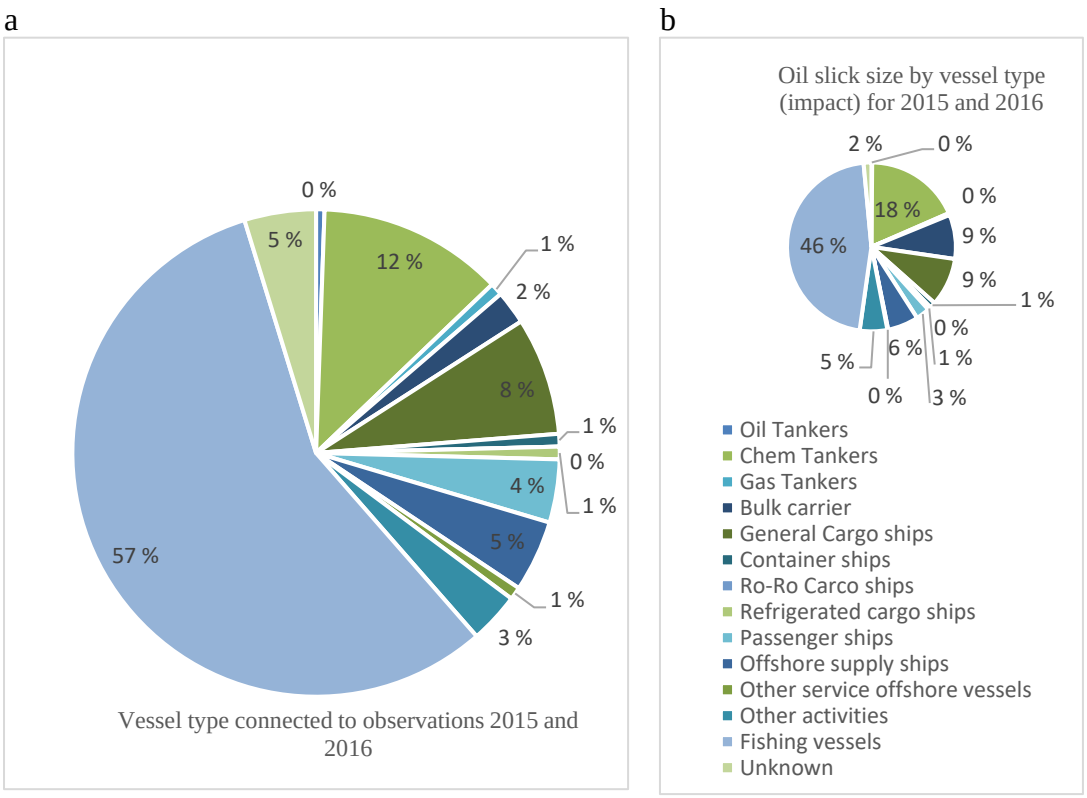

Figure 29: Ship category by the number of observations and by observation size. Shows both how often (a), (frequency) each ship type category is connected to an observation (Clockwise from 12), and (b) the impact of the different ship categories are connected to "possible oil spill" observations. Fishing vessels are dominant, and the second most dominant is Chemical tankers, in sum 69% frequency and 64% of the area, impact.

4.3.2 Oil spill size and type (substance impact)

The results on oil spill size and type first compare Sentinel-1 A/B and Radarsat-2 on oil spill size, secondly the overall impact (spill size and type) by all satellites is calculated, based on *in situ* data on substance from the offshore industry and the results from the source analysis.

Figure 30 shows a considerable contribution to the overall oil spill alerts from the two Sentinel-1 satellites from 2016. The most considerable difference in observations in the three different size categories is in the small size category, under 0.5 km^2 (Table 17 and Figure 30a). These results show that Sentinel-1 contributes to more oil spill alerts than Radarsat-2 in all size classes, and most of all, there are ten Sentinel-1 observations of every Radarsat-2 observation in the small size category, under 0.5km^2 (Table 17).

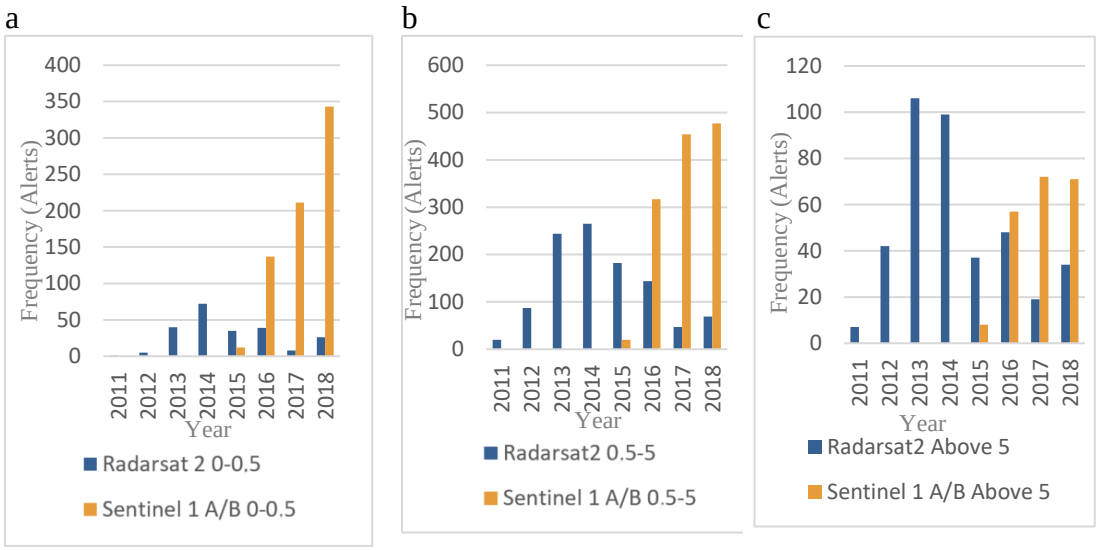

Figure 30: Observation size histogram on Radarsat-2 and Sentinel-1. Number of observations for Sentinel-1 and Radarsat-2 on (a) small size observations (0-0.5km^2), (b) medium size observations (0.5-5km^2) and (c) large size observations (over 5km^2)

Table 17. Ratio Radarsat-2/Sentinel-1 on the number of observations. The table shows the average number of observations and the ratio between Radarsat-2 and Sentinel-1 in 3 different size classes.

	0-0.5km^2		**0.5-5km^2**		**Over 5km^2**	
	2013-2015	2016-2018	2013-2015	2016-2018	2013-2015	2016-2018
Radarsat-2	49	24.3	230.3	86.7	80.7	33.7
Sentinel-1A/B	4	230.3	6.7	416	2.6	66.7
Ratio Radarsat-2/Sentinel-1		0.106		0.207		0.505

The following results relate to the estimation of the observation size and type.

Investigating NCA data for 2015 (Kystverket, 2015) and 2016 (Kystverket, 2016), most of the checked observations connected to offshore facilities are confirmed mineral oil, both on confidence A and confidence B level. The *In situ* data from these verifications on possible oil spill alerts and oil and gas installations is shown inTable 18. 97.5 % of all alerts connected to an oil and gas facilitation are verified as mineral oil from these data. A more conservative sample probability of 95% is used to calculate mineral oil when oil and gas facilities are the most likely source.

Table 18: In situ verification data on mineral oil, ref ancillary dataset 9.0. In situ verification of mineral oil connected to "possible oil spill alerts." The data supplied from NCA follow-up records on satellite observations most likely connected gas facilities in 2015 and 2016. The possible oil spill alerts that were not verified to be mineral oil were reported to be a calm sea area.

	2015		**2016**		**2015-2016**
confidence	**A**	**B**	**A**	**B**	**A/B**
Number of NCA "alert" follow-ups	35	24	110	33	202
Verified as mineral oil	34	21	110	32	197
% Verified as mineral oil	97.1%	87.5%	100%	97.0%	97.5%

The result of the overall impact on the environment, based on observation surface size, sorted by source and substance, is presented in Figure 31.
The histogram shows an overall increase of an unknown substance. The unknown substance (UNK) in the histogram are the observations that are not connected to any probable source plus 5% of oil rig source alerts (95% is considered mineral oil). The results of ships and other substances (SHIP_OTH) have their origin where oil slicks

are connected to fishing vessels and chemical tankers and show a general increase, although a high number in 2013. The results of ships and mineral oil are connected to all other vessel classes than fishing vessels and chemical tankers. Here one can see is a slightly decreasing trend in the oiled area. The oil and gas industry and mineral oil have their origin connected to surface offshore rigs, and there is a slightly increasing trend to be detected in the histogram.

Three years of oil slick size data before the "shift" detected in 2015 and three years of oil slick size data after the shift is used to test the hypothesis (Table 19.) The result is an increase of mineral oil by 2.65%, where the increase contributing to an increase is the oil and gas results.

The number of alerts and the source/substance distribution is presented in Figure 32. This figure also gives a result where an increase in mineral oil substance alerts is primarily due to the oil and gas industry contribution.

Table 19: Results of substance size and percentage change. Result of the period before and after 2016.

Substance	**UNK**		**SHIP OTH**		**SHIP_M_Oil**		**RIG M_ Oil**	
Oil spill alert period	2013-2015	2016-2018	2013-2015	2016-2018	2013-2015	2016-2018	2013-2015	2016-2018
Observation Area Average (km^2)	460	880	390	691	387	275	367	499
Percentage change 2013-2015 to 2016-2018 (%)	91.3		77.18		-28.94		35.97	
Substance					**M_OIL**			
Oil spill alert period					2013-2015		2016-2018	
Sum M_Oil					754		774	
Percentage change mineral oil 2013-2015 to 2016-2018 (%)					2.65			

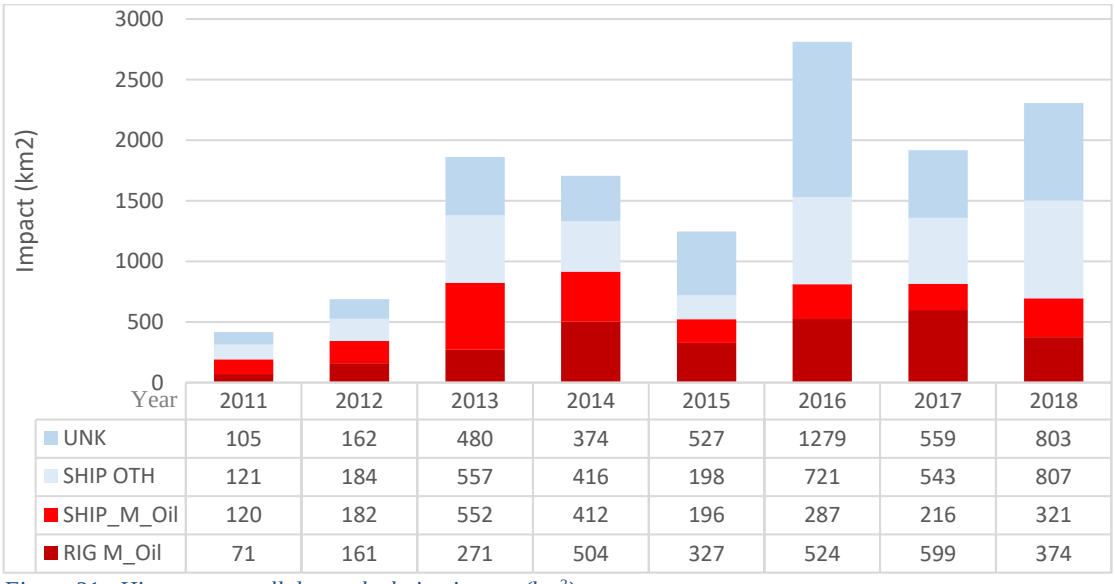

Figure 31: Histogram on all data calculating impact (km^2).

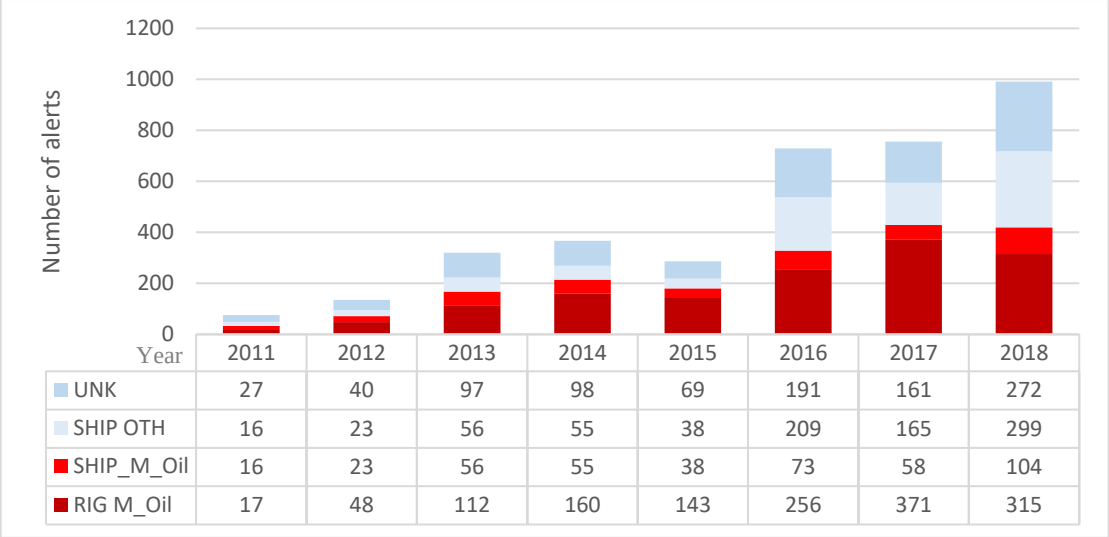

Year	2011	2012	2013	2014	2015	2016	2017	2018
UNK	27	40	97	98	69	191	161	272
SHIP OTH	16	23	56	55	38	209	165	299
SHIP_M_Oil	16	23	56	55	38	73	58	104
RIG M_Oil	17	48	112	160	143	256	371	315

Figure 32: Histogram on all data calculating the number of alerts.

4.3.3 Oil spill variability analysis (non-spatial methods)

4.3.3.1 *Analyzing oil spill alert observation size (km2) distribution.*

The results of the descriptive analysis of the oil spill alert observation size (km^2) on a monthly temporal resolution are shown in Figure 33. All plots show median oil spill size for 2011-2018 for all oil spill alerts. The plot shows a decreasing oil spill alert size (km^2) trend from 2011 until 2018 for all months. However, there are some decreasing/increasing variations from year to year, especially during winter. Also, looking at the yearly median and yearly mean oil spill size (Table 20), the same decreasing trend can be observed on both the yearly median size and the mean size values.

Table 20: Median and mean oil slick size per year. Median, all data used (n=3694). Mean value where outliers (slick size above 100km2) are removed (n= 3679).

	2011	**2012**	**2013**	**2014**	**2015**	**2016**	**2017**	**2018**
Observation s(n) median/mean	76/76	135/134	320/313	367/364	288/287	735/734	768/768	1 005/1003
Median	2.87	2.93	2.18	1.73	1.47	1.14	1.04	0.76
Mean	5.50	5.14	5.94	4.69	3.15	3.08	2.50	2.30

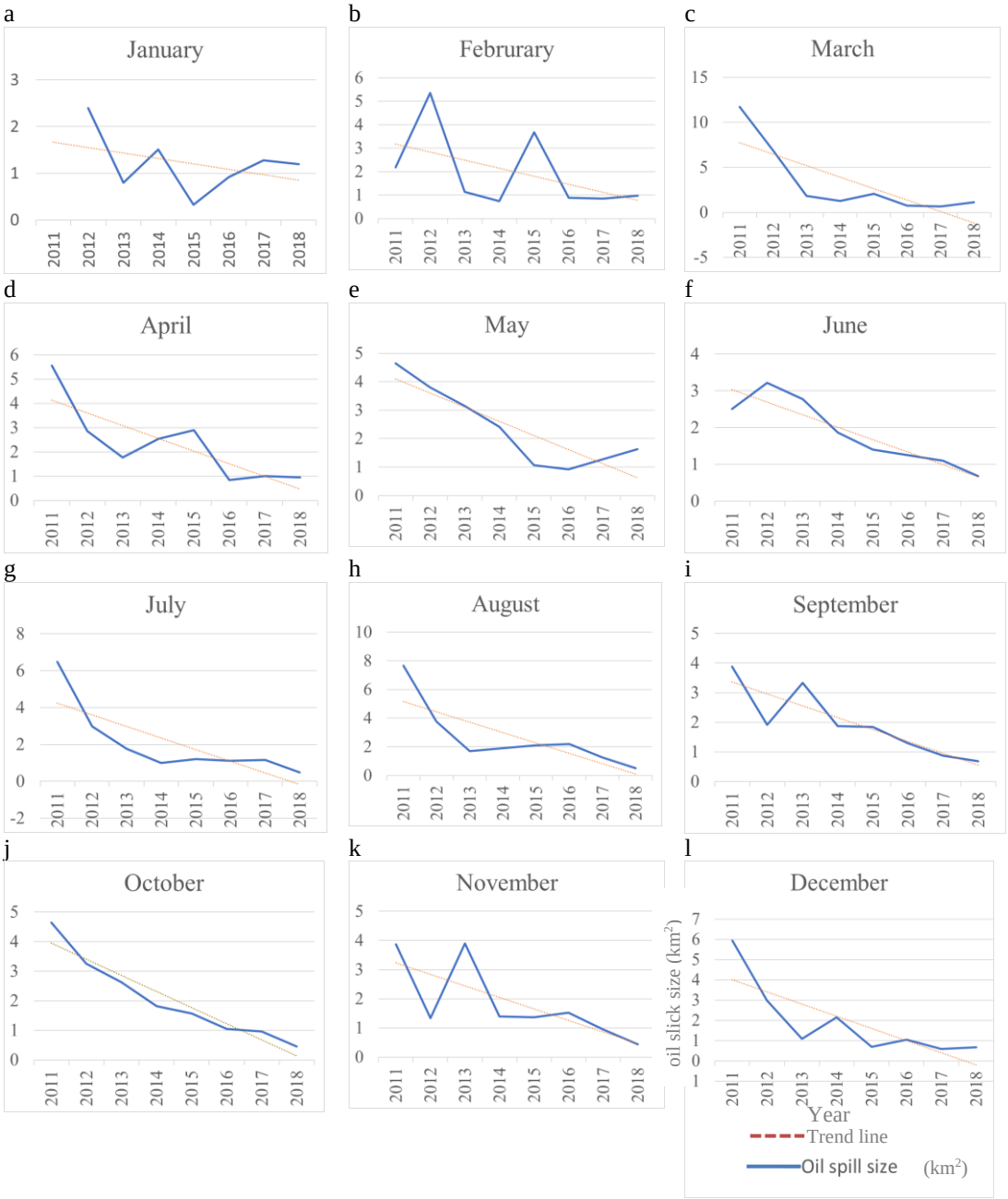

Figure 33: Spill size (km^2) trend plot, per month for 2011-2018. The median plot shows spill size per month for (a) January - (l) December from 2011 to 2018. The data for all months, (a) January,(b) February, (c) March, (d) April, (e) May, (f) June, (g) July, (h) August, (i) September, (j) October, (k) November, (l) December shows a general decrease in spill size over the years.

4.3.3.2 *Analyzing Seasonal variations on the number of oil spill alerts*

Figure 34a shows a distinct distribution over the year on the number of alerts. The result is a bell-shaped curve, indicating an increase in spills from January to a top in July, and there is a decreasing trend towards December. Seasonal data on the number of satellite images (Figure 34b), oil rig discharges of oil into the sea, Figure 34c, sailing/working hours of vessels, Figure 34d, and "climate factors" Figure 34e, are all considered factors that can influence the number of observations. Seasonal data on the number of satellite images (Figure 34b) is relatively uniform throughout the year. Oil

rig discharges of oil into the sea (Figure 34c) are relatively uniform throughout the year, although some lower discharge values during summer indicate a slightly bimodal distribution. The result of operating hours of vessels (Figure 34d) is also relatively uniform throughout the year. The data on climate factors, where the wind is the main factor, Figure 34e, this curve show a percentage of the time during each month, where the wind is within conditions for a satellite to be able to detect an oil spill at sea, show a unimodal distribution.

The following results are from Spearman's rank tests applied on the datasets (see Table 21), indicating a positive correlation (ρ=0.942) between alerts and climate factors (wind). The Spearman's ρ correlation coefficient indicates positive correlation at 1, no correlation at 0, and negative correlation at -1.
There is also a slight negative correlation between observations and discharges from oil rigs (ρ=-0.594).

Table 21: Spearman's rank test on seasonal distribution.

		Dependent variable	**Independent variables**			
		Number of alerts	**Number of images**	**Oil Discharge in tons by Oil rigs**	**Working Hours Ships**	**Climate factors**
N(data)		3684	7593	96	96	120 (10 years)
N(mean) regression		12	12	12	12	12
Mean (pr month)		38.375	79.094	23.505	283940.133	23.3333
Std. Deviation		20.756	7.185	4.841	13844.305	19.297
	Spearman's ρ		-0.203	-0.594	-0.357	0.942
	Significance		0.527	0.042	0.255	0.000

Figure 34: Histogram plot of the number of observations and possible influences. Figure (a) shows the distribution of observation over 12 months for the dataset on Radarsat-2 and Sentinel-1A/B. Figure (b) shows the distribution of the number of satellite scenes from the three satellites. Figure (c) shows the distribution of discharges for four of the oil rigs in 2015 and 2016, with most observations connected. Figure (d) shows working hours for four ship classes for 2015 and 2016, with most observations connected. Figure (e) shows the distribution of favorable condition for the use of chemical dispersants applied by ship within the study area (Strong parallels to the climate limitations that applies to radar satellites)

4.3.4 Test for spatial randomness

A Ripleys K function test has been done to oil spill alert observations (n=3694). The analysis has been run for ten different neighborhoods showing that oil spill alerts (incident) are not randomly distributed spatially. In Figure 35, the oil spill alert data (red line) shows clustering up to approximately 650 km neighborhood distance, as it is above the expected K line (black line) showing the random distribution. The observed K then crosses the expected K line and shows dispersed distribution from 650km to 900km. The two dotted lines in the figure are a confidence envelope where the tool is running random datasets (9), with the same number of incidents and same shape area (study area).

So by comparing the observed K line (red line) and the confidence envelope (two dotted lines), the spatial distribution of oil spill alerts shows clustering at all neighborhood distances from 1 km to 900 km, above the confidence envelope lines.

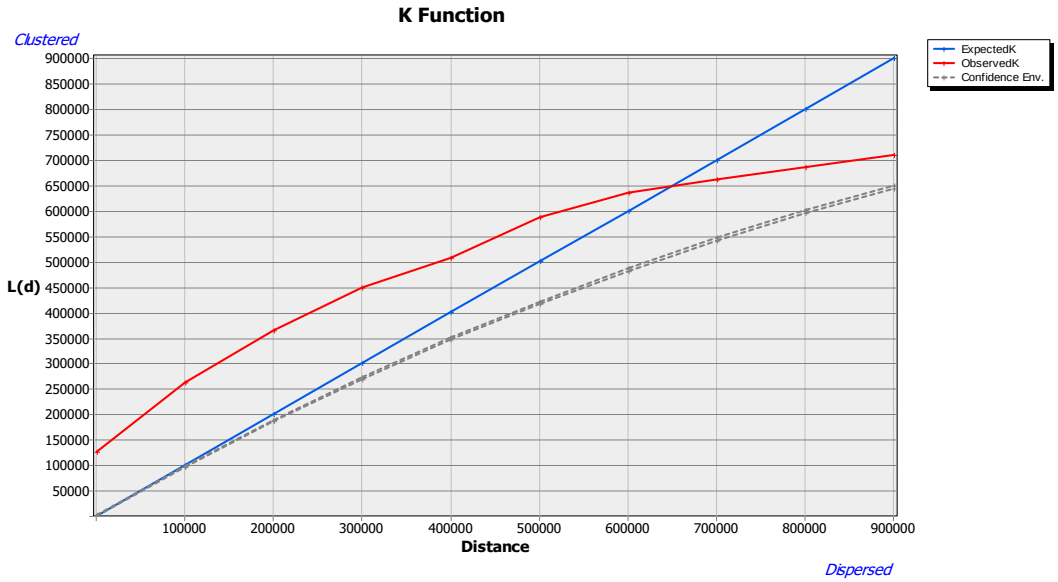

Figure 35: Ripleys K function test. Multi distance neighborhood plot from 1 000 – 900 000 m neighborhood distances.

4.3.5 Hotspot analysis all data and Ship + unknown as a source

The result where all (n=3694) oil spill alerts are included is shown in Figure 36. The figure shows three maps analyzed with different neighborhood distances. Figure 36a shows the maximum area (red and orange) with significant clustering, above 90% occurring (Z-score above 1.65). Figure 36b shows a map analyzed with half the neighborhood distancing used in map Figure 36a. The resulting map shows areas of higher Z scores than map Figure 36a, indicating more intense clustering. Figure 36c shows a map analyzed with half the neighborhood distancing used in map Figure 36b. The resulting map shows higher Z scores than map Figure 36b, indicating more intense clustering. This resulting map with very high z scores shows intense clustering around the fixed oil and gas surface installations offshore (black.

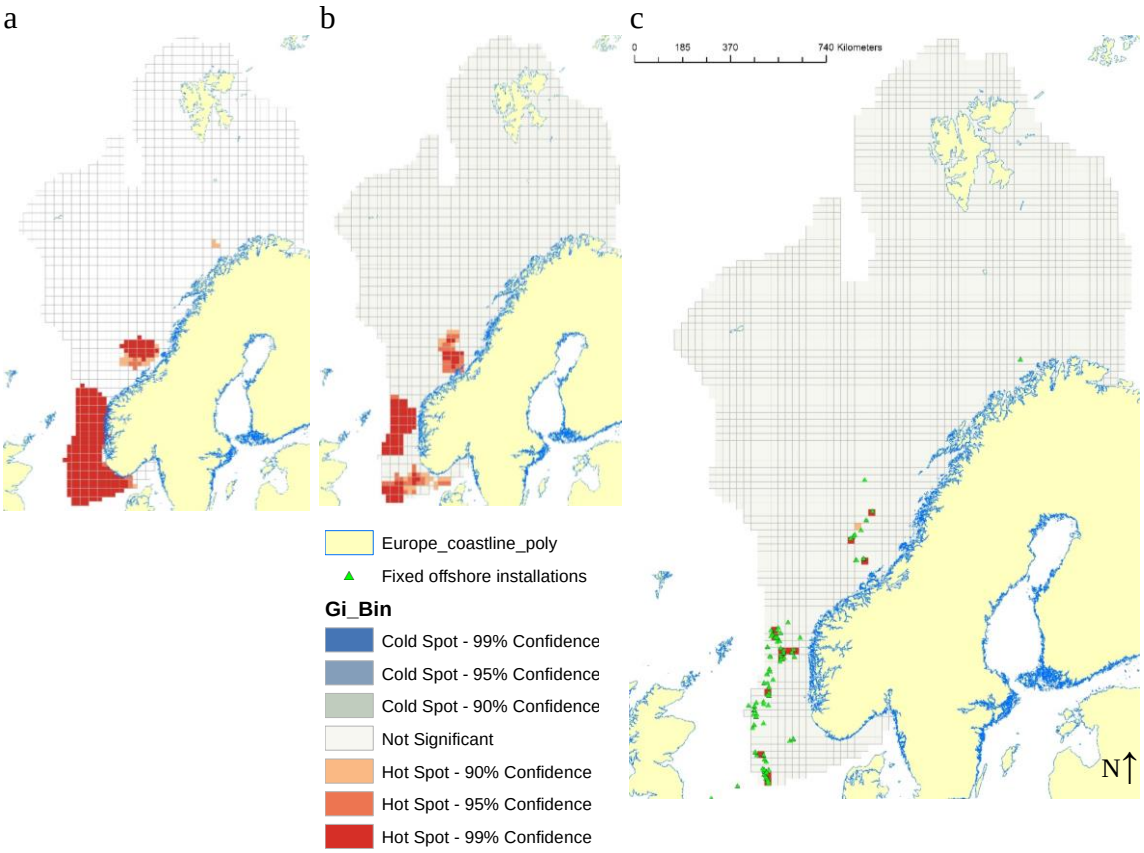

Figure 36: Maps of all observations, Optimized Hotspot Analysis with different distances to nearest neighbors, a), 160 km distance, b), 80km distance, and c), 25km including offshore fixed surface installations.

The optimized hot spot analysis is repeated on a dataset where all Rig source data is excluded from analyzing hotspots further.

The result where all (n=2190) oil spill alerts are included is shown in Figure 36. The figure shows three maps analyzed with different neighborhood distances. Figure 36a shows the maximum area (Red and orange) with significant clustering, above 90% occurring (Z-score above 1.65). Figure 36b show a map analyzed with half the neighborhood distancing used in map Figure 36a. The resulting map shows areas of higher Z scores than map Figure 36a, indicating more intense clustering. Figure 36c shows a map analyzed with half the neighborhood distancing used in map Figure 36b. the resulting map shows higher Z scores than map Figure 36b, indicating more intense clustering. This resulting map with very high z scores shows intense clustering in areas where ships have been connected to observations.

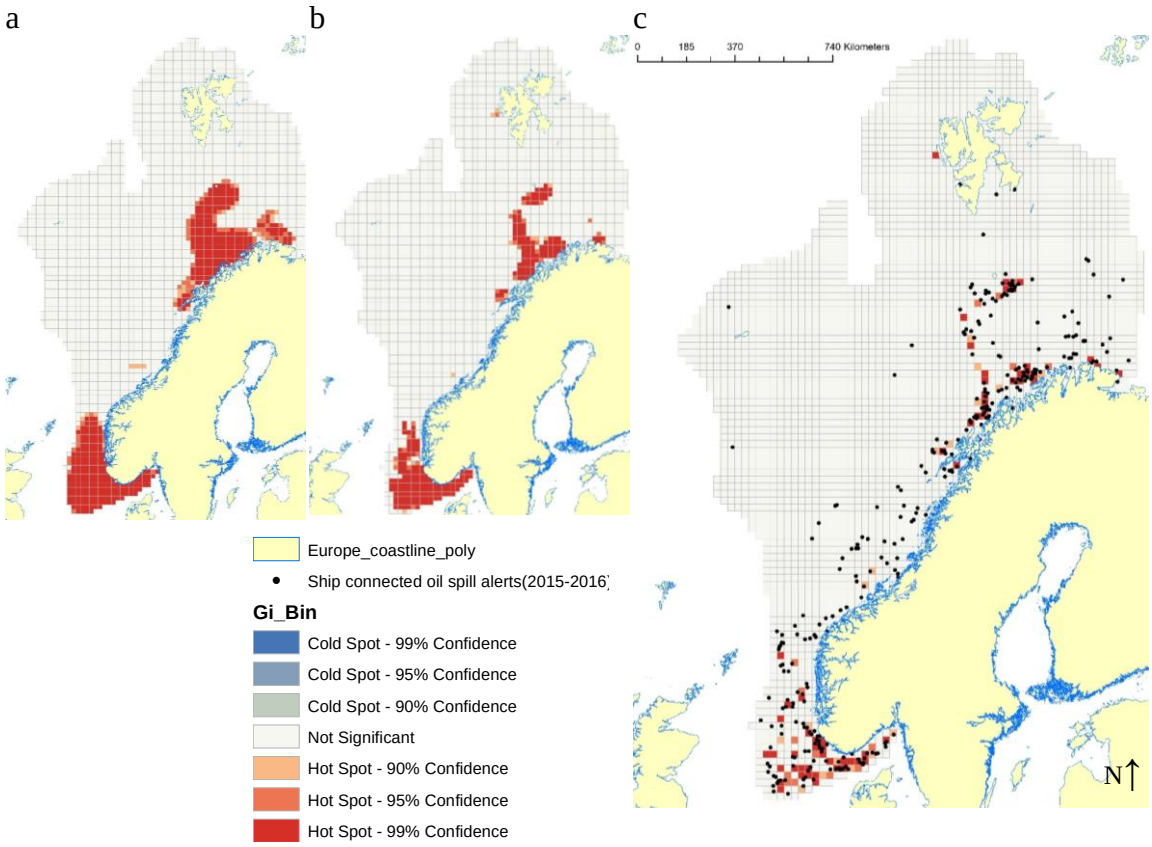

Figure 37: Maps of observations not connected to oil rigs. Optimized Hotspot Analysis with different distances to the nearest neighborhood, a), 88 km distance, b), 40 km distance and c), 20 km.

The last results are aggregating all the oil spill alert data (n=3694) into a raster, 10x10km grid. This is presented on the top of a footprint frequency raster with the same extension and alignment grid (10x10km). The results of this aggregation are shown in Figure 38. The map shows five different classes on the number of oil spill alerts, where all eight years of alerts are counted. The lowest class, 1-7 alerts over eight years, do not indicate a hotspot, and the other classes show different repetition strengths.

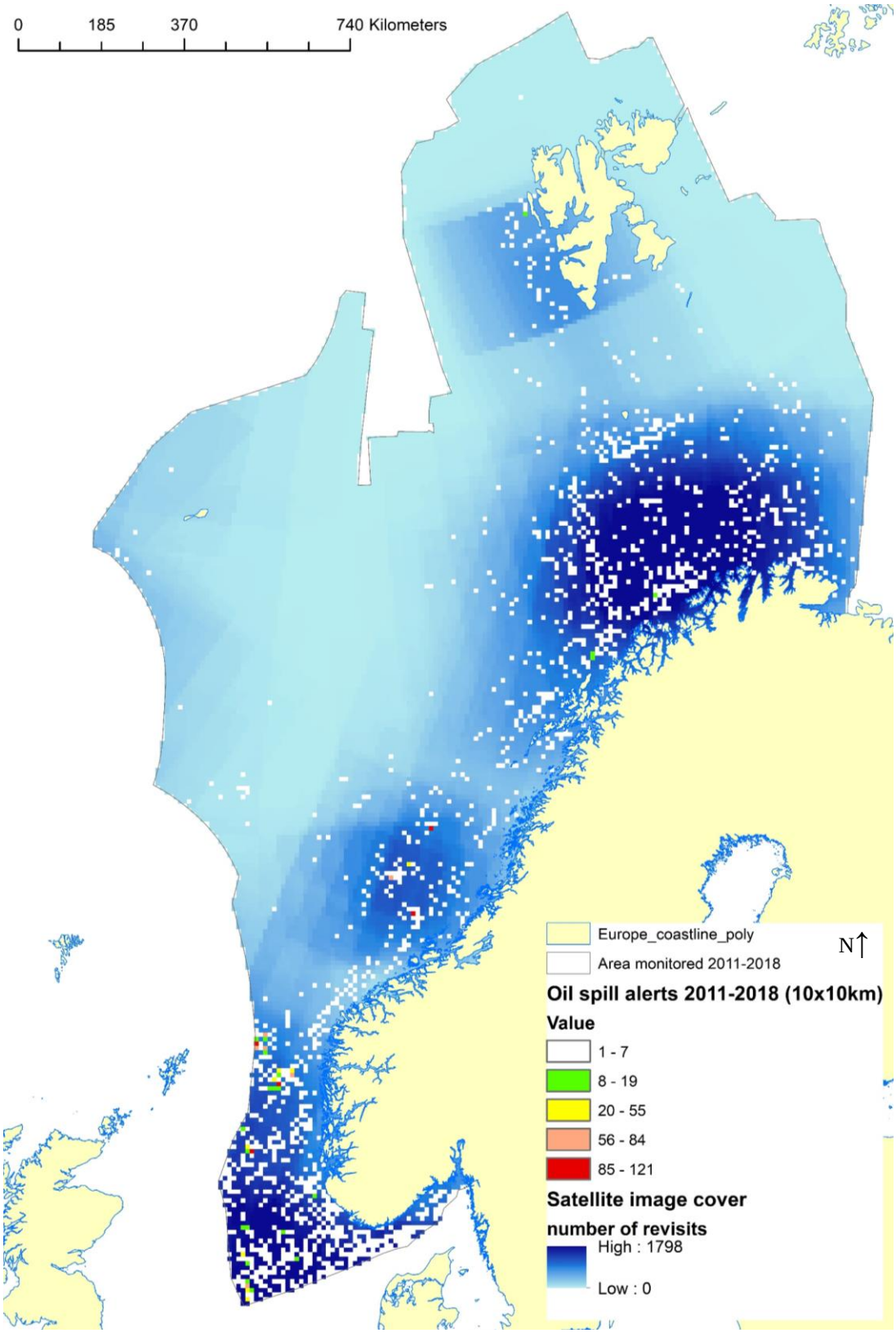

Figure 38: Raster map of observations and monitoring frequency. Map shows a 10 x10 km raster on total satellite footprint frequency, and the number of observations when aggregating observations on the same raster grid.

4.3.6 Hotspot analysis all data and Ship + unknown as source analyzed on impact.

When analyzing by observation size, outliers over 100km2 are subtracted from the dataset, as they will influence the result. Two maps are produced analyzing how clustering by size/impact of the observations are distributed (Figure 39 and Figure 40). The maps show hotspots in red where there is significant spatially clustering of high values on oil slick size. The maps show cold spots where there is significant spatially clustering of low values on oil slick size. Both maps also include a source layer on offshore oil and gas surface installations and a point layer of ships connected to oil spill alerts (the results of the 2015-2016 source analysis)

Looking at the pattern of Figure 39, where all observations (n=3679) are analyzed, the map show clustering of hotspots within six geographical areas. Many of these areas are outside the human activity (ship-based observations and offshore installations) shown in this map. However, cold spots in this map occur in and around the offshore areas, indicating clusters of small size oil slicks.

Looking at the pattern of Figure 40, where all observations connected to the ship and unknown origin (n=2175) are analyzed, the map shows multiple hotspots in six geographical areas. Many of these areas are still outside the human activity shown on this map. Here, no cold spot areas occur in and around the offshore areas, indicating clusters of small size oil slicks. The south area still indicates clusters of hotspots when the offshore linked alerts are removed from the analyzed dataset.

Both maps show pattern much the same areas of hotspots, but there are less significant hotspots in the results where all offshore connected oil slicks are subtracted (Figure 40)

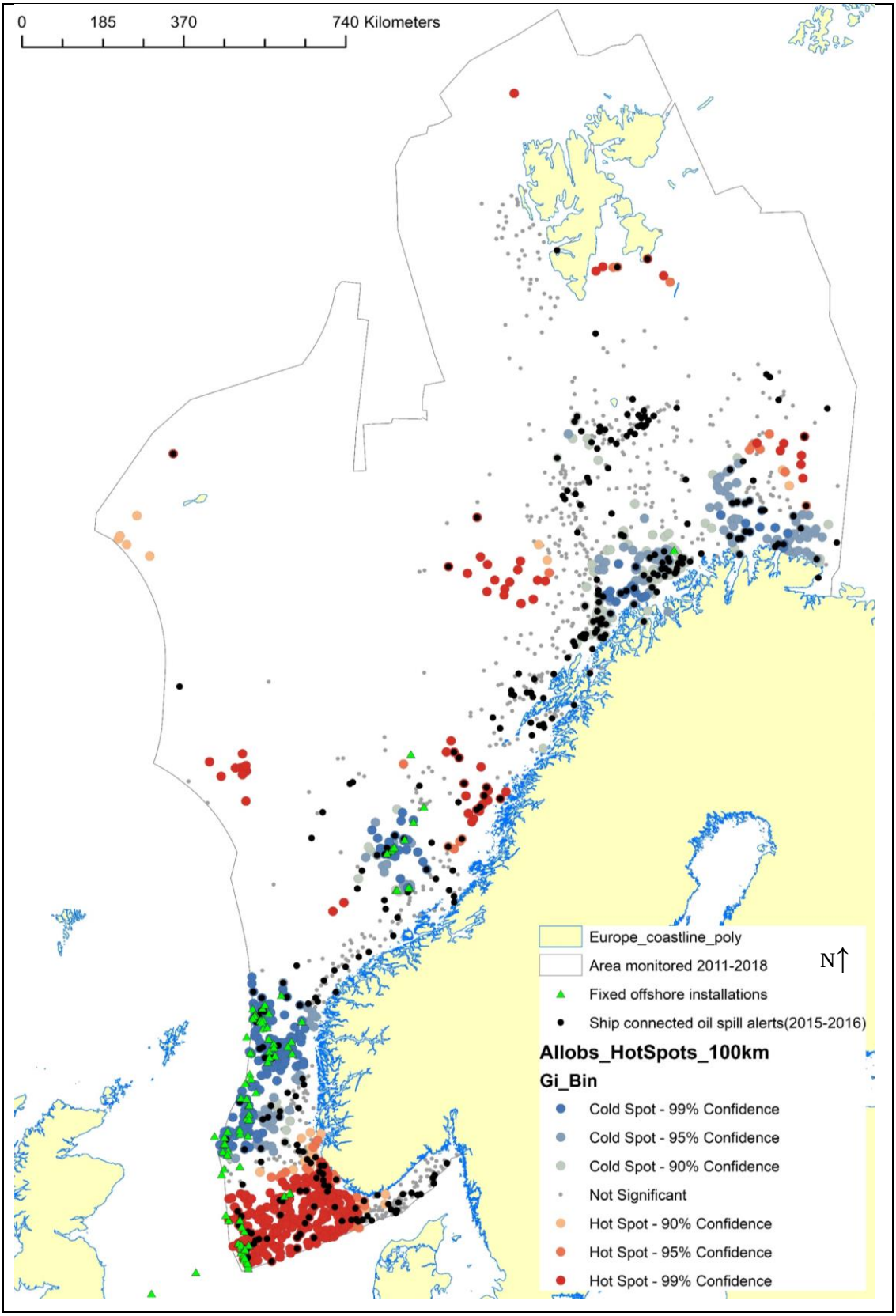

Figure 39: Hotspot analysis on the size of observation, all oil spill alerts. A map on all observations up to 100km2. Source data is added.

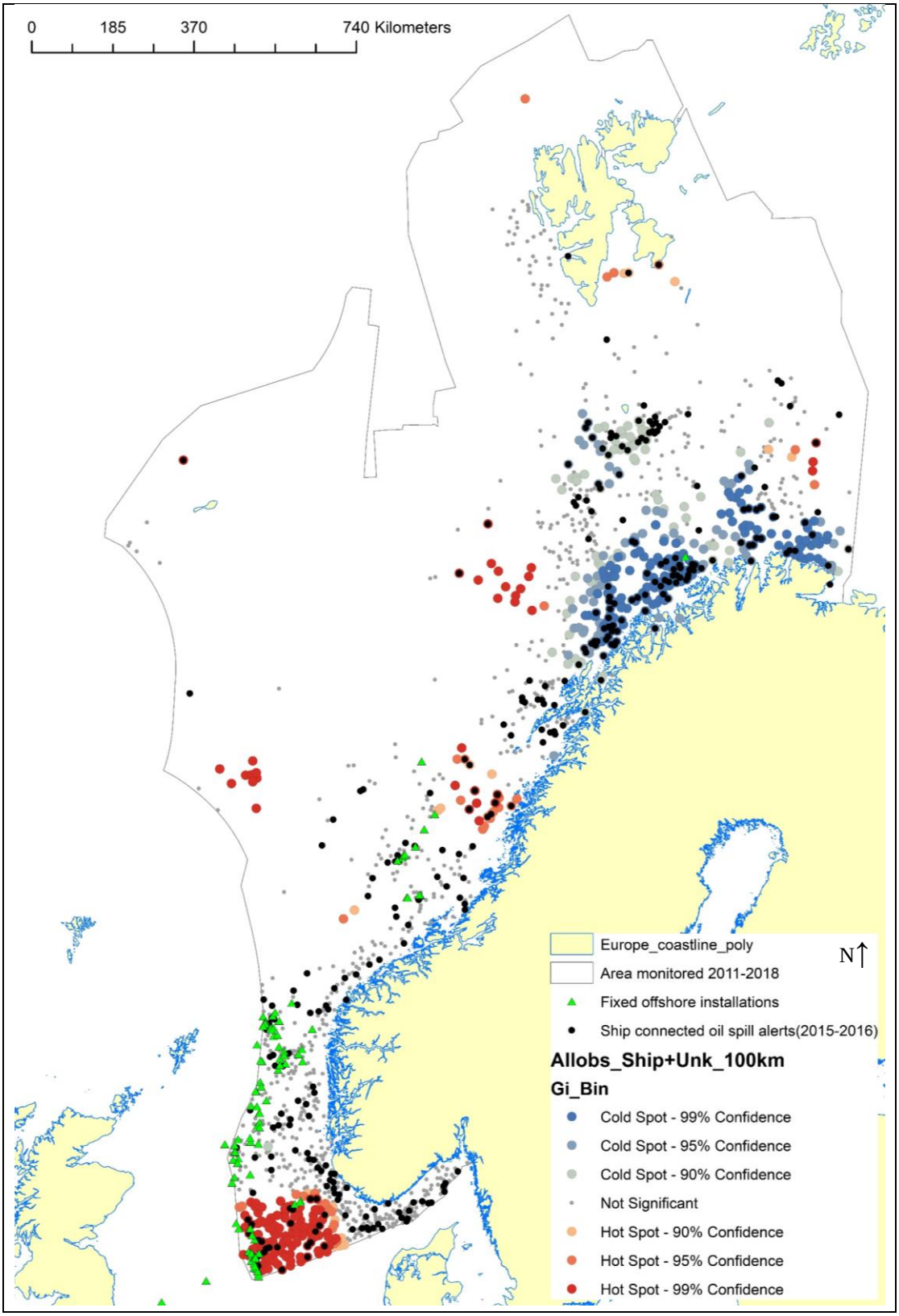

Figure 40: Hotspot analysis on oil slick size connected to ships and unknowns. Map to all observations with Ship and Unknown as the source. Source data is added.

4.4 Objective 3: To validate/verify the service provider's likelihood settings with historical observations.

The results of the confidence A and confidence B distribution on all Sentinel-1A/B and Radarsat-2 alerts for 2015 and 2016, concerning the source and observation size, are shown in Figure 41. The distribution shows 476 Radarsat-2 alerts and 542 Sentinel-1 alerts.

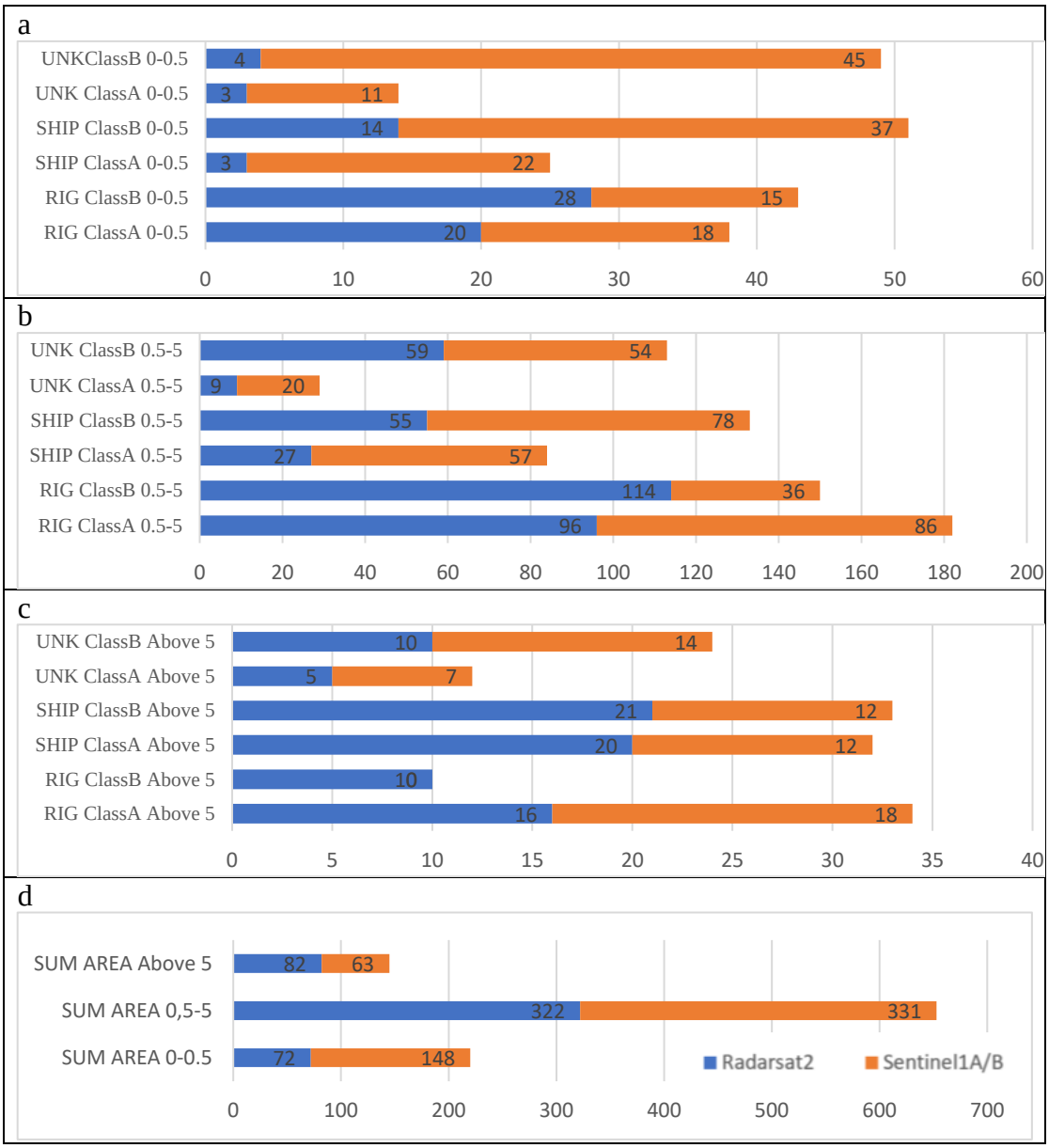

Figure 41: Source and classification results from 2015 and 2016. Alert and source data. The distribution show 476 Radarsat-2 alerts and 542 Sentinel-1 alerts for: Figure (a) A and B Confidence level for 0-0.5 km² Slick size, (b) 0.5-5 km², (c), above5 km² and (d) the sum of all observation within each size category.

The results of small-sized spills, 0-0.5 km² (Figure 41a and d), show approximately twice as many Sentinel-1 alerts than Radarsat-2 alerts. There are 77 confidence A alerts within this size category, most likely mineral oil, and 143 confidence B alerts, most likely ***not*** mineral oil.

The results of medium size spills, 0.5-5km², Figure 41b and d, show an approximately even contribution of Sentinel-1 alerts and Radarsat-2 alerts. There are 295 confidence

A alerts within this size category, most likely mineral oil, and 396 confidence B alerts, most likely ***not*** mineral oil.
The results of large-sized spills, Above 5km^2, Figure 41c and d, show a slightly smaller contribution of Sentinel-1 alerts to Radarsat-2 alerts. There are 78 confidence A alerts within this size category, most likely mineral oil, and 143 confidence level B alerts, which are most likely ***not*** mineral oil.

Furthermore, the results of how confidence levels relate to sources are shown in Table 22. The probability of an oil spill alert being mineral oil alerts is estimated/calculated. Oil and gas industry connected oil spill alerts mineral oil probability derives from the *in situ* data presented in section 4.3.2. The ship and unknown mineral oil probability are calculated, and the red rows in Table 22 show this probability.

In situ data show that 95% of oil spills connected to RIG are probably mineral oil Hence, 95% of the alerts connected RIG should be a confidence A alert (Most likely mineral oil). Source analysis results (Figure 32) show that 16% of oil spills connected to SHIP are most probably mineral oil. Hence 16% of the alerts connected SHIP to should be a confidence A alert (Most likely mineral oil)

The other probability calculations in Table 22 are based on the actual alert confidence settings connected to the alerts by the service provider. By calculating these probabilities, the alert classification performance can be evaluated.

Figure 42 shows how all results are distributed along a likelihood curve.

First, looking at the RIG alerts data in Table 22, the red row being the ground truth of an observation being mineral oil is placed on the curve at 0.95 probability. The results of the confidence A calculated in all alerts connected to RIG as source shows a ratio (probability) of 0.63 for Sentinel-1, 0.55 for Radarsat-2, and all satellites 0.62.

Next, looking at the SHIP + OTH alerts data in Table 22, the red row being the ground truth of an observation being mineral oil is relatively small and placed on the line at 0.16 probability. The results of the confidence level A calculated in alerts connected to ship and unknown as source show a ratio (probability) of 0.41 for Sentinel-1, 0.34 for Radarsat-2, and all satellites 0.42.

Another fascinating result is looking at all data delivered (2011-2018) to NCA by all satellites. This calculates to 49.9% (1835 alerts) of the observations is Confidence A, and 50.1% (1844 alerts) is confidence B alerts (the sum of the two blue rows in Table 22)
Also, for alerts delivered in 2015-2018 by the three satellites Radarsat-2, Sentinel-1A, and Sentinel-1B, 48.4% are confidence A alerts, and 51.6% are confidence B alerts (the sum of the two green rows in Table 22).

Further on, the result of mineral oil/No oil for the same period (2015-2018) 1358 /2763, resulting in a probability of 0.49 (sum of results for 2015-2018 in Figure 32).

Table 22: Distribution of the number of alerts for the confidence level. Confidence A and B for Radarsat-2, Sentinel-1A/B, and all satellites were sorted for RIG and SHIP+UNK as sources.

Source	Period	Alerts	Satellite	Sentinel-1A/B			Radarsat-2			All satellites		
			Observation Size\probability\ Confidence	**A**	**B**	**P= A/AB**	**A**	**B**	**P=A/AB**	**A**	**B**	**P= A/AB**
RIG Alerts	**2015-2018**	**N=2763**	0-0.5km^2	137	122	0.53	21	31	0.40			
			0.5-5km^2	355	185	0.66	115	83	0.58			
			Above 5km^2	41	6	0.87	18	11	0.62			
			All sizes	533	313	0.63	154	125	0.55	687	438	
			P source *In situ* based M Oil/no M oil			0.95			0.95			
	2011-2018	**N= 3679**	All Sizes							928	574	0.62
SHIP + UNK Alerts	**2015-2018**	**N=2763**	0-0.5km^2	141	296	0.32	10	35	0.22			
			0.5-5km^2	294	386	0.43	66	164	0.29			
			Above 5km^2	88	61	0.59	50	47	0.52			
			All sizes	523	743	0.41	126	246	0.34	649	989	
			P Source M Oil/no M oil 273//1678			0.16			0.16			
	2011--2018	**N=3679**	All Sizes							907	1270	0.42

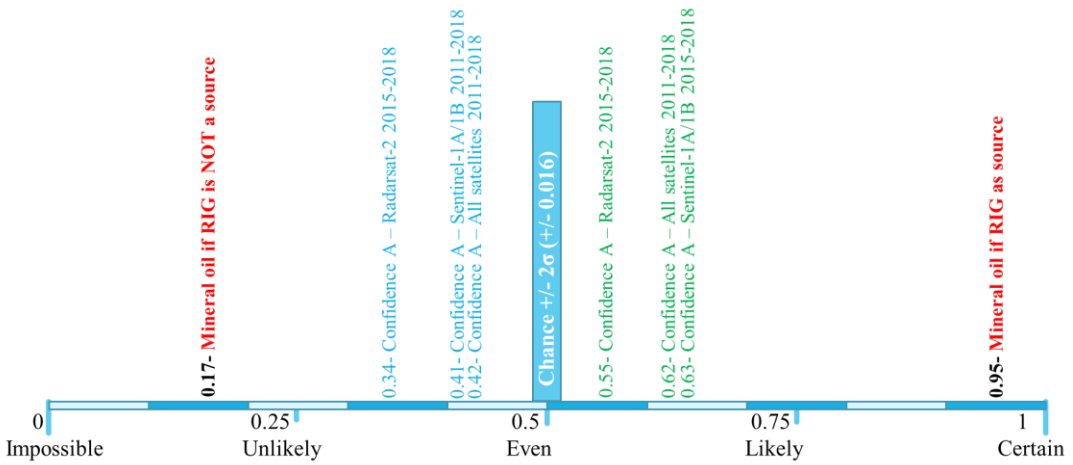

Figure 42: Likelihood line for an observation being mineral oil. Observations confidence A likelihood where Rig (green) is Source and Ship + unknown (blue) is the source.

5 Discussion

The main objective of this study has been to analyze an unexpected increase in oil spill alerts in Norwegian waters since 2015. The increase in oil spill alerts is not supported by other surveillance data (*in situ*), such as surveillance flights within the area of the Bonn Agreement (Bonn_Agreement, 2018a). Two new satellites with better resolution were introduced into the service in 2015 and 2016. *EMSA, as one of the major oil spill alert service providers, points towards this introduction of Sentinel-1 A/B satellites as a possible cause, with more and smaller spills detected which would not have been detected previously (EC, 2018).* However, an increase in oil spill alerts is not necessarily connected to mineral oil, even though this is the oil spill alert service (Alpers et al., 2017, Fingas and Brown, 2018).

A hypothesis was introduced along with the objectives of the study:

> H_0: The increase in alerts is not due to increased "mineral oil" at sea.

5.1 Intensity analysis of oil spill alerts.

The main problem stated in the introduction was based only on a count of oil spill alerts received by the end-user, not accounting for variation in monitoring cover and frequency by the satellites used. There was a need to recalculate the problem of oil spill alerts in a measure also accounting for satellite cover and frequency.

The new measure of the problem, where a ratio of spills per area observed is calculated, confirms and exceeds the 249% increase found by counting oil spill alerts from 2015 to 2018. The new calculated increase in the ratio is 297%.

This ratio uses all 3694 oil spill alerts, accounting for all 9442 satellite scenes analyzed within the study area from 2011 until 2018. By producing a ratio based on geographical analysis and the actual cover (footprint) of all satellite images, the result also accounts for areas of images outside the study area (other nation's waters or land areas). This measure will be "more correct" than only counting oil spill alerts and more correct than calculating a ratio of the number of spills per image.

The fact that the monitoring is not uniform in frequency or area covered has to be considered in all parts of the analysis done in this thesis. However, by analyzing and focusing the results on relative change rather than absolute measurement, this bias is accounted for or discussed further in different analyses of this study.

The most surprising finding is that there is still a large increase in ratio from 2017 to 2018, where the proportion of Radarsat-2 and Sentinel-1 for these two years is quite similar (Figure 21). *In situ* measurements of actual oil observations (Bonn_Agreement, 2018a) and the oil and gas industry's discharge of mineral oil (Norsk_OljeogGass, 2019) do not indicate any shift or increasing trend. The increase seems to be related to other factors.

5.2 Objective 1: To determine if the increase in alerts is due to the use of Sentinel-1.

5.2.1 Visual analysis of Sentinel-1 and Radarsat-2 radar images

The visual analysis clearly shows the difference in performance between Radarsat-2 and Sentinel-1A. One can visually observe that Sentinel-1A presents a clearer oil spill signature on a smoother surrounding area (backscatter/noise), hereby also able to detect smaller oil spills than Radarsat-2.

The higher resolution and all-over performance of Sentinel-1A show that Sentinel-1A can present a radar image where very small oil slicks can be identified as a possible oil spill. *One has to bear in mind that all alerts are visually analyzed/confirmed by the service providers. Hence, the visual performance is essential for connecting a suspected feature to be a possible oil spill alert and then setting the confidence level of the alert as mineral oil.* By visually analyzing the two images, the flattening of the capillary waves due to the oil is apparent in both images as a dark feature against a homogenous surrounding area.

In these two images, one can also observe the low observation size threshold, where Sentinel-1 can detect and differ from Radarsat-2, where the same area blends into the backscatter/noise. Because of this, and as the recognition that images are analyzed manually by a radar operator, images from Sentinel-1A can present radar images where smaller possible oil slick features will be found compared to Radarsat-2. This result supports that resolution and smaller spills can be part of the overall increase in the number of oil spill alerts as discussed as one likely cause discussed in 1.1 Rationale. EMSA also points at resolution as a possible cause of the increase (EC, 2018).

This visual analysis is very valuable, as one can directly compare the performance of the two instruments. Also, by having *in situ* data on the substance being mineral oil, this rare example shows a “ground truth” of the results by these two satellites in an oil spill service.

Furthermore, this is an example where further work on comparing satellites in “operational mode” on verified *in situ* mineral oil data could benefit end-users, service providers, instrument owners/designers, and researchers. Such valuable research has been done on incidents with oil spills and trials (Del Frate et al., 2011, Garcia-Pineda et al., 2017, Garcia-Pineda et al., 2013a, Garcia-Pineda et al., 2013b, Ivanov, 2010, Skrunes et al., 2012, Skrunes et al., 2015). However, many of these studies lack satellite data and overlapping *in situ* data, or the radar mode is different from the used/available operationally. For end-users, and service providers, a comparing study on differences in operational mode data, would be beneficial. Using well-known static sources (platforms) that discharge mineral oil as part of the production process, with visible mineral oil on the water under some weather conditions, might be a good subject for further study on overlapping radar data.

By resampling Radarsat-2 radar scene resolution to Sentinel-1A resolution, pixel-by-pixel analyses could give further insight into performance, limitations, and difference.

5.2.2 The detection performance of the instruments

Sentinel-1 performs significantly better than Radarsat-2 on small oil spills, detecting more small spills, indicating that the large increase in the number of spills from 2015 does not indicate a similar increase in "environmental impact" of the increase consists of small size possible oil spills.

The main result in this analysis shows that Sentinel-1 detects significantly more oil spills that cover less than 1 km^2 of the sea surface than Radarsat-2. On oil spills larger than 1 km^2, no such difference in performance is detected.

Regardless of the big increase in the number of spills after the introduction of the Sentinel1 satellites in late 2015, also detected at the European scale, there have not been any significant studies conducted regarding Radarsat-2 vs. Sentinel-1 on the ability to detect oil spills.

The *Sentinel-1A and 1B instruments have the same sensor* characteristics (ESA, 2016), though operated on different satellites, following the same polar orbit, 180 degrees apart. Radarsat-2 (Maxar_Technologies_Ltd, 2018) has a lower spatial resolution than Sentinel-1, flying at different altitudes. To measure how the two (three, Sentinel-1A and 1B and Radarsat-2) instruments/satellites perform against each other, a statistical test on the instruments' ability towards observation size is performed in two steps.

The change/shift in the number of observations per area monitored (Figure 21 b) is lined up with the introduction of two new satellites, Sentinel-1A and Sentinel-1B. These two satellites, together with Radarsat-2, have worked in parallel since late 2015, and those three satellites include 79% of all satellite data in the study (see Table 7).

The dataset is considered suitable for doing an oil spill size analysis of significance between the different instruments.

The first step was to establish the distribution of the data, showing no normal distributed data on oil spill size, and then to choose and perform a suitable test of significance.

A correlation test on oil slick size between the three satellites/instruments is applied to study the difference in performance. As a test for normal distribution does not support normal distribution, a Mann Whitney U test was chosen (rank test) is applied on all three instruments.

The result from the Mann Whitney U test between the two Sentinel-1 instruments shows no significant difference in performance regarding all observation sizes. This is as expected, as Sentinel-1A and Sentinel-1B carry the same instrument, flying the same altitude, following the same orbit, only 180 degrees, which means when 1A passes the north pole, 1B passes the south pole (ESA, 2019c, ESA, 2016).

The result from the Mann Whitney U test between the Radarsat-2 and the two Sentinel1 instruments together shows a significant difference in performance regarding the observation sizes. The difference is shown in Figure 26, organized by

rank from small observation size, where Radarsat-2 shows fewer small observations than Sentinel-1A/B. *This is an essential and significant finding of this study, and it confirms the assumption that the difference in radar resolution contributes to the increase in the number of observations.* This is also supported by EMSA, which points towards resolution as one possible explanation to the registered trend shift registered in European waters (EC, 2018).

A spatial analysis of the footprint of the three satellites is done for 2015 - 2018. The resulting ratio plot (Figure 27) clearly shows the impact of Sentinel-1A and Sentinel-1B observations and their contribution to the increase.

Sentinel-1 and Radarsat-2 show a significant difference in detecting oil spills by size, including all spill sizes. The data are categorized into size intervals to see in what spill size category significant difference is detected. The Mann-Whitney U test shows only significant differences in the observation size interval of 0-1km^2. *This proves that Radarsat-2 and Sentinel-1 perform significantly differently on small oil spills.* When analyzing size intervals over 1km^2, none of these show a significant difference due to observation size. This is also expected when detecting an observation over 1km^2. The area will probably vary some in size between the representation of the observation instrument, but not significantly. Especially towards the edge of the observation, it might appear differently. Still, an observation larger than 1km^2, if it is a homogenous "slick" and within acceptable wind limits (Fingas and Brown, 2011), it will be visible for Radarsat-2 and Sentinel-1A/B due to their resolution, Table 1. The visual analyses (section 5.2.1) support this result and show that there are only minor differences in the overall "oiled" area of the two satellites' radar images.

A result that proves the difference in performance and how the Sentinel-1 and Radarsat-2 differ is an important result usable for further studies on environmental impact. It is also applicable operationally for the end-user regarding how and where one could apply filtering in alert level if this is implemented (Ferraro et al., 2010). In simple terms, with limited resources, one could decide not to follow up on observations smaller than 0.5km^2, based on an environmental impact assessment.

One possible bias, and maybe a subject for further studying, is if Sentinel-1A/B with its higher resolution and instrument characteristics have the same cut-off regarding the ability to detect "oil" in low and high wind? Wind does influence the ability to detect oil on water, and the "environmental window of application" is considered between 1.5 m/s and 10 m/s (Fingas and Brown, 2011). *Is this still applicable for Sentinel-1, or does it perform differently at winds over 10m/s?*

As this study is based upon alerts, where the geographical feature is not the satellite image itself, but a representation of the "oil slick" as a polygon, with the correct shape, area, and orientation, there is a need to explore further how the difference appears in multiple radar satellite images. This study only explores the visual difference in performance and characteristics by one example (Figure 22 and Figure 23).
Still, to have this one example, with an *in situ* verified mineral oil observation, both by the platform right after the detection and by surveillance aircraft (+ 20 hours), and parallel satellite images is very valuable and demonstrates the whole essence of the results in this thesis.

5.3 Objective 2 To Quantify oil spill type, size, and variability

5.3.1 Oil spill origin (source analysis)

Mineral oil spills in Norwegian waters are most connected to human activity as discharges from offshore installations and shipping. Having a source connected to the oil spill alert, down to offshore installation name and ship size and type, has revealed new knowledge, especially for the impact of shipping and the type of ship connected to oil spills alerts.

When looking at each source from 2015 to 2016, the number of oil spill alerts from the oil and gas industry has increased by 79%. Ships do by far contribute most to the increase in observations with a 271% increase. There is also a large increase in observations not connected to any source (189%). However, the impact per oil spill alert is decreasing due to smaller oil slick sizes for both the oil and gas industry and ships, where the average oil slick size is decreasing. The oil slick size where no source has been found is increasing (Table 15).

This indicates less mineral oil per oil spill.

The connection between source and observation is needed to estimate the most likely substance of the observation. Data on substance, and the mineral oil distribution between the three likely sources, ship, rig, and unknown, can be used for estimating the impact of the increase in oil spill alerts. The two years of data, 2015 and 2016, were chosen as the change/shift is registered (Figure 21). These two years include the implementation of Sentinel-1A/B, in parallel with the use of Radarsat-2. It is also two years of good coverage, with 3023 satellite images, see Table 7. Also, in this period, the availability of source data was good.

In this part of the analysis, the method and the assumptions are well worth discussing, as the source data format and content influence how the method is developed.

The method used to connect oil spill alerts to the most likely source is based on the activity near the oil spill at the time of the satellite image acquisition. Fixed oil and gas surface installations connect platform and alerts with a 3000 m buffer analysis on polygon alerts and 6000 m buffer analysis on point alerts. This assumption is documented in the method section.

The method of moving possible sources (ships) is more complex, as both the source and the oil spill are moving, and the satellite alert is only status at an exact given time. A highly generalized model is used to analyze a 2 nautical mile buffer over 6 hours to connect the ship to oil spill alerts. The assumptions are also well-documented in the methods section.

Both these general assumptions are considered reasonable estimates, where the dynamics regarding the oil, weathering of oil, oil drift, and environmental parameters factors are taken into account as part of the method settings. The connection between source and observation within these assumptions is regarded as of high likelihood. As discussed in the background chapter, a mineral oil discharge within the study area has a very high likelihood of being connected to human activities as Oil and gas industry and shipping. Also, some “oil spill lookalikes” originate from human activities, where other oil types will appear on the sea surface due to (legal) activities from some ship

categories. However, all assumptions will yield a bias in the results. *However, as the bias will perform quite equal on the results compared in this study, the resulting relative difference should be considered a good measure when analyzing trends.*

As the oil and gas industry offshore discharges oil into the sea as part of the day-to-day production, more images over such offshore areas will most likely increase the number of observations. So if the sea conditions are suitable for satellite detection, and the platforms injection system of produced water usually causes visible oil with the same conditions, the monitoring frequency will also affect the number of oil spill alerts. In the context of *in situ* measurements, Bonn Agreement surveillance flights have been conducted for many decades on Oil and gas industry in the North Sea (Tour d'Horizon Flights). These remote sensing flights collect *in situ* measurements of mineral oil on the sea surface. The surveillance frequency in the offshore industry is limited to once every two months. The decreasing trend in shipping within the Bonn agreements flight data (chapter 1 Introduction) does not apply to offshore industry surveillance flight data. There is no clear trend in the surveillance flight data, and the Bonn agreement has concluded that weather and sea state around offshore installations influence the data and findings. Low wind conditions show many observations by surveillance aircraft, and high wind conditions might give no observations (Bonn_Agreement, 2018b, Carpenter, 2007). Natural dispersion into the water column and weathering of oil and sea state contribute to this (Fingas, 2016). The trend from *in situ* measurements on actual discharge is decreasing in the same period. Reports from the industry to the regulators show a decrease from 1900 tons of oil in 2015 to 1800 tons in 2016 (Norwegian_oil&gass, 2019). The increase registered on oil and gas industry connected observations might be random, and this trend is further discussed in section 5.3.5.

Ships contribute, by far, most to the increase in observations by 271%. Regarding impact from ships to the environment, discharges into sea and air from ships are regulated in MARPOL (IMO regulations). As expected, the two ship categories with both the highest frequency and impact are fishing vessels and chemical tankers, see Table 16.
Both are allowed to discharge non-mineral oils, like vegetable oils, animal oil, fish waste (MARPOL Annex V and Annex II needed). Examining the impact, fishing activities, and "Noxious Liquids" from tank cleaning hold 517km^2 of the 617km^2 increase. Fishing vessels and chemical tankers are set to OTH oils, both due to regulations and in situ follow-up data from surveillance aircraft. The Surveillance aircraft has intensified the fishery patrolling the last three years, and in 2018, well over 400 flights hours were aimed at fisheries, also controlling for mineral oil spills. No mineral oil spills were detected when looking at 2016-2018, except for fishery vessels involved in accidents (NCA, 2016a, NCA, 2017b, NCA, 2018b).

The increase connected to the rest of the ship categories is assumed to be mineral oil. These ship types are not allowed to discharge oil visible on the sea surface(IMO, 2019), ref 2.4.1.1, and the total increase from 2015-2016 is 100 km^2.

In the category unknown, no source is likely to have caused the observation. These observations are most likely to be something else than oil. There is a large increase in the number of observations not connected to any source (189%). Examining the distribution between SHIP, RIG, and UNK per year, Figure 28 shows that the UNK

observation category has a small increase from 22% of all observations in 2015 to 24% in 2016. The size per observation increases the number of unknowns. The impact of unknowns is also discussed further regarding the spatial trend analysis, section 5.3.3. These oil spill alerts are very interesting in terms of origin and if they tend to cluster.

5.3.1 Oil spill size and type (substance impact)

Even though oil spill alerts per area monitored have increased by nearly 300% from 2015-2018, the mineral oil affecting the sea surface is close to the same in 2018 as in 2015.

The results from the overall impact of mineral oil on the environment show a marginal increase of 2.65% when comparing the average impact of the years 2013-2015 to the average impact for the years 2016-2018.

The overall impact is measured by the observation's size and the most likely source. One can assume the substance (oil type) by knowing specific data on the source, like the type of ship. Data from two years is in-depth analyzed, and data from these two years are also used to estimate/assume some impact parameter for the rest of the oil spill alert dataset.

All the oil spill alerts in the study are analyzed towards oil and gas installations as a source. The connected oil spill alerts are adjusted by a 0.95 mineral oil probability (from *in situ* data) (Table 18). The impact is the sum of observation sizes for each year. This is the most reliable data in the dataset, as there is a good amount of validation data on mineral oil connected to oil rigs. One must also consider a discharge of mineral oil as long as there is production at the platform. The source is also static, so the link between observations and source connection is of high likelihood.

When analyzing Ship as a source, this will impact mineral oil and other oils. Follow-up *in situ* data indicates that there is a good estimation to let chemical tankers and fishing vessels relate to other oils regarding the activity and connection to the observations. Regarding fishing vessels, there is a large increase in observations.

Oil spill alerts connected to ship as a source outside the period analyzed in the source analysis (2015-2016) are estimated. This estimation assumes the yearly distribution between ships and unknowns to follow a constant ratio calculated from the 2015 and 2016 data. There is a shift in the main used satellites in the service and data, from Radarsat-2 in 2015 and the years before, to Sentinel-1A/1B from 2016 and forward, Table 7. Based on this, two distribution ratios are calculated. The ratio from 2015 data is applied on 2011-2014 oil spill alerts. The other ratio is calculated from the 2016 data and applied to the 2017-2018 alerts. Similarly, an oil type ratio constant, where a ship is assumed to be the source, is calculated and applied to the dataset.
The result is shown in Figure 31, with a total mineral oil impact of 695 km^2 in 2018. Analyzing the shift, registered in 2016, Figure 21, the average mineral oil spill for 2013-2015 is 754 km^2 and from 2016-2018 is 774km^2. This indicates a marginal increase in impact after the shift. There is also a decreasing trend from 2016-2018, with an impact of 695 km2 in 2018. In the same periods, the average number of

observations for 2013-2015 is 325, where for 2016-2018 is 825, Table 6. There is some variation in the six years of data within the calculation. *Using the average of three years before Sentinel-1 against the average of three years including Sentinel-1, the impact of variation in the data is minimized.* The average increase in the number of oil spill alerts spills is 154%, where the impact (mineral oil spill area) is only 2.65%.

Based on the average impact of mineral oil, the null hypothesis has to be rejected and that there is probably a marginal increase regarding the impact of mineral oil on the sea. Still, this increase is marginal, with 2.65% against the average 154% increase in the number of observations.

On the human activity for the period analyzed, there is an increasing trend for shipping in operation hours, Figure 5. The Oil and gas industry has a decreasing trend on oil discharge into the sea in the same period (Norwegian_oil&gass, 2019).

Regarding these two trends connected to source, one could suspect a slight increase in impact towards shipping as a source and a slight decrease towards Oil and Gas industry as a source. The results do not contradict such a scenario. However, there is a difference in coverage and monitoring frequency throughout the dataset, and this also needs to be considered. There is also a drop in the number of observations (Figure 21) and impact in 2015, Figure 31. There is no apparent cause for this drop when analyzing the available data in this study. The low number of oil spill alerts in 2015, in reference to 2014 and 2016, holding a higher number of oil spill alerts are also registered by EMSA CleanSeaNet for the whole North Sea basin (Bonn_Agreement, 2015, Bonn_Agreement, 2016, Bonn_Agreement, 2017).

5.3.2 Oil spill variability analysis (non-spatial methods)

5.3.2.1 *Analyzing oil spill alert observation size (km2) distribution*

The observation size of the oil spill alert has a decreasing trend counteracting the "impact" of the increasing trend of the number of alerts.

Analyzing the temporal trend from 2011 until 2018, including the seasonal resolution by month on median observation size, the trend is decreasing on observation size.

Median observation size is used to avoid the influence of outlier observations in the dataset. There have not been any major oil spills within the study area in 2011-2018 that would cause large areas of oil at sea (ITOPF, 2018). Therefore, observation size over 100 km^2 is considered to be an outlier concerning mineral oil.
The overall trend from 2011 until 2018 tends to support the null hypothesis, where observation sizes decrease (Figure 33).

5.3.2.2 *Analyzing Seasonal variations on the number of oil spill alerts*

The wind influence on the radar satellite's ability to detect oil spills is very clear when examining the monthly distribution on oil spill alerts in this dataset and average wind month by month within the study area.

The main result is that the climate factor, wind, and sea-state most influence the distribution of oil spill alerts.

The seasonal trend in the dataset shows a bell-shaped curve in the number of observations from January until December (Figure 34 a). The number of satellite scenes is relatively evenly distributed throughout the year, indicating other causes than a seasonal change in observation frequency.
The main influence on the distribution of oil spill alerts found in the correlation analysis is the climate, where wind/waves are the main factors (Dahlslett et al., 2018). This is not unexpected, as both low wind and high wind are sea state conditions where radar satellite's ability to detect oil on the sea surface is limited (Fingas and Brown, 2011). This means that there might be the same amount of “oil slicks” during the winter months as the summer months, where the rougher sea state during the winter months is less favorable for detection (Figure 6).

Examining sources of mineral oil slicks, the oil and gas industry and ships do not indicate any trends that support less mineral oil discharged during winter than summer. The small dataset on oilrigs (A/S_Norske_Shell, 2016, A/S_Norske_Shell, 2017, Statoil, 2016a, Statoil, 2016b, Statoil, 2017a, Statoil, 2017b, Wintershall, 2016, Wintershall, 2017) shows a negative correlation, where slightly more oil is discharged during the winter months than the summer months.
Another source of alerts is natural films from biological activity, such as algae blooms, as these phenomena also give “false” oil spill alerts on the satellite services (Espedal, 1999, Gade et al., 1998). Biological activity, especially in arctic waters, has a general and similar bell-shaped biomass curve (Richardson, 1989). This probably adds observations during spring and summer, more than in autumn and winter, enhancing the shape of observation when looking at this seasonal.

This analysis is very general, and some of the data used are limited in terms of sample size and geographical extent. However, it adds general knowledge of the oil spill distribution within the study area and the major factors influencing the result.

5.3.3 Test for spatial randomness.

There is significant spatial clustering revealed examining oil spill alerts within the study area.

The result for the spatial randomness test, Ripleys K function test, shows clustering for the spatial distribution of the alerts (incidents).

Regarding the confidence envelope not following the expected K-line, this can happen when the shape of the study area is rather complex (ESRI, 2011). With a simple shape study area, as a rectangle or square, the confidence envelope would have the expected K line inside the two dotted lines (see Figure 35). However, in this analysis, using a more complex study area (where oil spill alerts can occur), the envelope curve follows the blue random expected K line up to approximately 100km neighborhood distance and then drops below the expected K line.

5.3.4 Hotspot analysis all data and Ship + unknown as a source

Significant spatial clustering is revealed by examining oil spill alerts within the study area, especially in areas of human activity.

The main finding in this analysis is clustering connected to the offshore industry, where high Z values correspond with offshore installation areas.

Local spatial statistic methods have been conducted, on various scale inputs, to see the magnitude of the maximum spatial autocorrelation and analyze it on a smaller/local scale. Looking at all data with maximum spatial autocorrelation settings, in Figure 36a, three areas are revealed as clustered. These can be further investigated pixel-by-pixel on z-scores, but they are all significant in the analysis at 90%, 95%, and 99% confidence levels. Running the analysis with smaller-scale data down to where scale stops influencing the clustering, Figure 36b/c shows "strong" clustering in offshore industry areas.

The same analysis is also done on a dataset containing only data not connected to the oil and gas industry. At maximum autocorrelation (**Feil! Fant ikke referansekilden.** a), the map is still quite similar in terms of spatial pattern in the North Sea area, indicating clustering in this area outside the offshore industry. One bias here is that when removing some data, new clusters will form. Still, investigating the oil spill alert dataset without "RIG" source data reveals new clustering areas in the Norwegian Sea and the Barents Sea.

Feil! Fant ikke referansekilden.b/c also shows new patterns, where some of the hotspots are still in offshore areas, some have a good overlap with the ship as source data from the 2015-2016 analysis. Some clusters are in areas outside where a likely source is connected. For instance, the hotspot west of Ny Ålesund (Svalbard) is interesting, as this is a low human activity area. This finding, where there is no known source for such a hotspot, can point at unknown sources such as a shipwreck or an area of natural seepage.

The aggregated oil spill alert map (Figure 38) is also an important one. *This map does not yield statistically significant findings but shows oil spill alerts added up within a fixed 10x10km grid, giving an oil spill frequency. Such a frequency map also can reveal important spatial patterns missed by hotspot analysis*. However, the results of this map and pattern are much in line with the results of the hotspot analysis. Looking at the two classes, 8-19 and 20-55, where there is some repetition of oil spill alerts observed. This can indicate that some activity within this area should cause this repetition in oil spill alerts. The pattern we see is much in alignment with shipping activity, especially repeating activity for fishing vessels, using the same fishing areas repeatedly. The two last classes, 56-84 and 85are to be considered hotspots, and they only occur in areas with stationary oil and gas installations.

This map can also use raster calculations to produce pixel-by-pixel ratios, as monitoring frequencies are available in the same raster format. The frequencies are shown as background in the map in Figure 38. Areas of low monitoring frequency and repeating oil spill alerts should be investigated further, as there could be significant hotspots in such areas. This is also a bias in the study, as the monitoring is not

uniform, either in frequency or spatial cover. This is further discussed at the end of the next section, 5.3.5, and this applies to the study in general.

Also, many ancillary datasets in Norway are also available as 10x10 km raster. This includes data on metrological data, environmental resources, marine wildlife, natural resources, and others. Such standardized datasets might then be used as input for other assessments and studies.

5.3.5 Hotspot analysis all data and Ship + unknown as source analyzed on impact.

When analyzing how oil slick size and spatial relationships occur within the study area, clustering of small size slicks is found in offshore industry areas, and some clustering of large size slicks is found in areas outside typical human activity.

The main finding in this analysis is clustering connected to the offshore industry, where high Z values correspond with offshore installation areas.

The results here are also related to the results of section 4.3.1 on oil spill origin, where the 2016 results show an average observation size varies by the three sources, Rig (2.05km^2), Ship (3.58km^2), and Unknown (5.68km^2). The hotspot analysis on observation size also shows clustering of low values in the oil and gas installations area. Figure 39shows significant cold spots. Analyzing the data without "RIG" source data reveal only hotspots with high values in the southern North Sea of the study area and some other smaller clusters. The hotspot area in the south is a little smaller, analyzing the data without oil rig connected alerts. However, it has not changed much in the southern oil rig areas, so the contribution on high values clustering in the southern North Sea is not connected to oil and gas activity. Both heat maps (Figure 39 and Figure 40) also show some other cluster areas, where the large size observations cluster are likely to be unknowns. The unknowns are discussed as oil spill lookalike signatures. The operative "mineral oil" service should ideally be left out of the alert service or at least categorized as something other than mineral oil. These clusters of most likely unknowns and all related attribute data could be investigated further. Clustering cold spots (small size oil slicks) is interesting in terms of natural seepage, as the higher resolution images (Sentinel-1) are now used more extensively. Future data use should certainly be analyzed for such clustering.

One general bias in this thesis's spatial study is that some areas do have less confidence in the data because the area has not been revisited by satellites more than a few times. The reason is that the operational satellite service is aimed at coastal waters, typical of shipping activity, and at some larger, more "rural" areas where the offshore industry is established. However, a raster extraction of footprint data (monitoring frequency) for all the 3694 observations reveals that only two observations are within areas covered less than 30 times by satellite. Looking at how many observations are in areas covered by satellite 100 times and less, only 23 of the 3694 oil spill alerts are in these less frequently monitored areas. Accordingly, the findings within this study should be considered based on a good and valid dataset for the statistical analysis methods used, and much of the uncertainty lies in areas less monitored. These less monitored areas are not of a priority at the time being, but a change in shipping traffic patterns, offshore industry, or other activities might shift or enlarge the monitoring effort.

5.4 Objective 3: To validate/verify the service provider's likelihood settings with historical observations.

The results from this part of the study indicate that the classification of A/B, where confidence A is more likely mineral oil and confidence B is less likely mineral oil, do not work well as an independent measure for decision making for the end-user.

The main result of this analysis shows that a confidence A is more likely to be mineral oil than a confidence B oil spill alert.

The oil spill alert services deliver very close to 50/50% on confidence A/B alerts, and actually within a random chance 0.5 probability ± 2σ, based on the 3679 observations, giving a 0.4835 – 0.5165 span, as shown in Figure 42.
The result of calculating the total number of mineral oil spills in 2015-2018 against the other oils/UNK (No mineral oils) seems to be spot on with 49% mineral oil alerts. However, as Figure 42 shows, when evaluating the confidence classes when connected to a source, the confidence levels do not perform as well. One cannot conclude that a confidence A alert equals a mineral oil observation.
When connecting the observation to RIG as a source, the classification presented to the end-user is on the correct side of the probability threshold of 50% set by the service providers. *In situ* data shows that 95% of the RIG connected alert is mineral oil, so the majority of these alerts should then be classified as confidence A, and they are. Here Sentinel-1A/B performs best with a probability of 0.63.

When the observation is not connecting to RIG as a source, being either SHIP or UNK, the classification presented to the end-user is on the correct side of the probability threshold of 50% set by the service providers. A calculation of mineral oil connected to SHIP+UNK and the number of observations data shows that 17% of the SHIP+UNK connected alert is mineral oil, so the majority (83%) of these alerts should then be classified as confidence B. Here Radarsat-2 performs best with a probability of 0.42.

The results on RIG as a source, connected to mineral oil, the number of confidence A alerts received by end-user is highly underestimated. Where the shipping is the source, confidence A is highly overestimated.

These results show the end-user difficulties using the classification, especially as a sole indicator of what is mineral oil or not mineral oil. This result shows that a source analysis is more important than the confidence class of the observation to the end-user.

Setting the confidence level is a complex task for the service provider. Ideally, oil lookalikes should not be reported at all, where the end-user wishes for a robust "no mineral oil"/"mineral oil" classification. The classification results from a set of rules, analyzing complexity in a radar image and oil spill candidates. The different natural phenomena as sea state, ice conditions, and biological activity add to the complexity in classifying an oil spill candidate (Brekke et al., 2014, Espedal, 1999, Ferraro et al., 2010).

The results in this study indicate that both classes should be considered a “feature of interest” as a starting point. Considering the high number of alerts, still increasing, source information is of high importance in enforcing appropriate remedial actions by the end-user. This approach has been discussed (Ferraro et al., 2010) and implemented at EMSA CleanSeaNet, allowing a set of rules applying on ancillary data and observation data, resulting in a red, yellow, or green alert. Today there are some limitations in how the filter algorithm can be built, and there are also limitations on how attributes can be part of the algorithm. Ship type is one set of information that cannot be used today in the algorithm, although this information might target the follow-up more efficiently. For example, observations connected to fishing vessels could give a yellow alert, and observations connected to other vessels could give a red alert. In this case, the yellow alert indicates that this is less likely to be mineral oil, and a random check on, for example, 10% of these alerts, might be sufficient and correct level of resources used for follow-up.

6 Conclusions

The Norwegian Coastal Administration has experienced a large increase in oil spill alerts since 2015. The increase is lined up with the introduction of two new Sentinel-1 satellites. However, *in situ* data indicated a general decreasing/flat trend in mineral oil spills in the Norwegian area in the same time frame. As radar satellites also detect oil spill lookalikes, end-users need to consider uncertainty when deciding corrective measures on a possible oil spill alert. In sum, the NCA faces a knowledge gap on ***what, where,*** and ***why*** there is a major increase in possible oil spill alerts and the impact.

The thesis objectives were to: one, explore the increase in oil spill alerts and establish the influence of Sentinel-1A and 1B, two, quantify the increase of mineral oil, and three, assess the confidence setting for an observation being mineral oil used by the service providers.

A hypothesis was established as part of one of three specific objectives set to meet the aim of the study, stating *that the increase in alerts is not due to increasing "mineral oil" at sea.*

The hypothesis is rejected as there is an estimated increase in mineral oil impact. The increase is though marginal, with its 2.65% on a 154% increase in observations.

The main objectives of the study are all met, were the *three* specific objectives have all contributed to the main findings:

- The Sentinel-1 satellites perform significantly differently than Radarsat-2 concerning oil slick size. The increase in the number of oil spill alerts is connected to the use of the Sentinel-1 satellites. This finding is probably due to higher spatial resolution, resulting in the instruments' ability to detect smaller size oil slicks and lookalike oil slicks than Radarsat-2.
- The increase in the number of observations from the Sentinel-1 satellites in comparison with Radarsat-2 contributes most in the small size observations category, under 0.5km2, and most of the newly added observations contributing to the increase are found among small observations.
- There is a large increase in the number of observations connected to ships as a likely source, though observation size decreases.
- The two most represented ship types where ship and observation connect are fishing vessels and chemical tankers. The observations are most probably animal/vegetable oils and fall into the category of legal discharges.
- The analyses show that the "oil spill " classification, with confidence A and B, used by the service providers, where A is more probable to be mineral oil/oil spill than B category, do not work well as a mineral oil/other observation categorization. In consequence, it is not recommended for end-users to base follow-up solely on category.

Even there is a large increase in the number of oil spill alerts for 2016-2018, the increase in mineral oil discharged is small. More small-size mineral oil spills and more large-sized non-mineral oil spills contribute to this.

There is also an increase in “spills” that fail to connect to any likely source, so there is still a need for further work/research connected to these observations and their origin/substance/phenomena. The results also show the very high importance of analyzing all observations for a likely source connection. This is essential for establishing what type of product the oil spill observation most likely consists of, and next, what measures the end-user wants/needs to apply towards the “oil spill alert” and the source. This source analysis is partly available at the services today, and additional ancillary data that can add to the service's quality is easily accessible. Service providers should offer more refinement in applying ancillary data and filters/algorithms for classifying the observations on end-user terms.
As new satellites are implemented, the results in this study reveal a need to undertake comparative analysis/sensor-shift analyses, primarily aimed at detection characteristics in the mode available for day-to-day service.

7 References

A/S_NORSKE_SHELL. 2016. *Utslipp fra Draugenfeltet 2015* [Online]. Stavanger, Norway: Norsk olje & gass. Available: https://www.norskoljeoggass.no/contentassets/a980907016bd4bb89ee6fdac0ad9a7b5/nea_2015_draugen.pdf [Accessed 19th November 2019].

A/S_NORSKE_SHELL. 2017. *Utslipp fra Draugenfeltet 2016* [Online]. Stavanger, Norway: Norsk olje & gass. Available: https://www.norskoljeoggass.no/contentassets/858441a2af864132b23c5237836ffb1e/draugen.pdf [Accessed 19th November 2019].

AIRHISTORY.NET. 2018. *LN-LMD* [Online]. AirHistory.net Available: https://www.airhistory.net/photo/63023/LN-LMD [Accessed 19th October 2021].

ALPERS, W., HOLT, B. & ZENG, K. 2017. Oil spill detection by imaging radars: Challenges and pitfalls. IEEE.

BERN, T.-I., WAHL, T., ANDERSEN, T. & OLSEN, R. 1993. Oil spill detection using satellite based SAR-experience from a field experiment. *Photogrammetric Engineering and Remote Sensing;(United States),* 59.

BONN_AGREEMENT. 2011. *BAOAC Photo Atlas* [Online]. London, United Kingdom: Bonn Agreement. Available: https://www.bonnagreement.org/site/assets/files/1081/photo_atlas_version_20112306.pdf [Accessed 1st November 2019].

BONN_AGREEMENT. 2015. *Annual report on aerial surveillance for 2014* [Online]. London, United Kingdom: Bonn Agreement. Available: https://www.bonnagreement.org/site/assets/files/3949/2014_report_on_aerial_surveillance-1.pdf [Accessed 15th November 2019].

BONN_AGREEMENT. 2016. *Annual report on aerial surveillance for 2015* [Online]. London, United Kingdom: Bonn Agreement. Available: https://www.bonnagreement.org/site/assets/files/3949/2015_report_on_aerial_surveillance.pdf [Accessed 15th November 2019].

BONN_AGREEMENT. 2017. *Annual report on aerial surveillance for 2016* [Online]. London, United Kingdom: Bonn Agreement. Available: https://www.bonnagreement.org/site/assets/files/3949/2016_report_on_aerial_surveillance.pdf [Accessed 15th November 2019].

BONN_AGREEMENT. 2018a. *Annual report on Aerial Surveillance for 2018* [Online]. London, United Kingdom: Bonn Agreement Available: https://www.bonnagreement.org/site/assets/files/3949/2018_aerial_surveillance.pdf [Accessed 15th November 2019].

BONN_AGREEMENT. 2018b. *Summary Record OTSOPA 2018* [Online]. London, United Kingdom: Bonn Agreement. Available: https://www.bonnagreement.org/meetings/summary-records?q=&y=&s=-date_start [Accessed 7th November 2019].

BREKKE, C., HOLT, B., JONES, C. & SKRUNES, S. 2014. Discrimination of oil spills from newly formed sea ice by synthetic aperture radar. *Remote Sensing of Environment,* 145**,** 1-14.

CARPENTER, A. 2007. The Bonn Agreement Aerial Surveillance programme: Trends in North Sea oil pollution 1986–2004. *Marine Pollution Bulletin,* 54**,** 149-163.

CARPENTER, A. 2018. Oil pollution in the North Sea: the impact of governance measures on oil pollution over several decades. *Hydrobiologia*.

CLEANSEANET, E. 2019. *Earth Observation Services* [Online]. Lisbon, Portugal: European Maritime Safety Organisation. Available: http://www.emsa.europa.eu/csn-menu.html [Accessed 11th November 2019].
CSA. 2019a. *RADARSAT satellites: Technical comparison* [Online]. Quebec, Canada: Canadian Space Agency. Available: http://asc-csa.gc.ca/eng/satellites/radarsat/technical-features/radarsat-comparison.asp [Accessed 12th November 2019].
CSA. 2019b. *Technical features* [Online]. Quebec, Canada: Canadian Space Agency Available: http://www.asc-csa.gc.ca/eng/satellites/radarsat/technical-features/default.asp [Accessed 12th November 2019].
DAHLSLETT, H. P., AARNES, Ø., RUDBERG, A., GRAVIR, G., BRUDE, O. W., LUNDE, S. & BERGSTRØM, R. 2018. Oil Spill Response Viability Analysis for the Norwegian Continental Shelf Integrated in a Web Based Planning Tool. *SPE International Conference and Exhibition on Health, Safety, Security, Environment, and Social Responsibility.* Abu Dhabi, UAE: Society of Petroleum Engineers.
DALING, P. S. & STRØM, T. 1999. Weathering of Oils at Sea: Model/Field Data Comparisons. *Spill Science and Technology Bulletin,* 5**,** 63-74.
DEL FRATE, F., GIACOMINI, A., LATINI, D., SOLIMINI, D. & EMERY, W. J. 2011. The Gulf of Mexico oil rig accident: analysis by different SAR satellite images. *Proceedings of SPIE,* 8179**,** 81790F.
DLR. 2011. *Ölteppich vor der norwegischen Küste* [Online]. Köln, Germany: Standort Oberpfaffenhofen des Deutschen Zentrum für Luft- und Raumfahrt (DLR. Available: https://activations.zki.dlr.de/de/activations/items/ACT095.html [Accessed 16th November 2019].
DNV-GL 2018. Oil Spill Response Viability Analysis Model. Limited access.
EC. 2018. *Mid-term evaluation of Regulation (EU) No 911/2014 on multiannual funding for the action of the European Maritime Safety Agency in the field of response to marine pollution caused by ships and oil and gas installations* [Online]. Brussels, Belgium: European_Commission. Available: https://eur-lex.europa.eu/resource.html?uri=cellar:02e15f94-9712-11e8-8bc1-01aa75ed71a1.0001.01/DOC_1&format=PDF [Accessed 20th August 2019].
EMSA. 2010. *Welcome to CleanSeaNet 2nd generation* [Online]. Lisbon, Portugal: European Maritime Safety Agency. Available: https://portal.emsa.europa.eu/web/csn [Accessed 19th October 2021].
EMSA. 2013a. *Addressing Illegal Discharges in the Marine Environment* [Online]. Lisbon, Portugal: European Maritime Safety Agency. Available: http://www.emsa.europa.eu/news-a-press-centre/external-news/2-news/1879-addressing-illegal-discharges-in-the-marine-environment.html [Accessed 10th October 2019].
EMSA. 2013b. *CleanSeaNet* [Online]. Lisbon, Portugal: European Maritime Safety Agency Available: http://www.emsa.europa.eu/csn-menu/download/438/711/23.html [Accessed 19th October 2021].
ESA. 2016. *Sentinel-1 Product Definition* [Online]. Paris, France: European Space Agency. Available: https://sentinels.copernicus.eu/documents/247904/1877131/Sentinel-1-Product-Definition.pdf/6049ee42-6dc7-4e76-9886-f7a72f5631f3?t=1461673251000 [Accessed 12th November 2019].

ESA. 2019a. *COSMO-SkyMed (Constellation of 4 SAR Satellites)* [Online]. Paris, France: European Space Agency. Available: https://directory.eoportal.org/web/eoportal/satellite-missions/c-missions/cosmo-skymed [Accessed 12th November 2019].
ESA. 2019b. *EnviSat (Environmental Satellite)* [Online]. Paris, France: European Space Agency. Available: https://earth.esa.int/web/eoportal/satellite-missions/e/envisat [Accessed 12th November 2019].
ESA. 2019c. *Sentinel-1* [Online]. Paris, France: European Space Agency. Available: https://sentinel.esa.int/web/sentinel/missions/sentinel-1 [Accessed 11th November 2019].
ESA. 2019d. *TDX (TanDEM-X: TerraSAR-X add-on for Digital Elevation Measurement)* [Online]. Paris, France: European Space Agency. Available: https://earth.esa.int/web/eoportal/satellite-missions/t/tandem-x [Accessed 12th November 2019].
ESA. 2019e. *TSX (TerraSAR-X) Mission* [Online]. Paris, France: European Space Agency. Available: https://earth.esa.int/web/eoportal/satellite-missions/t/terrasar-x [Accessed 12th November 2019].
ESPEDAL, H. Detection of oil spill and natural film in the marine environment by spaceborne SAR. IEEE 1999 International Geoscience and Remote Sensing Symposium. IGARSS'99 (Cat. No.99CH36293), 28 June-2 July 1999 1999. 1478-1480 vol.3.
ESRI. 2011. *Ripley's K Confidence Envelope doesn't follow the blue expected line* [Online]. ESRI. Available: https://community.esri.com/t5/spatial-statistics-questions/ripley-s-k-confidence-envelope-doesn-t-follow-the-blue-expected/m-p/232299 [Accessed 25th March 2021].
FERRARO, G., BASCHEK, B., DE MONTPELLIER, G., NJOTEN, O., PERKOVIC, M. & VESPE, M. 2010. On the SAR derived alert in the detection of oil spills according to the analysis of the EGEMP. *Marine Pollution Bulletin,* 60**,** 91-102.
FFI. 2003. *Satellittovervåkning* [Online]. Kjeller, Norway: Forsvarets Forskningsinstitutt. Available: https://publications.ffi.no/nb/item/asset/dspace:6131/FFIs-historie-nr20.pdf [Accessed 20th October 2021].
FINGAS, M. 2016. *Oil spill science and technology*, Gulf professional publishing.
FINGAS, M. 2018. The challenges of remotely measuring oil slick thickness. *Remote sensing,* 10**,** 319.
FINGAS, M. & BROWN, C. E. 2011. Chapter 6 - Oil Spill Remote Sensing: A Review. *In:* FINGAS, M. (ed.) *Oil Spill Science and Technology*. Boston: Gulf Professional Publishing.
FINGAS, M. & BROWN, C. E. 2018. A Review of Oil Spill Remote Sensing. *Sensors (14248220),* 18**,** 1-N.PAG.
FINGAS, M. F. & BROWN, C. E. 1997. Review of oil spill remote sensing. *Spill Science and Technology Bulletin,* 4**,** 199-208.
GADE, M., ALPERS, W., HÜHNERFUSS, H., MASUKO, H. & KOBAYASHI, T. 1998. Imaging of biogenic and anthropogenic ocean surface films by the multifrequency/multipolarization SIR-C/X-SAR. *Journal of Geophysical Research. Oceans,* 103**,** 18851.
GARCIA-PINEDA, O., HOLMES, J., RISSING, M., JONES, R., WOBUS, C., SVEJKOVSKY, J. & HESS, M. 2017. Detection of Oil near Shorelines during

the Deepwater Horizon Oil Spill Using Synthetic Aperture Radar (SAR). *Remote Sensing,* 9**,** 567.
GARCIA-PINEDA, O., MACDONALD, I. & GREEN, R. Detection of thick patches of floating oil emulsions using X, C, and L-band SAR during Deep water Horizon oil spill. Geoscience and Remote Sensing Symposium (IGARSS), 2013 IEEE International, 2013a. IEEE, 2007-2010.
GARCIA-PINEDA, O., MACDONALD, I. R., LI, X., JACKSON, C. R. & PICHEL, W. G. 2013b. Oil Spill Mapping and Measurement in the Gulf of Mexico With Textural Classifier Neural Network Algorithm (TCNNA). *IEEE Journal of Selected Topics in Applied Earth Observations and Remote Sensing,* 6**,** 2517-2525.
GETIS, A. & ORD, J. 1996. Spatial analysis and modeling in a GIS environment. *A research agenda for geographic information science***,** 157-196.
GYORY, J., MARIANO, A. J. & RYAN, E. H. 2013. *"The Spitsbergen Current." Ocean Surface Currents.* [Online]. Available: https://oceancurrents.rsmas.miami.edu/atlantic/norwegian.html [Accessed 1st Feb 2020].
HAUGAN, P. M., EVENSEN, G., JOHANNESSEN, J. A., JOHANNESSEN, O. M. & PETTERSSON, L. H. 1991. Modeled and observed mesoscale circulation and wave-current refraction during the 1988 Norwegian Continental Shelf Experiment. *Journal of Geophysical Research: Oceans,* 96**,** 10487-10506.
HOVLAND, M. 1990. Suspected gas-associated clay diapirism on the seabed off Mid Norway. *Marine and Petroleum Geology,* 7**,** 267-276.
HOVLAND, M. 1992. Hydrocarbon seeps in northern marine waters: Their occurrence and effects. *Palaios***,** 376-382.
IDAAS, K. 1995. NORWEGIAN POLLUTION CONTROL AUTHORITY WORK ON SHIPWRECKS. *International Oil Spill Conference Proceedings,* 1995**,** 733-735.
IMO. 2019. *IMO Annex I, Oil pollution* [Online]. London, United Kingdom: International Maritime Organisation. Available: http://www.imo.org/en/OurWork/Environment/PollutionPrevention/OilPollution/Pages/Default.aspx [Accessed 12th November 2019].
ITOPF. 2018. *Previous Spill Experience* [Online]. London , United Kingdom: ITOPF. Available: https://www.itopf.org/knowledge-resources/countries-territories-regions/countries/norway/ [Accessed 13.december 2019].
IVANOV, A. Y. 2010. The oil spill from a shipwreck in Kerch Strait: radar monitoring and numerical modelling. *International Journal of Remote Sensing,* 31**,** 4853-4868.
KSAT 2014. OIL DETECTION REPORT - RS2_20140807_053852_0045_SCNA_HHHV_SGF_340542_3460_9950271_KYSTVERKET_ODR. Internal Report to Norwegian Coastal Administration.
KSAT. 2019. *Earth observation services* [Online]. Tromsø, Norway: Kongsberg Satellite Services. Available: https://www.ksat.no/services/earth-observation-services/ [Accessed 11th November 2019].
KSAT. 2021. *Oil Spill Detection Service* [Online]. Tromsø, Norway: Kongsberg Satellite Services. Available: https://www.ksat.no/no/earth-observation/environmental-monitoring/oil-spill-detection-service/ [Accessed 19th October 2021].
KYSTVERKET 2016. Archive monitoring data Surveillance Aircraft. Unpublished - local database: Norwegian Coastal Administration.

MANN, H. B. & WHITNEY, D. R. 1947. On a Test of Whether one of Two Random Variables is Stochastically Larger than the Other. *Ann. Math. Statist.,* 18**,** 50-60.
MAXAR_TECHNOLOGIES_LTD. 2018. *RADARSAT-2 PRODUCT DESCRIPTION* [Online]. Westminister, Colorado, United States: Maxar_Technologies_Ltd Available: https://mdacorporation.com/docs/default-source/technical-documents/geospatial-services/52-1238_rs2_product_description.pdf?sfvrsn=10 [Accessed 15th November 2019].
MINISTRY_OF_CLIMATE_AND_ENVIRONMENT. 2020. *Marine and coastal waters* [Online]. Oslo, Norway. Available: https://www.environment.no/topics/marine-and-coastal-waters/ [Accessed 13th November 2019].
MORANDIN, L. A. & O'HARA, P. D. 2016. Offshore oil and gas, and operational sheen occurrence: is there potential harm to marine birds? *Environmental Reviews,* 24**,** 285-318.
MOUGINOT, J., RIGNOT, E., SCHEUCHL, B. & MILLAN, R. 2017. Comprehensive Annual Ice Sheet Velocity Mapping Using Landsat-8, Sentinel-1, and RADARSAT-2 Data. *Remote Sensing,* 9**,** 364.
NACHAR, N. 2008. The Mann-Whitney U: A test for assessing whether two independent samples come from the same distribution. *Tutorials in quantitative Methods for Psychology,* 4**,** 13-20.
NCA. 2016a. *Hendelser håndtert i 2016* [Online]. Ålesund, Norway: Norwegian Coastal Administration. Available: https://www.kystverket.no/globalassets/beredskap/publikasjoner-beredskap/hendelsesrapport-2016-endelig.pdf [Accessed 15th November 2019].
NCA. 2016b. *KYSTVERKETS ÅRSRAPPORT 2016* [Online]. Ålesund, Norway: Norwegian Coastal Administration. Available: https://www.regjeringen.no/contentassets/dfe89791d3744379b5242d79975ae528/arsrapport-2016-for-kystverket.pdf [Accessed 20th October 2021].
NCA. 2017a. *HAVBASE* [Online]. Norwegian Coastal Administration. Available: https://havbase.kystverket.no/havbase_report/doc/Havbase.pdf [Accessed 31st December 2018].
NCA. 2017b. *hendelsesrapport 2017* [Online]. Ålesund, Norway: Norwegian Coastal Administration. Available: https://www.kystverket.no/oljevern-og-miljoberedskap/rapporter-og-dokumenter/ [Accessed 15th November 2019].
NCA 2018a. Common operational picture MAP service https://beredskap.kystverket.no/: Norwegian Coastal Administration.
NCA. 2018b. *Hendelsesrapport 2018* [Online]. Ålesund, Norway: Norwegian Coastal Administration. Available: https://www.kystverket.no/globalassets/oljevern-og-miljoberedskap/hendelsesrapporter/hendelsesrapport-2018.pdf/download [Accessed 16th November 2019].
NCA. 2021. *Statlige beredskapsressurser* [Online]. Ålesund, Norway: Norwegian Coastal Administration. Available: https://www.kystverket.no/oljevern-og-miljoberedskap/ansvar-og-roller/statlige-beredskapsressurser/#j_1346 [Accessed 19th October 2021].
NEA. 2019. *Management Areas* [Online]. Trondheim, Norway: Norwegian Environment Agency. Available:

https://tema.miljodirektoratet.no/no/Havforum/Forside/English/Marine-management-plan-areas/ [Accessed 19th November 2019].
NORWEGIAN_GOVERNMENT. 2015. *Management plans for marine areas* [Online]. Oslo, Norway: Ministry of Climate and Environment. Available: https://www.regjeringen.no/en/topics/climate-and-environment/biodiversity/innsiktsartikler-naturmangfold/forvaltningsplaner-for-havomrada/id2076485/ [Accessed 29th May 2020].
NORWEGIAN_OIL&GASS. 2019. *Miljørapport* [Online]. Stavanger, Norway. Available: https://www.norskoljeoggass.no/contentassets/172447a918d14f13aee01614037954b7/norog-miljorapport19-orig.pdf [Accessed 12.dec 2019].
NORWEGIAN_SPACE_AGENCY. 2021. *TILGANG TIL DATA FRA RADARSAT-2* [Online]. Oslo, Norway: Norwegian Space Agency. Available: https://www.romsenter.no/no/Fagomraader/Jordobservasjon2/Tilgang-til-data-fra-Radarsat-2 [Accessed 19th October 2021].
OSPAR. 2020. *Discharges offshore industry* [Online]. London, United Kingdom: OSPAR. Available: https://www.ospar.org/work-areas/oic/discharges [Accessed 13th November 2020].
PEEL, M. C., FINLAYSON, B. L. & MCMAHON, T. A. 2007. Updated world map of the Köppen-Geiger climate classification. *Hydrology and Earth System Sciences, Vol 11, Iss 5, Pp 1633-1644 (2007)***,** 1633.
PELICH, R., LONGÉPÉ, N., MERCIER, G., HAJDUCH, G. & GARELLO, R. Performance evaluation of Sentinel-1 data in SAR ship detection. 2015 IEEE International Geoscience and Remote Sensing Symposium (IGARSS), 26-31 July 2015 2015. 2103-2106.
PRION, S. & HAERLING, K. A. 2014. Making Sense of Methods and Measurement: Spearman-Rho Ranked-Order Correlation Coefficient. *Clinical Simulation in Nursing,* 10**,** 535-536.
RAZALI, N. M. & WAH, Y. B. 2011. Power comparisons of shapiro-wilk, kolmogorov-smirnov, lilliefors and anderson-darling tests. *Journal of statistical modeling and analytics,* 2**,** 21-33.
RICHARDSON, K. 1989. Algal blooms in the North Sea: The good, the bad and the ugly. *Dana. Charlottenlund,* 8**,** 83-93.
RIPLEY, B. D. 1977. Modelling Spatial Patterns. *Journal of the Royal Statistical Society. Series B (Methodological),* 39**,** 172-212.
ROY, S., HOVLAND, M. & BRAATHEN, A. 2016. Evidence of fluid seepage in Grønfjorden, Spitsbergen: Implications from an integrated acoustic study of seafloor morphology, marine sediments and tectonics. *Marine Geology,* 380**,** 67-78.
SKRUNES, S., BREKKE, C. & ELTOFT, T. 2012. Oil spill characterization with multi-polarization C- and X-band SAR. IEEE.
SKRUNES, S., BREKKE, C., ELTOFT, T. & KUDRYAVTSEV, V. 2015. Comparing Near-Coincident C- and X-Band SAR Acquisitions of Marine Oil Spills. *IEEE Transactions on Geoscience & Remote Sensing,* 53**,** 1958.
STATOIL. 2016a. *Kristin - Årsrapport 2015*
[Online]. Stavanger, Norway: Norsk olje & gass. Available: https://www.norskoljeoggass.no/contentassets/a980907016bd4bb89ee6fdac0ad9a7b5/nea_2015_kristin.pdf [Accessed 19th november 2019].
STATOIL. 2016b. *Norne årsrapport 2015*

[Online]. Stavanger, Norway: Norsk olje & gass. Available: https://www.norskoljeoggass.no/contentassets/a980907016bd4bb89ee6fdac0ad9a7b5/nea_2015_norne.pdf [Accessed 11th November 2019].

STATOIL. 2017a. *Kristin - Årsrapport 2016* [Online]. Stavanger, Norway: Norsk olje & gass. Available: https://www.norskoljeoggass.no/contentassets/858441a2af864132b23c5237836ffb1e/kristin.pdf [Accessed 19th November 2019].

STATOIL. 2017b. *Norne årsrapport 2016* [Online]. Stavanger, Norway: Norsk olje & gass. Available: https://www.norskoljeoggass.no/contentassets/75083ada93904f22b979248850ddcd32/norne.pdf [Accessed 19th November 2019].

VAUGHAN, D. G., COMISO, J. C., ALLISON, I., CARRASCO, J., G. KASER, R., KWOK, P. M., MURRAY, T., PAUL, F., REN, J., RIGNOT, E., SOLOMINA, O., STEFFEN, K. & ZHANG, T. 2013. Observations: Cryosphere. In: Climate Change 2013: The Physical Science Basis. Contribution of Working Group I to the Fifth Assessment Report of the Intergovernmental Panel on

Climate Change. United Kingdom and New York, NY, USA: Contribution of Working Group I to the Fifth Assessment Report of the Intergovernmental Panel on

Climate Change [Stocker, T.F., D. Qin, G.-K. Plattner, M. Tignor, S.K. Allen, J. Boschung, A. Nauels, Y. Xia, V. Bex and

P.M. Midgley (eds.).

WINTERSHALL. 2016. *Årsrapport til Miljødirektoratet for 2015 - Brage* [Online]. Stavanger, Norway: Norsk olje & gass. Available: https://www.norskoljeoggass.no/contentassets/8edae75099714a1c85eeabb713b00132/nea_2015_draugen.pdf [Accessed 19th November 2019].

WINTERSHALL. 2017. *Årsrapport til Miljødirektoratet for 2016 - Brage* [Online]. Stavanger, Norway: Norsk olje & gass. Available: https://www.norskoljeoggass.no/contentassets/75083ada93904f22b979248850ddcd32/brage.pdf [Accessed 19th November 2019].

Series from Lund University

Department of Physical Geography and Ecosystem Science

Master Thesis in Geographical Information Science

1. *Anthony Lawther:* The application of GIS-based binary logistic regression for slope failure susceptibility mapping in the Western Grampian Mountains, Scotland (2008).
2. *Rickard Hansen:* Daily mobility in Grenoble Metropolitan Region, France. Applied GIS methods in time geographical research (2008).
3. *Emil Bayramov:* Environmental monitoring of bio-restoration activities using GIS and Remote Sensing (2009).
4. *Rafael Villarreal Pacheco:* Applications of Geographic Information Systems as an analytical and visualization tool for mass real estate valuation: a case study of Fontibon District, Bogota, Columbia (2009).
5. *Siri Oestreich Waage:* a case study of route solving for oversized transport: The use of GIS functionalities in transport of transformers, as part of maintaining a reliable power infrastructure (2010).
6. *Edgar Pimiento:* Shallow landslide susceptibility – Modelling and validation (2010).
7. *Martina Schäfer:* Near real-time mapping of floodwater mosquito breeding sites using aerial photographs (2010).
8. *August Pieter van Waarden-Nagel:* Land use evaluation to assess the outcome of the programme of rehabilitation measures for the river Rhine in the Netherlands (2010).
9. *Samira Muhammad:* Development and implementation of air quality data mart for Ontario, Canada: A case study of air quality in Ontario using OLAP tool. (2010).
10. *Fredros Oketch Okumu*: Using remotely sensed data to explore spatial and temporal relationships between photosynthetic productivity of vegetation and malaria transmission intensities in selected parts of Africa (2011).
11. *Svajunas Plunge:* Advanced decision support methods for solving diffuse water pollution problems (2011).
12. *Jonathan Higgins:* Monitoring urban growth in greater Lagos: A case study using GIS to monitor the urban growth of Lagos 1990 - 2008 and produce future growth prospects for the city (2011).
13. *Mårten Karlberg:* Mobile Map Client API: Design and Implementation for Android (2011).
14. *Jeanette McBride:* Mapping Chicago area urban tree canopy using color infrared imagery (2011).
15. *Andrew Farina:* Exploring the relationship between land surface temperature and vegetation abundance for urban heat island mitigation in Seville, Spain (2011).
16. *David Kanyari*: Nairobi City Journey Planner: An online and a Mobile Application (2011).

17. *Laura V. Drews:* Multi-criteria GIS analysis for siting of small wind power plants - A case study from Berlin (2012).
18. *Qaisar Nadeem:* Best living neighborhood in the city - A GIS based multi criteria evaluation of ArRiyadh City (2012).
19. *Ahmed Mohamed El Saeid Mustafa:* Development of a photo voltaic building rooftop integration analysis tool for GIS for Dokki District, Cairo, Egypt (2012).
20. *Daniel Patrick Taylor*: Eastern Oyster Aquaculture: Estuarine Remediation via Site Suitability and Spatially Explicit Carrying Capacity Modeling in Virginia's Chesapeake Bay (2013).
21. *Angeleta Oveta Wilson:* A Participatory GIS approach to *unearthing* Manchester's Cultural Heritage '*gold mine'* (2013).
22. *Ola Svensson:* Visibility and Tholos Tombs in the Messenian Landscape: A Comparative Case Study of the Pylian Hinterlands and the Soulima Valley (2013).
23. *Monika Ogden:* Land use impact on water quality in two river systems in South Africa (2013).
24. *Stefan Rova:* A GIS based approach assessing phosphorus load impact on Lake Flaten in Salem, Sweden (2013).
25. *Yann Buhot:* Analysis of the history of landscape changes over a period of 200 years. How can we predict past landscape pattern scenario and the impact on habitat diversity? (2013).
26. *Christina Fotiou:* Evaluating habitat suitability and spectral heterogeneity models to predict weed species presence (2014).
27. *Inese Linuza:* Accuracy Assessment in Glacier Change Analysis (2014).
28. *Agnieszka Griffin:* Domestic energy consumption and social living standards: a GIS analysis within the Greater London Authority area (2014).
29. *Brynja Guðmundsdóttir:* Detection of potential arable land with remote sensing and GIS - A Case Study for Kjósarhreppur (2014).
30. *Oleksandr Nekrasov:* Processing of MODIS Vegetation Indices for analysis of agricultural droughts in the southern Ukraine between the years 2000-2012 (2014).
31. *Sarah Tressel:* Recommendations for a polar Earth science portal in the context of Arctic Spatial Data Infrastructure (2014).
32. *Caroline Gevaert:* Combining Hyperspectral UAV and Multispectral Formosat-2 Imagery for Precision Agriculture Applications (2014).
33. *Salem Jamal-Uddeen:* Using GeoTools to implement the multi-criteria evaluation analysis - weighted linear combination model (2014).
34. *Samanah Seyedi-Shandiz:* Schematic representation of geographical railway network at the Swedish Transport Administration (2014).
35. *Kazi Masel Ullah:* Urban Land-use planning using Geographical Information System and analytical hierarchy process: case study Dhaka City (2014).
36. *Alexia Chang-Wailing Spitteler:* Development of a web application based on MCDA and GIS for the decision support of river and floodplain rehabilitation projects (2014).
37. *Alessandro De Martino:* Geographic accessibility analysis and evaluation of potential changes to the public transportation system in the City of Milan (2014).
38. *Alireza Mollasalehi:* GIS Based Modelling for Fuel Reduction Using Controlled Burn in Australia. Case Study: Logan City, QLD (2015).

39. *Negin A. Sanati:* Chronic Kidney Disease Mortality in Costa Rica; Geographical Distribution, Spatial Analysis and Non-traditional Risk Factors (2015).
40. *Karen McIntyre:* Benthic mapping of the Bluefields Bay fish sanctuary, Jamaica (2015).
41. *Kees van Duijvendijk:* Feasibility of a low-cost weather sensor network for agricultural purposes: A preliminary assessment (2015).
42. *Sebastian Andersson Hylander:* Evaluation of cultural ecosystem services using GIS (2015).
43. *Deborah Bowyer:* Measuring Urban Growth, Urban Form and Accessibility as Indicators of Urban Sprawl in Hamilton, New Zealand (2015).
44. *Stefan Arvidsson:* Relationship between tree species composition and phenology extracted from satellite data in Swedish forests (2015).
45. *Damián Giménez Cruz*: GIS-based optimal localisation of beekeeping in rural Kenya (2016).
46. *Alejandra Narváez Vallejo:* Can the introduction of the topographic indices in LPJ-GUESS improve the spatial representation of environmental variables? (2016).
47. *Anna Lundgren:* Development of a method for mapping the highest coastline in Sweden using breaklines extracted from high resolution digital elevation models (2016).
48. *Oluwatomi Esther Adejoro:* Does location also matter? A spatial analysis of social achievements of young South Australians (2016).
49. *Hristo Dobrev Tomov:* Automated temporal NDVI analysis over the Middle East for the period 1982 - 2010 (2016).
50. *Vincent Muller:* Impact of Security Context on Mobile Clinic Activities A GIS Multi Criteria Evaluation based on an MSF Humanitarian Mission in Cameroon (2016).
51. *Gezahagn Negash Seboka:* Spatial Assessment of NDVI as an Indicator of Desertification in Ethiopia using Remote Sensing and GIS (2016).
52. *Holly Buhler:* Evaluation of Interfacility Medical Transport Journey Times in Southeastern British Columbia. (2016).
53. *Lars Ole Grottenberg*: Assessing the ability to share spatial data between emergency management organisations in the High North (2016).
54. *Sean Grant:* The Right Tree in the Right Place: Using GIS to Maximize the Net Benefits from Urban Forests (2016).
55. *Irshad Jamal:* Multi-Criteria GIS Analysis for School Site Selection in Gorno-Badakhshan Autonomous Oblast, Tajikistan (2016).
56. *Fulgencio Sanmartín:* Wisdom-volkano: A novel tool based on open GIS and time-series visualization to analyse and share volcanic data (2016).
57. *Nezha Acil:* Remote sensing-based monitoring of snow cover dynamics and its influence on vegetation growth in the Middle Atlas Mountains (2016).
58. *Julia Hjalmarsson:* A Weighty Issue: Estimation of Fire Size with Geographically Weighted Logistic Regression (2016).
59. *Mathewos Tamiru Amato:* Using multi-criteria evaluation and GIS for chronic food and nutrition insecurity indicators analysis in Ethiopia (2016).
60. *Karim Alaa El Din Mohamed Soliman El Attar:* Bicycling Suitability in Downtown, Cairo, Egypt (2016).

61. *Gilbert Akol Echelai:* Asset Management: Integrating GIS as a Decision Support Tool in Meter Management in National Water and Sewerage Corporation (2016).
62. *Terje Slinning:* Analytic comparison of multibeam echo soundings (2016).
63. *Gréta Hlín Sveinsdóttir:* GIS-based MCDA for decision support: A framework for wind farm siting in Iceland (2017).
64. *Jonas Sjögren:* Consequences of a flood in Kristianstad, Sweden: A GIS-based analysis of impacts on important societal functions (2017).
65. *Nadine Raska:* 3D geologic subsurface modelling within the Mackenzie Plain, Northwest Territories, Canada (2017).
66. *Panagiotis Symeonidis*: Study of spatial and temporal variation of atmospheric optical parameters and their relation with PM 2.5 concentration over Europe using GIS technologies (2017).
67. *Michaela Bobeck:* A GIS-based Multi-Criteria Decision Analysis of Wind Farm Site Suitability in New South Wales, Australia, from a Sustainable Development Perspective (2017).
68. *Raghdaa Eissa*: Developing a GIS Model for the Assessment of Outdoor Recreational Facilities in New Cities Case Study: Tenth of Ramadan City, Egypt (2017).
69. *Zahra Khais Shahid*: Biofuel plantations and isoprene emissions in Svea and Götaland (2017).
70. *Mirza Amir Liaquat Baig*: Using geographical information systems in epidemiology: Mapping and analyzing occurrence of diarrhea in urban - residential area of Islamabad, Pakistan (2017).
71. *Joakim Jörwall*: Quantitative model of Present and Future well-being in the EU-28: A spatial Multi-Criteria Evaluation of socioeconomic and climatic comfort factors (2017).
72. *Elin Haettner*: Energy Poverty in the Dublin Region: Modelling Geographies of Risk (2017).
73. *Harry Eriksson*: Geochemistry of stream plants and its statistical relations to soil- and bedrock geology, slope directions and till geochemistry. A GIS-analysis of small catchments in northern Sweden (2017).
74. *Daniel Gardevärn:* PPGIS and Public meetings – An evaluation of public participation methods for urban planning (2017).
75. *Kim Friberg:* Sensitivity Analysis and Calibration of Multi Energy Balance Land Surface Model Parameters (2017).
76. *Viktor Svanerud:* Taking the bus to the park? A study of accessibility to green areas in Gothenburg through different modes of transport (2017).
77. *Lisa-Gaye Greene*: Deadly Designs: The Impact of Road Design on Road Crash Patterns along Jamaica's North Coast Highway (2017).
78. *Katarina Jemec Parker*: Spatial and temporal analysis of fecal indicator bacteria concentrations in beach water in San Diego, California (2017).
79. *Angela Kabiru*: An Exploratory Study of Middle Stone Age and Later Stone Age Site Locations in Kenya's Central Rift Valley Using Landscape Analysis: A GIS Approach (2017).
80. *Kristean Björkmann*: Subjective Well-Being and Environment: A GIS-Based Analysis (2018).
81. *Williams Erhunmonmen Ojo*: Measuring spatial accessibility to healthcare for people living with HIV-AIDS in southern Nigeria (2018).

82. *Daniel Assefa*: Developing Data Extraction and Dynamic Data Visualization (Styling) Modules for Web GIS Risk Assessment System (WGRAS). (2018).
83. *Adela Nistora*: Inundation scenarios in a changing climate: assessing potential impacts of sea-level rise on the coast of South-East England (2018).
84. *Marc Seliger*: Thirsty landscapes - Investigating growing irrigation water consumption and potential conservation measures within Utah's largest master-planned community: Daybreak (2018).
85. *Luka Jovičić*: Spatial Data Harmonisation in Regional Context in Accordance with INSPIRE Implementing Rules (2018).
86. *Christina Kourdounouli*: Analysis of Urban Ecosystem Condition Indicators for the Large Urban Zones and City Cores in EU (2018).
87. *Jeremy Azzopardi*: Effect of distance measures and feature representations on distance-based accessibility measures (2018).
88. *Patrick Kabatha*: An open source web GIS tool for analysis and visualization of elephant GPS telemetry data, alongside environmental and anthropogenic variables (2018).
89. *Richard Alphonce Giliba*: Effects of Climate Change on Potential Geographical Distribution of Prunus africana (African cherry) in the Eastern Arc Mountain Forests of Tanzania (2018).
90. *Eiður Kristinn Eiðsson*: Transformation and linking of authoritative multi-scale geodata for the Semantic Web: A case study of Swedish national building data sets (2018).
91. *Niamh Harty*: HOP!: a PGIS and citizen science approach to monitoring the condition of upland paths (2018).
92. *José Estuardo Jara Alvear*: Solar photovoltaic potential to complement hydropower in Ecuador: A GIS-based framework of analysis (2018).
93. *Brendan O'Neill*: Multicriteria Site Suitability for Algal Biofuel Production Facilities (2018).
94. *Roman Spataru*: Spatial-temporal GIS analysis in public health – a case study of polio disease (2018).
95. *Alicja Miodońska*: Assessing evolution of ice caps in Suðurland, Iceland, in years 1986 - 2014, using multispectral satellite imagery (2019).
96. *Dennis Lindell Schettini*: A Spatial Analysis of Homicide Crime's Distribution and Association with Deprivation in Stockholm Between 2010-2017 (2019).
97. *Damiano Vesentini*: The Po Delta Biosphere Reserve: Management challenges and priorities deriving from anthropogenic pressure and sea level rise (2019).
98. *Emilie Arnesten*: Impacts of future sea level rise and high water on roads, railways and environmental objects: a GIS analysis of the potential effects of increasing sea levels and highest projected high water in Scania, Sweden (2019).
99. *Syed Muhammad Amir Raza*: Comparison of geospatial support in RDF stores: Evaluation for ICOS Carbon Portal metadata (2019).
100. *Hemin Tofiq*: Investigating the accuracy of Digital Elevation Models from UAV images in areas with low contrast: A sandy beach as a case study (2019).
101. *Evangelos Vafeiadis*: Exploring the distribution of accessibility by public transport using spatial analysis. A case study for retail concentrations and public hospitals in Athens (2019).
102. *Milan Sekulic*: Multi-Criteria GIS modelling for optimal alignment of roadway by-passes in the Tlokweng Planning Area, Botswana (2019).

103. *Ingrid Piirisaar*: A multi-criteria GIS analysis for siting of utility-scale photovoltaic solar plants in county Kilkenny, Ireland (2019).
104. *Nigel Fox*: Plant phenology and climate change: possible effect on the onset of various wild plant species' first flowering day in the UK (2019).
105. *Gunnar Hesch*: Linking conflict events and cropland development in Afghanistan, 2001 to 2011, using MODIS land cover data and Uppsala Conflict Data Programme (2019).
106. *Elijah Njoku*: Analysis of spatial-temporal pattern of Land Surface Temperature (LST) due to NDVI and elevation in Ilorin, Nigeria (2019).
107. *Katalin Bunyevácz*: Development of a GIS methodology to evaluate informal urban green areas for inclusion in a community governance program (2019).
108. *Paul dos Santos*: Automating synthetic trip data generation for an agent-based simulation of urban mobility (2019).
109. *Robert O' Dwyer*: Land cover changes in Southern Sweden from the mid-Holocene to present day: Insights for ecosystem service assessments (2019).
110. *Daniel Klingmyr*: Global scale patterns and trends in tropospheric NO2 concentrations (2019).
111. *Marwa Farouk Elkabbany*: Sea Level Rise Vulnerability Assessment for Abu Dhabi, United Arab Emirates (2019).
112. *Jip Jan van Zoonen*: Aspects of Error Quantification and Evaluation in Digital Elevation Models for Glacier Surfaces (2020).
113. *Georgios Efthymiou*: The use of bicycles in a mid-sized city – benefits and obstacles identified using a questionnaire and GIS (2020).
114. *Haruna Olayiwola Jimoh*: Assessment of Urban Sprawl in MOWE/IBAFO Axis of Ogun State using GIS Capabilities (2020).
115. *Nikolaos Barmpas Zachariadis*: Development of an iOS, Augmented Reality for disaster management (2020).
116. *Ida Storm*: ICOS Atmospheric Stations: Spatial Characterization of CO2 Footprint Areas and Evaluating the Uncertainties of Modelled CO2 Concentrations (2020).
117. *Alon Zuta*: Evaluation of water stress mapping methods in vineyards using airborne thermal imaging (2020).
118. *Marcus Eriksson*: Evaluating structural landscape development in the municipality Upplands-Bro, using landscape metrics indices (2020).
119. *Ane Rahbek Vierø*: Connectivity for Cyclists? A Network Analysis of Copenhagen's Bike Lanes (2020).
120. *Cecilia Baggini*: Changes in habitat suitability for three declining Anatidae species in saltmarshes on the Mersey estuary, North-West England (2020).
121. *Bakrad Balabanian*: Transportation and Its Effect on Student Performance (2020).
122. *Ali Al Farid*: Knowledge and Data Driven Approaches for Hydrocarbon Microseepage Characterizations: An Application of Satellite Remote Sensing (2020).
123. *Bartlomiej Kolodziejczyk*: Distribution Modelling of Gene Drive-Modified Mosquitoes and Their Effects on Wild Populations (2020).
124. *Alexis Cazorla*: Decreasing organic nitrogen concentrations in European water bodies - links to organic carbon trends and land cover (2020).

125. *Kharid Mwakoba*: Remote sensing analysis of land cover/use conditions of community-based wildlife conservation areas in Tanzania (2021).
126. *Chinatsu Endo*: Remote Sensing Based Pre-Season Yellow Rust Early Warning in Oromia, Ethiopia (2021).
127. *Berit Mohr*: Using remote sensing and land abandonment as a proxy for long-term human out-migration. A Case Study: Al-Hassakeh Governorate, Syria (2021).
128. *Kanchana Nirmali Bandaranayake*: Considering future precipitation in delineation locations for water storage systems - Case study Sri Lanka (2021).
129. *Emma Bylund*: Dynamics of net primary production and food availability in the aftermath of the 2004 and 2007 desert locust outbreaks in Niger and Yemen (2021).
130. *Shawn Pace*: Urban infrastructure inundation risk from permanent sea-level rise scenarios in London (UK), Bangkok (Thailand) and Mumbai (India): A comparative analysis (2021).
131. *Oskar Evert Johansson*: The hydrodynamic impacts of Estuarine Oyster reefs, and the application of drone technology to this study (2021).
132. *Pritam Kumarsingh*: A Case Study to develop and test GIS/SDSS methods to assess the production capacity of a Cocoa Site in Trinidad and Tobago (2021).
133. *Muhammad Imran Khan*: Property Tax Mapping and Assessment using GIS (2021).
134. *Domna Kanari*: Mining geosocial data from Flickr to explore tourism patterns: The case study of Athens (2021).
135. *Mona Tykesson Klubien*: Livestock-MRSA in Danish pig farms (2021).
136. *Ove Njøten*: Comparing radar satellites. Use of Sentinel-1 leads to an increase in oil spill alerts in Norwegian waters (2021).